CHAPTER ONE - INTRODUCTION

The first part of this chapter gives background into mining activities within the Witwatersrand Basin, and the pollution resulting from it. The second part describes the mine pollution remediation options and considerations.

1.1 Mining and mine pollution on the Witwatersrand Basin

The Witwatersrand Basin has the world's richest deposits of gold and low-grade uranium, with South Africa being the world's leading producer of gold (Weiersbye *et al.*, 2006; Kumah, 2004). Mining started in the Witwatersrand in 1886, after an Australian prospector discovered gold, on what used to be a farm in the area (Sutton *et al.*, 2006). The Main Reef conglomerates spread in an arc from East-West over a length of 60 km, marking a shoreline of an ancient lake (McCarthy, 2006; Winde, 2005). Gold occurrence was of considerable significance, thus gold mining was highly feasible, leading to the development of townships, industries and secondary industries, which eventually gave rise to the large city of Johannesburg. Figure 1.1 shows the layout of the Witwatersrand Basin, including the mining regions.

Gold is generally found in conglomerates of rock, within a matrix of various other minerals. Gold bearing conglomerates contain a high percentage of pyrite and uranium content (Weiersbye *et al.*, 2006). The gold concentration only constitutes approximately 0.2 – 0.3 ounces of gold per tonne of milled ore (Douglas, 1961).

Gold was initially extracted by the mercury amalgam method, but in later years the cyanidation process was implemented, as it became more applicable, especially as mining became deeper and the conglomerate matrix contained more interference

(Naiker *et al.*, 2002). Gold ore was mined underground and brought to the surface, where it was crushed to fine sand. In the mercury amalgam method, the fine sand was exposed to a thin film of mercury spread on copper plates. The mercury-gold amalgam was scraped off the plates and later further distilled to recover gold (Naiker *et al.*, 2002).

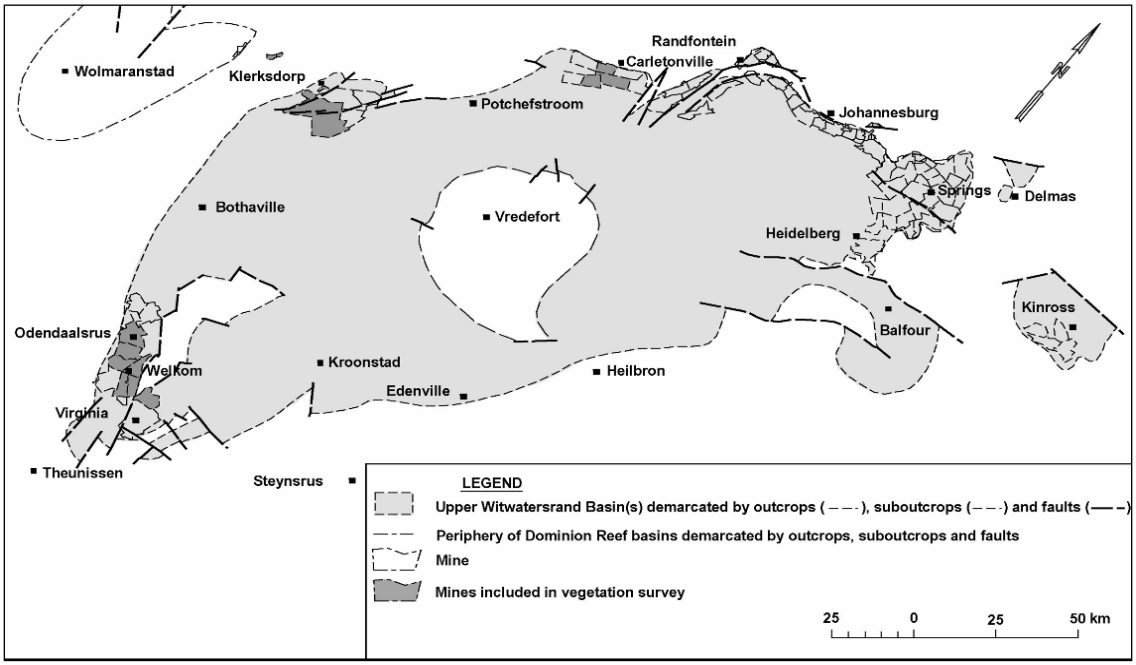

Figure 1.1 Layout of the Witwatersrand Basin, with the mining regions in an arc from East-West (Weiersbye *et al*., 2006)

The cyanide process on the other hand involves finer milling of the ore, which is then treated with a cyanide containing solution, which dissolves the gold. The solution is then separated to undergo further gold recovery processes (Naiker *et al.*, 2002). Extraction methods like the mercury amalgam method and the cyanidation process are highly selective for gold, thus all other minerals end up in the tailings. Large volumes of tailings are generated from gold mining, especially since gold only forms a small fraction of the conglomerates that were mined. These tailings form mountainous tailings storage facilities (TSF's) in the form of sand dumps, rock dumps and slimes

dumps (Weiersbye *et al.*, 2006). After mining ceased, these TSF's remained unused and untreated for over a century.

Mining produces more waste than any other industry (Brodie *et al.*, 1992). In South Africa 70% of all waste, i.e. 318 – 450 million tonnes a year, is generated by mining, mainly gold and uranium, platinum and coal sectors (Weiersbye, 2008). Mine wastes are disposed of on land and this type of waste is generally classified as non-hazardous, although they may have significant health and environmental risks (Brodie *et al.*, 1992). In the Witwatersrand Basin alone, there is approximately 400 km^2 of gold TSF's and footprints (Weiersbye *et al.*, 2006).

Soil contamination by mine TSF's can occur by any of the following mechanisms (Weiersbye *et al.*, 2006):

1. by windblown tailing material,
2. by the decomposition of spilled tailings,
3. through seepage due to water percolating through, and
4. By the precipitation of mineral salts on soil from seepage and shallow groundwater.

Acid rock drainage (ARD) is one of the most severe types of mine pollution. ARD emanates from mine waste rock, tailings, and mining structures (Akcil *et al.*, 2004). Acid rock drainage is caused mainly by the oxidation of sulphide minerals such as pyrite (FeS_2), which was originally present in the ore (Watzlaf, 2004). The ore is exposed to both oxygen and water, which acidifies the water leaching through the dumps. The following chemical equations represent the sequence of pyrite oxidation reactions (Weber, 2004):

$$FeS_2 + \frac{7}{2}O_2 + H_2O \rightarrow Fe^{2+} + 2SO_4^{2-} + 2H^+ \quad (1)$$

$$Fe^{2+} + \frac{1}{4}O_2 + H^+ \rightarrow Fe^{3+} + \frac{1}{2}H_2O \quad (2)$$

$$Fe^{3+} + 3H_2O \rightarrow Fe(OH)_{3(s)} + 3H^+ \quad (3)$$

$$FeS_2 + 14Fe^{3+} + 8H_2O \rightarrow 15Fe^{2+} + 2SO_4^{2-} + 16H^+ \quad (4)$$

In the first reaction pyrite is oxidised in the presence of water, to produce dissolved iron, sulphate, and hydrogen ions. The production of these ions in solution increases the total dissolved solids and acidity of water thus decreasing the pH (Akcil *et al.*, 2004). The ferrous iron is oxidised to the ferric iron in reaction (2). The reaction acts as the rate determining step in the sequence of pyrite oxidation reactions, and depends on whether the surrounding environment is sufficiently oxidising, i.e. dependant on oxygen concentration, pH and bacterial activity. In the third reaction, ferric iron is hydrolysed with water to form solid ferric hydroxide, which precipitates out at pH values 2.3 – 3.5. This reaction leaves little Fe^{3+} in solution, and simultaneously lowers the pH. The final step involves the further oxidation of the pyrite or ferric iron, with further acid production. This reaction occurs if any Fe^{3+} from reaction (2) doesn't precipitate out of solution by reaction (3), these ions may be used to oxidise additional pyrite and thus this reaction takes place in the absence of oxygen, and acid formation will continue until the supply of pyrite or the ferric iron is exhausted (Growitz, 2002; Akcil *et al.*, 2004).

The rate of acid generation is dependent on a number of factors (Akcil *et al.*, 2004):

- pH
- Temperature
- Oxygen content of the gaseous phase

- Oxygen content in the water phase
- Degree of saturation with water
- Chemical activity of Fe^{3+}
- Surface area of the exposed metal sulphide
- Chemical activation energy required to initiate acid generation
- Bacterial activity

By the above oxidation reactions, water percolating through the mine dumps becomes acidic and enters the ground water, then streams and ultimately enters rivers along the Witwatersrand. A problem associated with acid rock drainage is the contamination by metals and metalloids such as Fe, Mn, Ni, Co, Cu, Zn, Al, Cr, As, Hg, U, Bi, and Pb which could potentially a) be taken up by plants and be bio-accumulated, b) leach into the ground water (Naiker *et al.*, 2002), and c) enter surface water bodies and aquatic water systems. These all have negative impacts on the aquatic life in rivers and can also affect the vegetation on the banks of rivers and streams, by making the soil unsustainable for growth. Examples of rivers affected by acid rock drainage are the Wonderfonteinspruit (Winde, 2005) and also the Vaal River Basin. Some metals such as Fe, Mn, Ni, Co, Cu, and Zn are plant micro-nutrients which can be toxic at high concentrations. These factors should all be considered when considering rehabilitation of acid rock drainage.

Figure 1.2 is a conceptual model of acid rock drainage in the Witwatersrand region (Tutu *et al.*, 2008a). The model firstly highlights the main sources of acid rock drainage pollution, which includes active tailings dumps where deposition is occurring currently, tailings undergoing reprocessing, and tailings footprints and secondary sources, e.g. efflorescent crusts and polluted soils (Tutu *et al.*, 2008a). Secondly the model highlights the pollution dispersal pathways, which include surface flow and

groundwater which later enter surface water bodies, while wetlands are most affected as they are the main sinks for acid rock drainage pollution (Tutu *et al.*, 2008a).

Another contaminant which is sourced from tailings is that of uranium (U). Ore mined for gold had relatively high amounts of uranium compared to gold; Au – U ration ranges from 1:10 to 1:100 (Winde, 2004). After the ore was mined, milled, and leached, the remaining material was deposited as slurry in slimes dams. Uranium can be leached from the slimes dams at high concentrations, acting as a point source of pollution to streams, ground water systems and sediments, where it can pose a major risk to human health, as uranium is a highly radioactive heavy metal (Winde, 2004). Thus uranium contamination should also be considered when dealing with the rehabilitation of mine pollution.

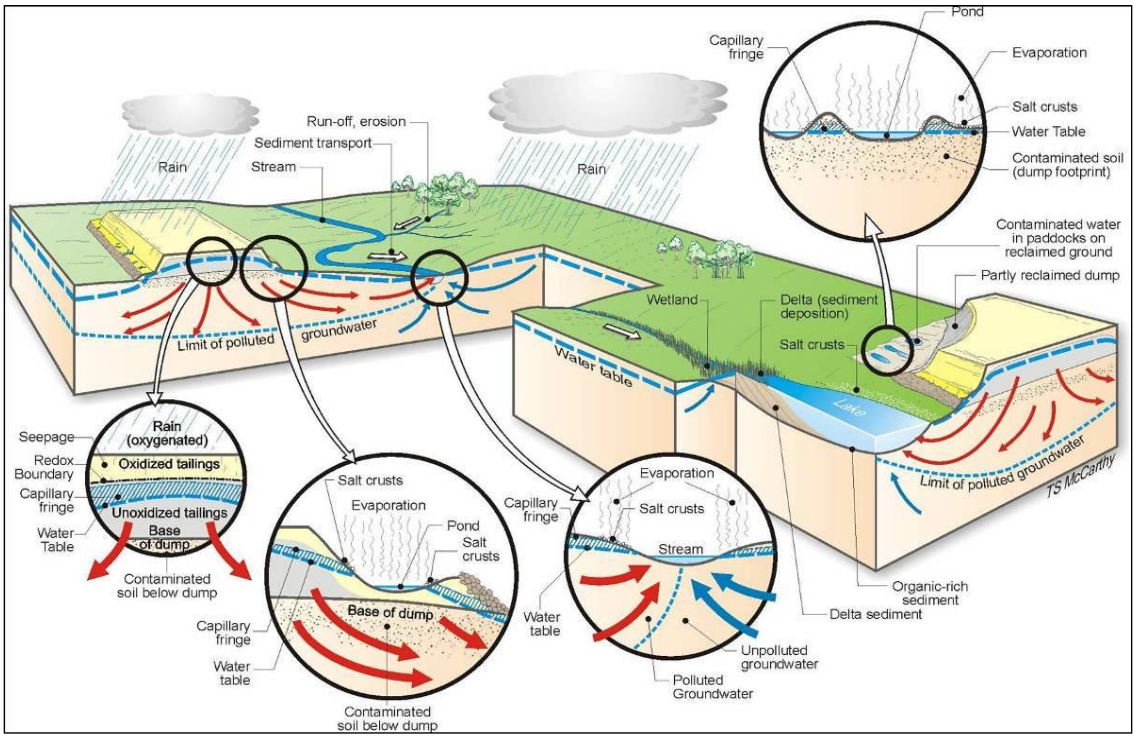

Figure 1.2 A conceptual model of acid rock drainage in the Witwatersrand region (Tutu *et al.*, 2008a)

1.2 Mine pollution remediation

Mine reclamation objectives are summarised under the following three broad categories (Brodie *et al*., 1992):

1. Physical Stability – There should be no hazard to public health and safety.
2. Chemical Stability – No chemicals should be released.
3. Land use and aesthetics – The appearance of the site should be compatible with surrounding lands.

Each of these objectives is important when considering the best fit remediation options.

Acid rock drainage remediation options can be divided into two broad categories, (i) source control options and (ii) migration control options (Johnson, 2005). Source control options of remediation are based on the concept of 'prevention is better than cure', while migration control involves minimising the impact of pollution of acidic mine water.

The source control remediation options are more desirable; however they are not always the most practical option. Figure 1.3 (Johnson, 2005) shows the summary of the source control remediation options.

Most of the source control options are based on reaction (1) above; just as water and oxygen are needed for acid rock drainage formation, so the exclusion of oxygen or water would prevent the oxidation of pyrite. In general due to the difficulty of implementing these source controls, migration controls are more favoured.

Migration controls for remediation can be subdivided into biological and non-biological activities and each of these can be further divided into 'active' and 'passive' processes

(Johnson, 2005). Active processes involve the application of chemicals to neutralise the acidic mine drainage waters, like alkaline solutions. Passive processes involve the use of wetlands, whether natural or man-made. These are summarised in Figure 1.4 (Johnson, 2005).

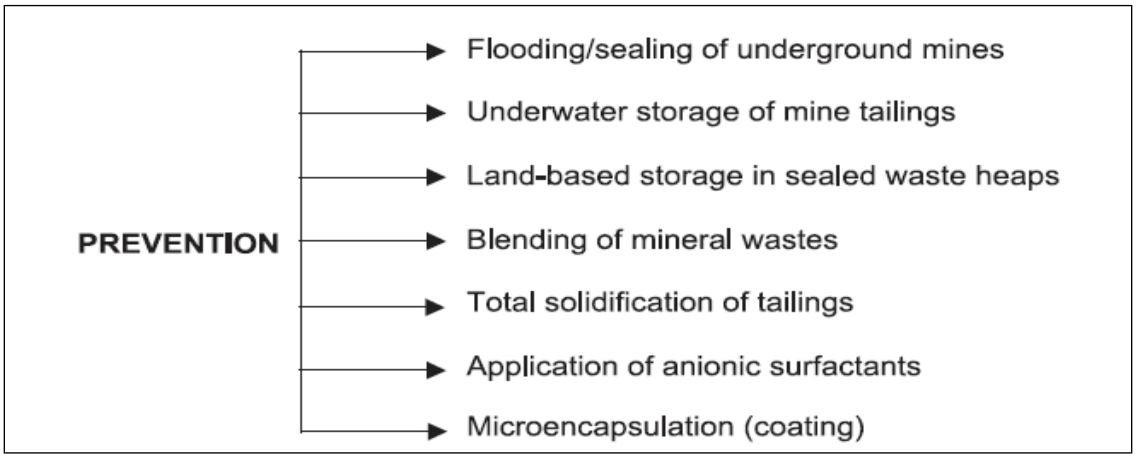

Figure 1.3 Source control options to minimise or prevent the generation of acid rock drainage (Johnson, 2005)

Deciding on which option is more suitable depends on a number of factors. One study (Steffen, 1986) involved the consideration of the following factors:

- How practical it is to implement
- The life expectancy of the remediation option
- Risk of failure
- Environmental impacts on implementation
- Duration and complexity of construction
- Maintenance requirements
- Effectiveness in reducing acid rock drainage

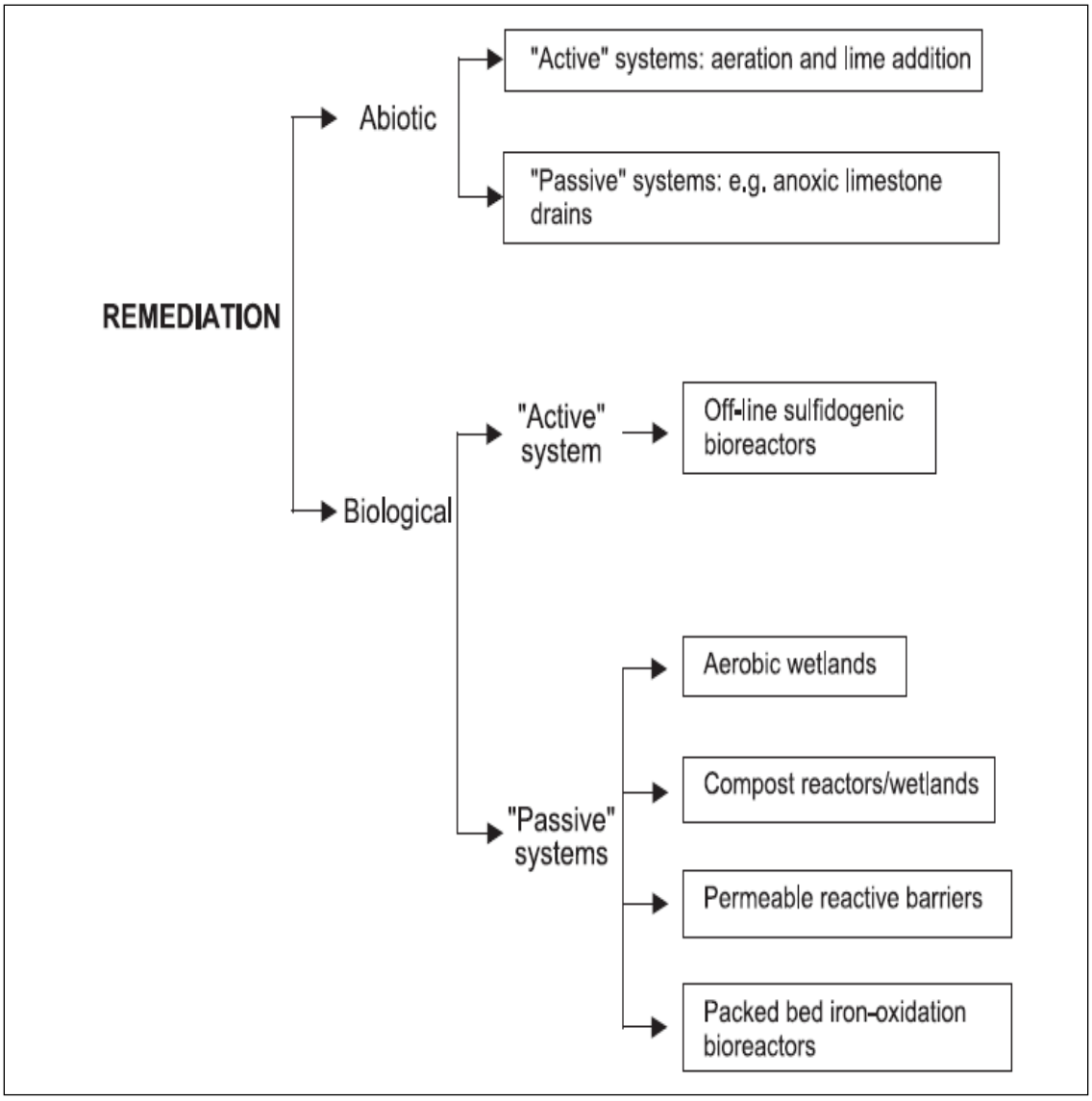

Figure 1.4 Migration control options to remediate acid rock drainage waters (Johnson, 2005)

Encompassing all these factors is the question of sustainability of the remediation system. Sustainable development is about finding a balance between the protection of human health and safety, and the natural environment, encompassing both sustained economic activity and growth (Brodie *et al.*, 1992). This concept of sustainable development is enforced in South African legislation and environmental legislation by the Constitution under Section 24 and by the National Environmental Management Act

(NEMA) (Act No 107 of 1998). Thus sustainable development should be the most critical factor in determining which remediation option is most favourable, as acid rock drainage is a form of pollution that will continue to pose a threat for many years to come (Johnson, 2005).

CHAPTER TWO - LITERATURE REVIEW

The first part of this chapter describes chemical speciation and how elements exist in the environment. The second part of the chapter describes the phytoremediation properties of certain plants, their ability to hyperaccumulate metals in their tissue, and a description of the technologies available.

2.1 Chemical speciation and metal mobility

Chemical speciation is the tendency of elements to exist in various forms in an environment, and that they can be transformed from one form into another or exist in different forms depending on the governing conditions (Martinez-Sanchez *et al.*, 2008). These conditions include the amount of organic matter, moisture content, cation exchange capacity, temperature, salinity and bacterial transformations, and also to a greater extent the pH, and Eh; oxidation-reduction potential.

The oxidation-reduction potential is the tendency of ions to acquire electrons. This value is more positive for oxidising ions and more negative for reducing ions (Symons *et al.*, 2000). The electron activity depends on pH, thus Eh vs. pH diagrams are useful in representing the range of elemental species, from soluble to insoluble, and species stability under varying conditions.

Figure 2.1 shows an Eh-pH diagram for Uranium speciation in high sulphate acid mine surface water (Tutu *et al.*, 2008b). The shaded regions show the species which are soluble, while the lighter regions show the species which are solid, and can precipitate out. Thus Eh-pH diagrams are useful in determining the mobility and bioavailability of

elements depending on the pH, thus predictions can be made as to the metals that could leach into groundwater due to acid rock drainage.

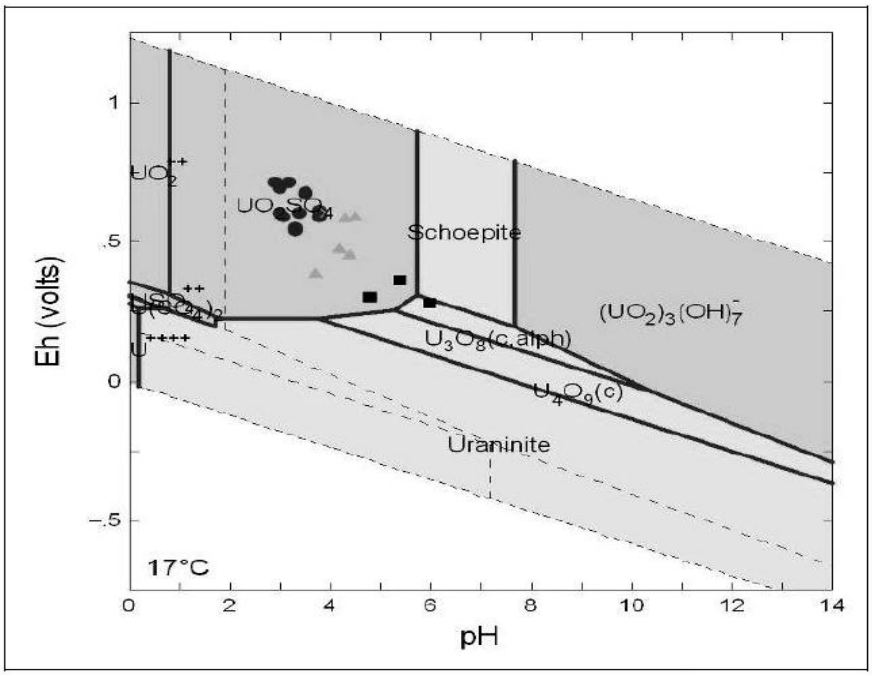

Figure 2.1 Eh-pH diagram for Uranium species in high sulphate acid mine surface water (Tutu *et al.*, 2008b)

2.2 Phytoremediation and metal hyperaccumulation in plants

Phytoremediation involves using plants and soil micro flora as well as non-living biomass to improve the quality of a substrate (Weiersbye, 2008). Although the term “phytoremediation” is not new, the concept of using plants has been around for a long time. By the end of the first century, *Thlaspi caerulescens* and *Viola calaminaria* were the first plants recognised for their ability to accumulate high levels of metals in their leaves (Baumann, 1885). The idea of using plants to extract metals from contaminated soil was first introduced by Chaney (1983).

Prasad *et al.* in 2003 described four different phytoremediation plant-based technologies, namely:

1. Rhizofiltration – This mechanism is used for water treatment. Plants are raised with their roots in water, and are then applied to contaminated waters. The plants absorb contaminants in their roots. Once the roots become saturated, they are then harvested and disposed of as hazardous waste.

2. Phytostabilization – This process involves the use of plants to stabilize rather than degrade contaminants. Plants immobilize contaminants by physical and chemical means, by root sorption and chemical fixation, in the soil.

3. Phytovolatilisation – In this technology plants take up contaminants from soil and release them into the atmosphere by volatilization. Plants absorb elemental forms of contaminants from the soil and biologically convert them to gaseous forms within the plant, and release them into the atmosphere by evapotranspiration.

4. Phytoextraction/ Phytoaccumulation – In Phytoextraction contaminants are absorbed from soil and are then stored and accumulated in aerial shoots, which can then later be harvested and disposed of. Plants are planted and cultivated in contaminated soils. These plants absorb contaminant elements from the soil and these are then translocated to above ground shoots where they accumulate. If metal availability is not sufficient for absorption by plants, chelating agents can be added to aide absorption. Once metal accumulation and plant growth is sufficient, then all above ground shoots and leaves are harvested, removed and disposed of as hazardous waste.

The PHYTO-3 document (ITRC, 2009) instead describes 6 major mechanisms associated with phytotechnologies. The difference between phytotechnologies and phytoremediation is that phytotechnologies involve containment in addition to phytoremediation strategies (ITRC, 2009). The six mechanisms associated with phytotechnologies are as follows (ITRC, 2009):

1. Phytosequestration – Also known as phytostabilisation, in Prasad et al.'s (2003) description above.

2. Rhizodegradation – This process involves the breakdown of a contaminant by increasing the bioactivity around the roots, which allows for the stimulation of microbial populations. The contaminants can be converted into harmless products, which can be converted into sources of food and energy for plants and soil organisms.

3. Phytohydraulics – In this technology plants take up surface- and ground-water and evapotranspire the water through the plant. The horizontal migration of groundwater can be contained and controlled using deep-rooted plants. This will limit the contamination of groundwater through the evapotranspiration by plants.

4. Phytoextraction – As described above by Prasad *et al.* (2003).

5. Phytodegradation/Phytotransformation – In phytodegradation contaminants taken up into the plant are subjected to biological processes in the plant, by internal enzymatic processes and metabolic processes, and the contaminant is subsequently broken down, mineralised or metabolised. This occurs either by plant enzymatic activity or by photosynthetic oxidation.

6. Phytovolatilisation – As described by Prasad *et al.* (2003) above.

The most applicable technology will depend on the specific site conditions, such as the contaminant matrix, the contaminated media, and also the clean-up goals, i.e. remediation and/or containment (ITRC, 2009).

Plants naturally take up metals from soil and water, as most of these elements act as macro- and micro-nutrients essential for growth. Most plants suffer toxicity effects when exposed to concentrations lower than what would be required for efficient phytoremediation of contaminants (Terry *et al.*, 2003) Metal hyperaccumulators on the

other hand are plant species that are capable of accumulating high concentrations of metals and metalloids in their tissues (Soriano *et al.*, 2003), thus making them highly applicable for mine remediation purposes, where metal concentrations can be very high. Metal hyperaccumulators are formally defined as species having a bio-concentration factor greater than 1, i.e. concentration of contaminant within plant can be greater than the concentration in the surrounding environment (McGrath *et al.*, 2003) Threshold limits for plant hyperaccumulation have been set by Reeves and Baker (2000) as 10000 mg kg^{-1} (1%) Zn, 100 mg kg^{-1} (0.01%) Cd and 1000 mg kg^{-1} (0.1%) Pb for shoot dry weight (Reeves and Baker, 2000).

Phytoremediation technologies are viable methods of cleaning large areas of soil, as it is cheaper per unit area and it may be an effective alternative to other soil clean-up methods (Salido *et al.*, 2003). It is an ecological technology and offers simultaneous decontamination and rehabilitation, while maintaining biodiversity (Rodriguez *et al.*, 2003; Weiersbye, 2007; Prasad *et al.*, 2003). In the USA the costs of non-biological treatments are in the range of US$ 100000 – US$ 2000000 per hectare of soil and <US$ 1 – US$ 300 per Kilo-litre of water. Biological or phytoremediation treatments however are much cheaper in the range of US$ 200 – US$ 100000 per hectare of soil and US$ 0.02 and US$ 40 per Kilo-litre of water (Weiersbye, 2007). Prices are even lower in Africa.

Apart from being cheaper phytoremediation has other advantages. Phytoremediation is more publicly acceptable and aesthetically pleasing. Also it can reduce the total volume and mass of waste to as low as 1% of the original contaminated soil (Salido *et al.*, 2003). Phytoremediation also has its disadvantages with the main limitation being that it is a lengthy process, with slow growth rates (Terry *et al.*, 2003).

CHAPTER THREE - MOTIVATION

This chapter describes the aims and objectives of this research report. The proposed hypotheses that were expected from this research are also presented.

3.1 Aims and objectives

The aim of this project was as follows:

- To assess whether two species of trees, with contrasting sulphur requirements, have the potential to remediate acid rock drainage through modifying the physical and chemical properties of the substrate, in particular the mobility of elements.

The objectives of the project were as follows:

1. To compare the physical and chemical properties of the substrata under woodland (two tree species with contrasting sulphur nutrition requirements) versus adjacent non-woodland (grassland) treatments. Two soil types (on two mining sites) were studied.
2. To assess if either of the tree species show potential for remediation of acid rock drainage-impacted substrata.
3. To assess the differences between the two sites, and between the tree species.

3.2 Hypotheses

It is expected that trees planted on ARD-polluted substrata will change the concentrations, and mobility, of major nutrients, metals and metalloids in their rooting substrate due to:

a) Hydraulic effects due to tree water-use could increase the concentration of some ions in the root zone,

b) Uptake of nutrient ions by trees could remove them from the soil solution,

c) Drying effects could result in changes in moisture content and precipitation of minerals with varying solubility,

d) The acquisition of ions from the substrata by roots and shoots and recycling to the top soil (though litter from falling leaves) could result in ion removal from the sub-soil and lead to their enrichment in the top soil.

Through some or all of these mechanisms, trees would be expected to reduce the impacts of ARD on deeper groundwater, as leaching of sulphate and metals from the soil is less likely to occur.

CHAPTER FOUR - ANALYTICAL TECHNIQUES

The chapter describes the analytical techniques that were used in this research project. It describes the theory behind the techniques, the process involved in each and the instrumentation.

4.1 Inductively coupled plasma – Optical emission spectroscopy (ICP-OES)

Inductively coupled plasma – optical emission spectroscopy is also known as inductively coupled plasma – atomic emission spectroscopy. In atomic spectroscopy concentrations of atoms are measured based on the emission or adsorption of characteristic wavelengths of radiation (Harris, 2002). It is considered to be one of the most important tools in analytical chemistry as it is highly sensitive; it easily differentiates between elements in a complex matrix, it can perform several element analyses concurrently, and it easily analyses samples automatically. In atomic spectroscopy, the analyte is usually atomised in a flame, a furnace, or plasma (Harris, 2002). Emission spectroscopy uses an inductively coupled plasma. A plasma is a hot gas containing ions and free electrons. Inductively coupled plasmas have the advantage that there is little interference due to the stable, high temperature, inert argon environment associated with it. These conditions make ICP–AES highly favourable for simultaneous multi-element analysis, even though it costs more to purchase and operate than instruments that use flames for atomisation.

The atomic emission process is shown in the schematic in Figure 4.1. A liquid sample is injected into the spectrometer; where it is nebulized into an aerosol. This aerosol is fed into an inductively coupled plasma where it is vaporised at 6000 – 8000 K. The molecules within the sample dissociate into atoms. These atoms are excited and

partially ionized, and emit an elementary specific radiation. This radiation is fed through transfer optics, into an optical system, where the radiation is diffracted into its spectral components. The intensity of the components is measured using semi-charge conductor detectors (CCD). The measured element intensities are processed in the unit, and evaluated by the smart analyser software. The methods on the software are set-up prior to measuring, and have elemental calibration functions stored within. These methods calculate the concentrations from the spectral intensities and results are reported in concentrations.

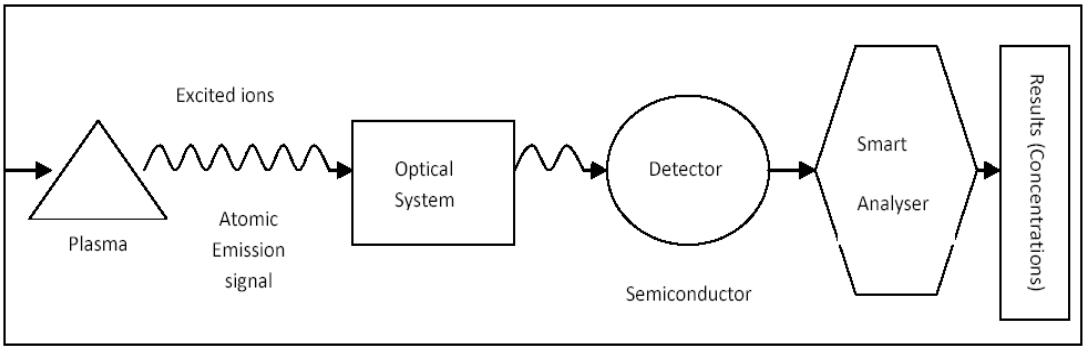

Figure 4.1 Schematic diagrams representing the atomic emission process

4.2 Carbon, hydrogen, nitrogen and sulphur elemental analysis (CHNS)

Commercial CHNS analysers allow for the rapid determination of the major elements i.e. carbon, hydrogen, nitrogen and sulphur, in organic substances (Fadeeva *et al.*, 2008). CHNS analysers are constructed in modular sections, such that different configurations can be set-up for different applications, e.g. CHN, CHNS, CNS, or N analysis (Thompson, 2008).

CHNS analysis involves oxidative combustion at high temperatures. Combustion takes place at a temperature of 1000ºC, with the conversion of carbon to carbon dioxide,

hydrogen to water, nitrogen to nitrogen gas or an oxide of nitrogen, and sulphur to sulphur dioxide (Thompson, 2008). Other elements present are also converted to combustion products; however these are removed by a variety of adsorbents (Thompson, 2008). The combustion products are carried out of the chamber by an inert gas, e.g. helium, and carried over high purity, heated copper, which acts to remove any excess oxygen not consumed during combustion (Thompson, 2008). The gases are then further passed through adsorbent traps, to remove any unwanted combustion products, and leave only carbon dioxide, water, nitrogen and sulphur dioxide (Thompson, 2008).

CHNS instrumentation requires 2 gas supplies, firstly an inert carrier gas, and secondly a high purity oxygen (minimum 99.9995% purity) (Thompson, 2008). The sample introduction system is dependent on the application for which it will be used and the type of samples which will be introduced, solids are weighed out in tin capsules, while liquids can be sealed in individual aluminium sample vials, and can be introduced via an auto-sampler (Thompson, 2008).

The combustion section allows for both complete combustion of the sample, as well as the conversion of nitrogen oxides to nitrogen gas (Thompson, 2008). Copper is most commonly used in the reduction stage, for the removal of excess oxygen; the oxidation and reduction can be housed in a single furnace, while in other cases it can be housed in two separate furnaces (Thompson, 2008). Catalysts and absorbents are also added at times, to aid combustion and remove potential contaminants (Thompson, 2008).

Instruments can either be described as static or dynamic based on the combustion conditions, and introduction of oxygen into the chamber (Thompson, 2008). Static conditions involves the introduction of a set volume of oxygen into the chamber before the sample is introduced, while dynamic conditions involves the oxygen is introduced with the sample, and continues to flow (Thompson, 2008).

Detection of the combustion gases are carried out by either using a) GC separation, with thermal conductivity detection; b) partial GC separation with thermal conductivity detection; or c) a series of IR and thermal conductivity cells for detection (Thompson, 2008). The entire instrument is usually controlled through a computer program, which allows for control of set-up, instrument calibration, monitor the instrument, sample introduction and data collection.

4.3 X-ray fluorescence spectroscopy (XRF)

The underlying principle in X-ray methods is that when an atom is excited by a source of radiation, electrons are removed from the inner shell; the atom usually returns to its normal state by transferring an electron from one of the outer shells to the vacancy in the inner shell, with the resultant emission of energy as X-rays, i.e. photons characteristic of high energy and short wavelengths (Willard *et al.*, 1981). The X-ray emission wavelengths are related by Moseley's law to the atomic number of the atom (Jenkins, 2000). A series of wavelengths, each representative of an atom, is produced for a sample made up of different atoms, making up the total X-ray emission of the sample (Jenkins, 2000). The intensity of the wavelengths is proportional to the number of excited atoms in the sample (Willard *et al.*, 1981), giving an indication of the respective concentrations.

X-ray fluorescence (XRF) spectrometry involves the irradiation of a sample with X-rays of a shorter wavelength (Willard *et al.*, 1981). Upon being excited, electrons are removed from the inner shell of an atom, and are later replaced by electrons from the outer shell, with the emission of fluorescent X-rays. The intensity of the fluorescent X-rays are of a much lower intensity than the X-rays obtained by direct excitation with a beam of electrons (Willard *et al.*, 1981).

All conventional X-ray spectrometers comprise of 3 basic parts: The primary source unit, the spectrometer itself and the detector (Jenkins, 2000). The primary source unit needs to be a very stable, high voltage generator (Jenkins, 2000), usually an X-ray tube. An X-ray tube is a large vacuum tube, which consists of a cathode, which emits electrons, and an anode, which captures electrons, through a high voltage field, resulting in a continuous flow of electrons in the tube. The electrons transfer energy to the atoms of the material in the anode; some of this energy is emitted as a continuous spectrum of X-rays which cover a broad wavelength range (Willard *et al.*, 1981).

There are two types of spectrometers used in XRF analysis, wavelength dispersive- or energy dispersive spectrometers. Wavelength dispersive spectrometers make use of an analysing crystal, where specific wavelengths of X-rays are diffracted onto the detector (Jenkins, 2000). The angle between the sample and the crystal, and the crystal and the detector needs to be kept the same (Jenkins, 2000). Energy dispersive spectrometers on the other hand have no analysing crystal, and X-rays are focused directly onto the detector (Willard *et al.*, 1981; Jenkins, 2000). Figure 4.2 shows a schematic of the setup of an energy dispersive spectrometer (Khalid *et al.*, 2011).

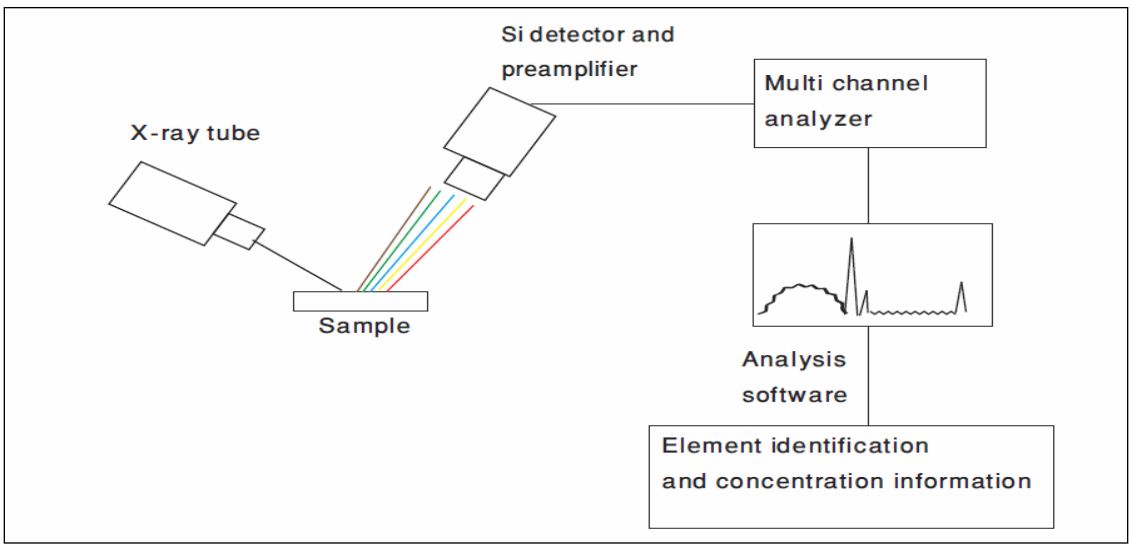

Figure 4.2 A schematic diagram of the setup of an energy dispersive spectrometer (Khalid *et al.*, 2011)

Lastly the X-ray detector transforms X-ray photon energy into voltage pulses (Jenkins, 2000). This is done by the production of electrons, resulting from the entering X-rays photon energy and their interaction with the active detector material (Jenkins, 2000). These electrons produce a current, which is converted to a voltage pulse, by a capacitor and a resistor (Jenkins, 2000). One voltage pulse is produced for each X-ray photon that enters (Jenkins, 2000). The most common detectors used are the semiconductor detectors (Khalid *et al.*, 2011).

CHAPTER FIVE - METHODOLOGY

Chapter five describes in detail the experimental design, sample collection and preparation, laboratory analysis, and statistical analysis that was used. Firstly, the chapter describes the study area, the tree species that were used, and the factorial experimental design. Secondly the chapter goes into detail on how the samples were taken, and how the samples were prepared. Then the physical and chemical analyses; and the methods, which were performed on the samples, are explained, including the description of the certified reference material. Lastly the statistical analysis that was performed on the data is described.

5.1 Experimental design

The experimental design describes the study area, the tree species, i.e. *Rhus lancea* and *Tamarix usneoides*, and expands on the experimental design in terms of the number of factors.

5.1.1 The study area

The woodland trials were conducted on two tailings storage facilities (TSFs) located at two mining sites in the western part of the Witwatersrand Basin, namely at the Vaal River West Complex (VRWC) and the Vaal River Mispah (VRMP). This area is characterised by natural soils and 560 mm per annum of rainfall. Figure 5.1 shows the woodland trial locations within the Witwatersrand Basin.

The Anglo Gold Ashanti Ltd (AGA) - Vaal River mining operation consists of an area of approximately 12 000 hectares and is located on the northern and southern side of the Vaal River (Wanenge, 2009). This area has polluted ground water due to the occurrence of acid rock drainage from the TSF's.

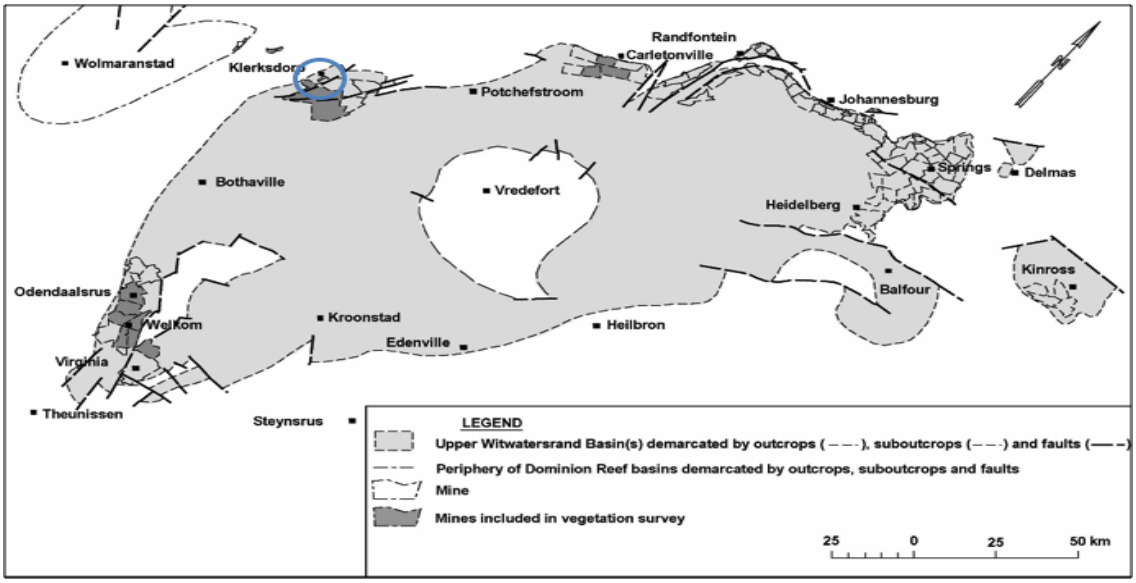

Figure 5.1 Location of the trials within the Witwatersrand Basin

The West Complex (VRWC) TSF has dolomitic, high clay soils, has an effective rooting zone of 0.5 to 1.5 metres and the depth to polluted groundwater is 0.6 to 0.8 metres (Wanenge, 2009). Mispah (VRMP) TSF is characterised by well-drained, sandy, red Hutton soil, has an effective rooting zone of 3.5 metres to 4 metres, and the depth to polluted groundwater is 5 to 6 metres (Wanenge, 2009). Figure 5.2 shows the Vaal River mining operation and the location of the two TSF's. Figures 5.3 and 5.4 show the layout of the woodland trials at VRWC TSF and VRMP TSF respectively.

Figures 5.5 and 5.6 show the groundwater plumes, in terms of the total dissolved solids (TDS) at the VRWC and VRMP TSF's respectively (AGA, 2007). The areas highlighted in red are the TSF's. At VRWC TSF the pollutants leach towards the Vaal River Basin,

as seen by the concentration of the TDS. The dark red areas show areas of salt accumulation. Pollutants from the VRMP TSF also leach towards the Vaal River Basin, however these sites are much younger, and thus the TDS values are less than those for VRWC.

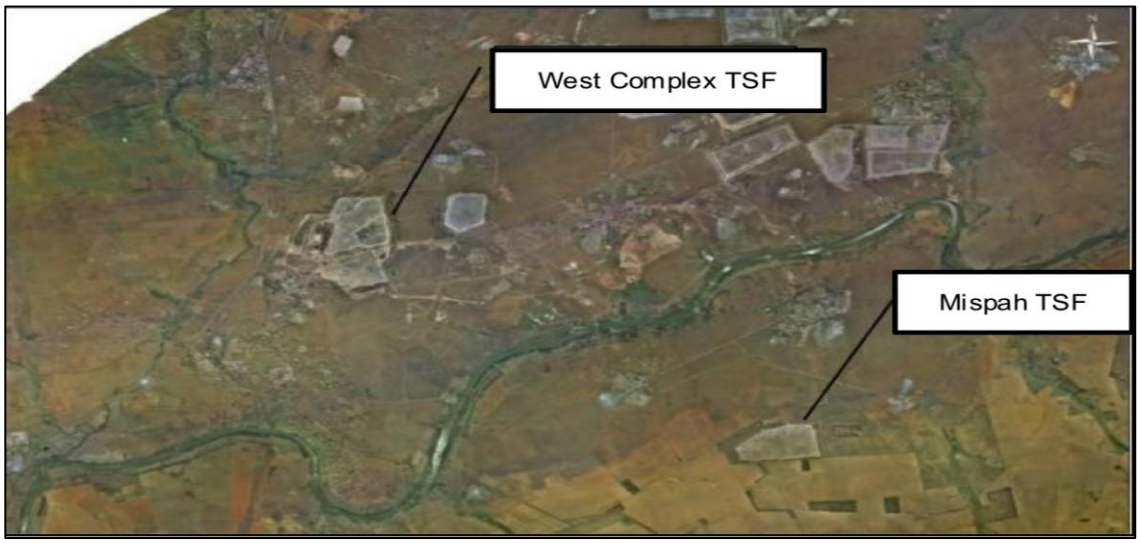

Figure 5.2 An aerial photo of the Vaal River mining operation near Klerksdorp

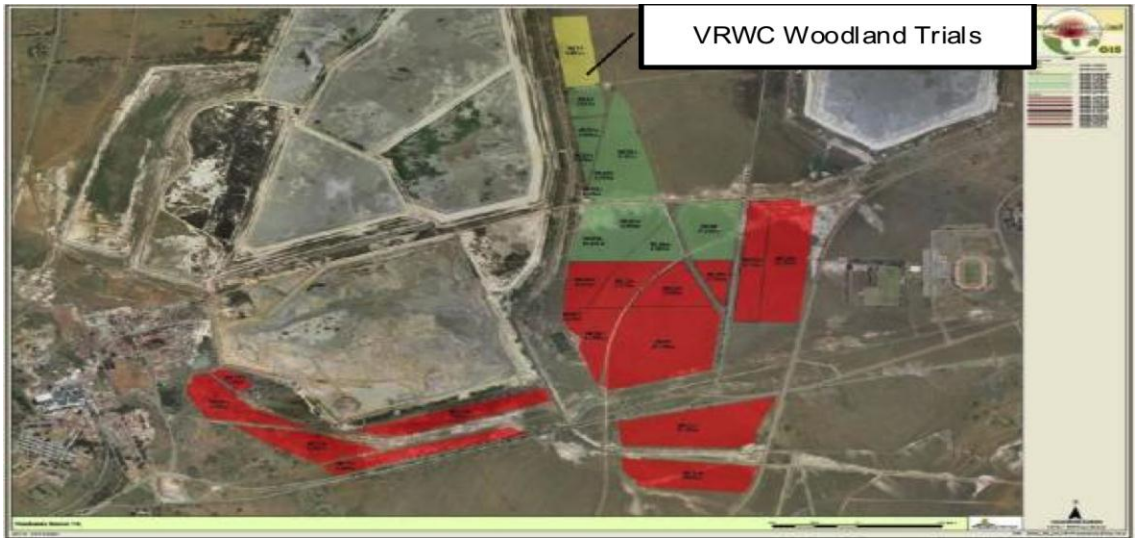

Figure 5.3 The layout of the woodland trials at the Vaal River West Complex site

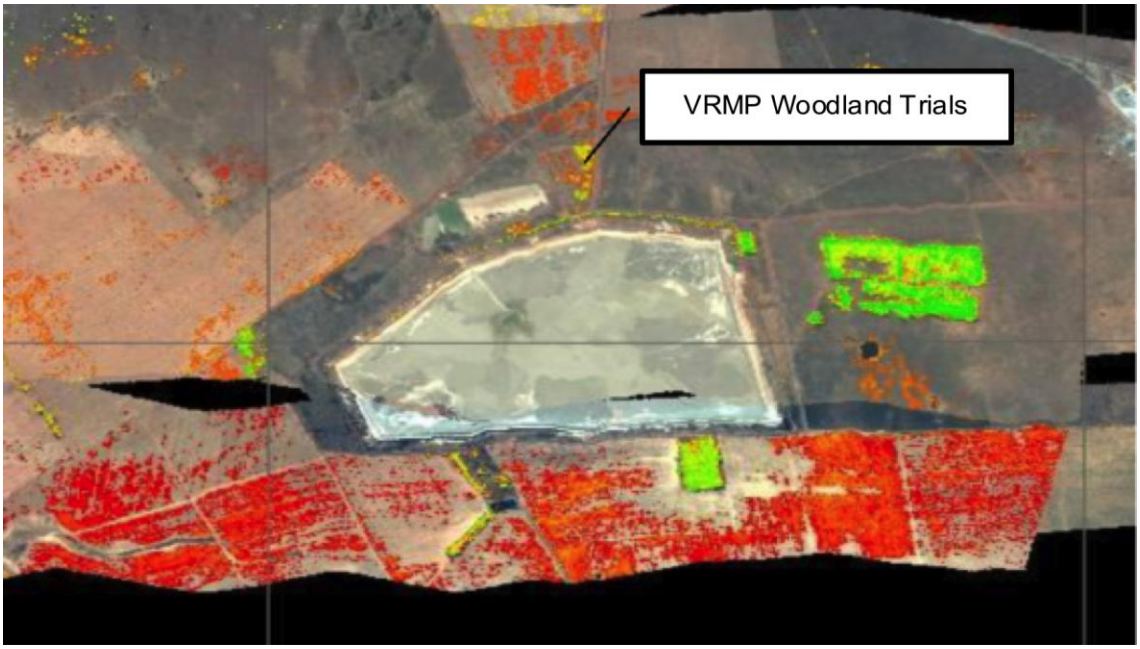

Figure 5.4 The layout of the woodland trials at the Vaal River Mispah site

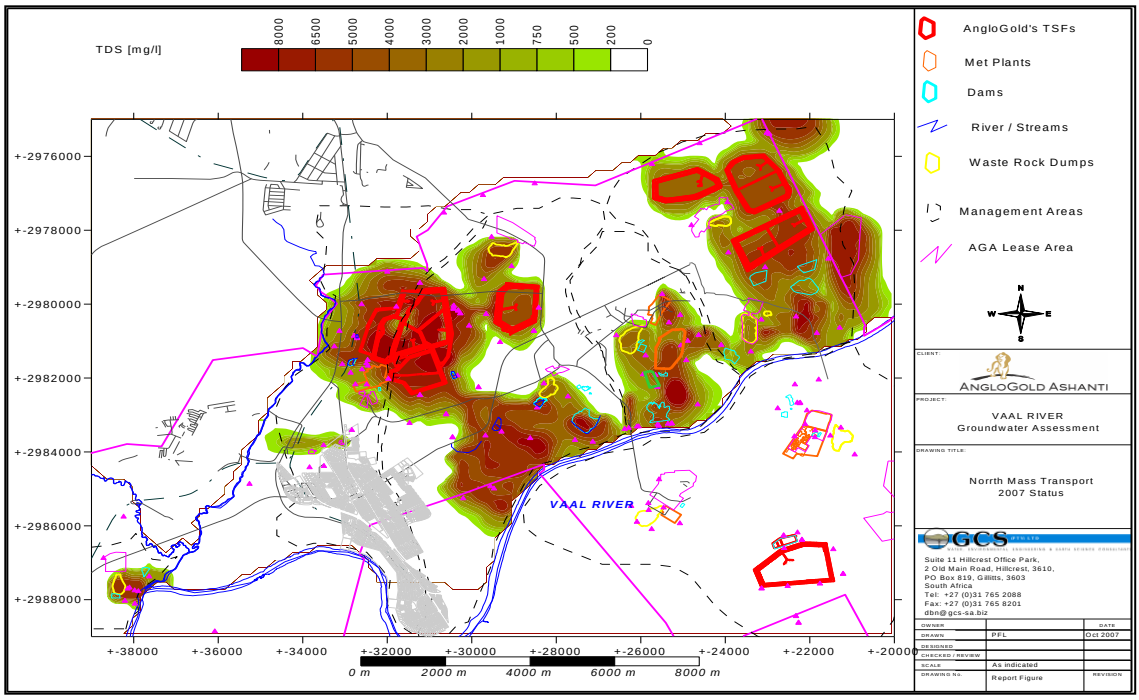

Figure 5.5 Groundwater plumes at the VRWC TSF (AGA, 2007)

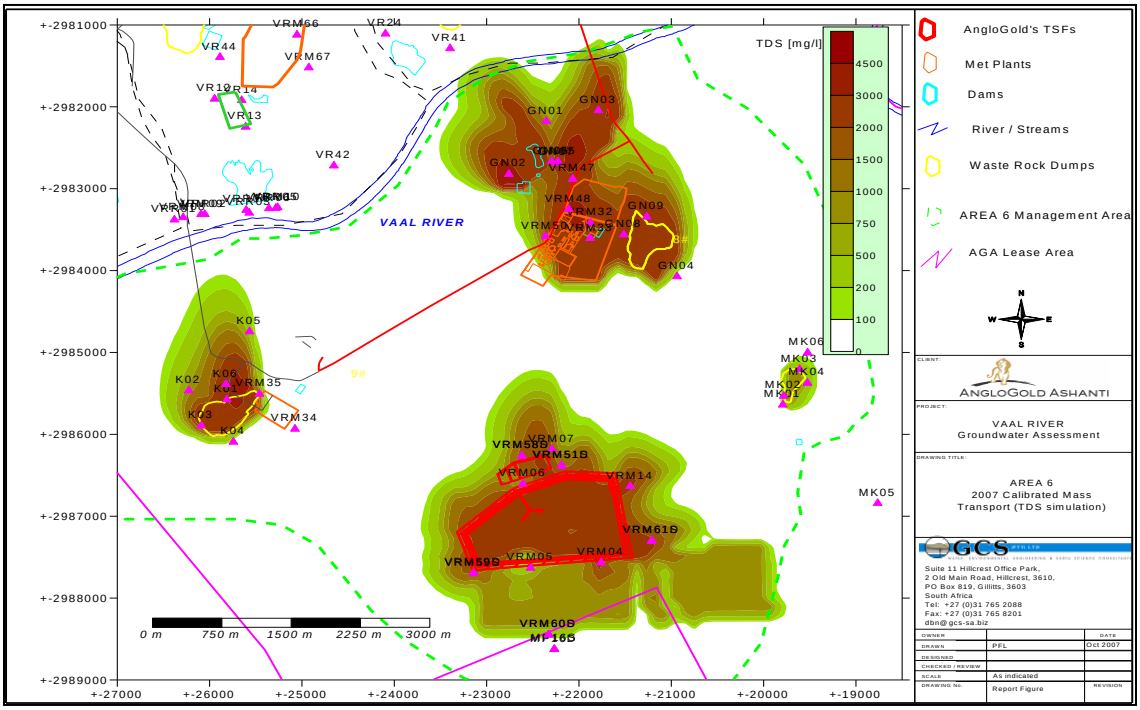

Figure 5.6 Groundwater plumes at the VRMP TSF (AGA, 2007)

5.1.2 The tree species

Two indigenous tree species planted at the mine site were studied. Samples were taken in the rooting zones of these tree species. The first tree species was *Rhus lancea* (*Searsia lancea*) also known as the Karee Boom, and the second species was *Tamarix usneoides*, which is commonly called the Salt Cedar. Both tree species were 4 years old when the samples were taken.

Species description of Rhus lancea

Rhus lancea trees are indigenous and evergreen, calcicole species, which have a high leaf index all year round (Wanenge, 2009). These trees are characterised by high water use, of approximately 1100 mm (Dye *et al*, 2008). They have a dense root mat for microbial activity, binding and/or the uptake of metals. It is highly tolerant to

competition from adjacent trees, and has been shown to be highly tolerant to ARD and salinity (Weiersbye and Witkowski, 2007). Lastly, it is able to accumulate high concentrations of sulphur in its leaves, or approximately 1.46 – 2.83% compared to 0.1 – 0.5% for other plants (Wanenge, 2009). Figure 5.7 shows a picture of 4-year old *Rhus lancea* trees at the VRWC.

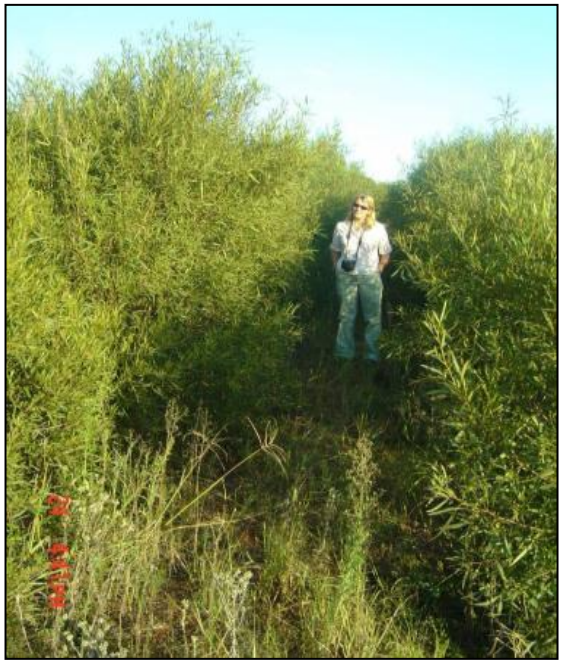

Figure 5.7 A photo of 4-year old *Rhus lancea* trees at the VRWC

Species description of Tamarix usneoides

Tamarix usneoides is a halophyte and a salt hyper-accumulator (Weiersbye *et al*, 2006; Weiersbye, 2008). Plant hyperaccumulators have been defined as having the following threshold limits for shoot dry weight: 10000 mg kg^{-1} (1%) Zn, 100 mg kg^{-1} (0.01%) Cd and 1000 mg kg^{-1} (0.1%) Pb (Reeves and Baker, 2000). It has been found to hyper-accumulate NaCl, sulphate and other halogens (Weiersbye and Witkowski, 2007). Figure 5.8 shows a picture of 4-year old *Tamarix usneoides* species at the VRMB.

Figure 5.8 A photo of 4-year old *Tamarix usneoides* trees at the VRMB

Salts taken up in the roots are translocated to the shoots and excreted by foliar glands as gypsum ($CaSO_4$), which has low solubility and is chemically non-toxic. The total sulphur shoot content can be up to 30% of the dry mass leaves. Figure 5.9 shows a scanning electron micrograph of salt crystals on *Tamarix usneoides* foliar salt glands (Weiersbye, unpublished).

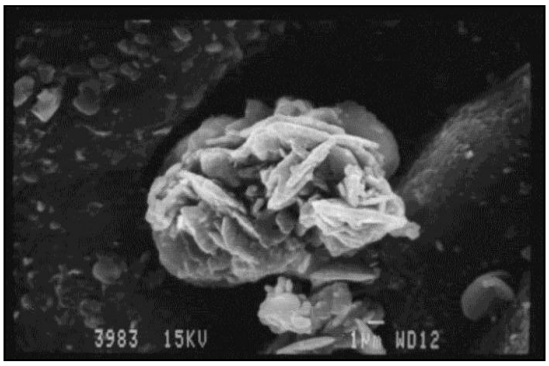

Figure 5.9 A scanning electron micrograph of salt crystals on *Tamarix* usneoides foliar glands (Weiersbye, unpublished)

Differences between species

Due to varying characteristics between the two species, we can expect differences in:

- Soil preferences,
- Physical-chemical properties (pH, Eh, EC),
- Total elemental concentrations (C, N, H, S),
- Soil organic carbon concentrations,
- Soil solution chemistry, of major nutrients: Calcium (Ca), magnesium (Mg), phosphorous (P), potassium (K), and sulphur (S), and trace elements: Aluminium (Al), arsenic (As), chromium (Cr), copper (Cu), iron (Fe), lead (Pb), manganese (Mn), mercury (Hg), nickel (Ni), titanium (Ti), uranium (U), vanadium (V) and zinc (Zn).

5.1.3 Experimental design

The experimental design is as follows for the soil core samples:

1. 2 sites: VRWC and VRMP. The mine areas are combined as the sites are within the same geographical location, hence are characterised by the same soil genesis and classification, climate and amount of rainfall.
2. 2 treatments: (+) woodland vs. (-) grassland treatment substrates at the two mining sites.
3. 2 species: *Rhus lancea* and *Tamarix usneoides* tree species at the two mining sites.
4. Depths: 0-10 cm, 10-20 cm, 20-30 cm at the VRWC site; 0-10 cm, 10-20 cm, 20-30 cm, 30-40 cm, 40-50 cm at the VRMP site.
5. 3 BCR Sequential extraction steps: 1 – represents ions bound to carbonates, 2 – represents ions bound to oxides, and 3 – represents ions bound to organics.

5.2 Sample collection

Samples were taken in the dry season in the May – August 2009 period, as rain could have caused leaching and dilution of salt and metal concentrations.

Core soil samples were taken under the two different tree species – (1) *Rhus lancea* (*Searsia lancea*, Karee Boom) and (2) *Tamarix usneoides* (Salt Cedar), within 30 cm distance of the stem of the tree, to the maximum possible depth, at both sites. Control core soil samples were taken from non-woodland substrates, i.e. under grass, within 50 m of the tree species, within the same soil and geology, around the same time as the tree soil cores. Figure 5.10 shows how the soil core samples were collected.

Figure 5.10 A photo showing how the soil core samples were collected in the rooting zone (The plant in the photo is *Rhus lancea*)

Core samples from VRWC were approximately 30 cm in depth and split into depths of 0 – 10 cm, 10 – 20 cm, and 20 – 30 cm. Core samples from VRMP were approximately 50 cm in depth, with one sample being 90 cm in depth. The 50 cm samples were split into depths of 0 – 10 cm, 10 – 20 cm, 20 – 30 cm, 30 – 40 cm and 40 – 50 cm, while the 90 cm sample was split into depths of 0 – 10 cm, 10 – 20 cm, 20 – 30 cm, 50 – 60 cm, and 80 – 90 cm.

The total number of soil core samples, including the controls, is shown in Table 5.1. From the total amount of samples, only a subset of replicate samples was extracted by the BCR sequential extraction procedure.

Table 5.1 The total number of soil core samples, i.e. control samples and tree samples, taken at the Vaal River sites

Location	**Soil core sample substrate**	**Number of samples including samples at all depths**
Vaal River West Complex	*Tamarix usneoides* (rooting zone)	9
	Rhus lancea (rooting zone)	9
	Control (degraded grassland)	12
Vaal River Mispah	*Tamarix usneoides* (rooting zone)	15
	Rhus lancea (rooting zone)	15
	Control (degraded grassland)	15
Total Soil Core Samples		75

5.3 Sample preparation

Figures 5.11 and 5.12 show flow diagrams of the sample preparation protocol that was followed. Figure 5.11 explains how fresh soil core samples were treated and prepared

after collection, while Figure 5.12 shows analysis schemes that were done on the soil core samples.

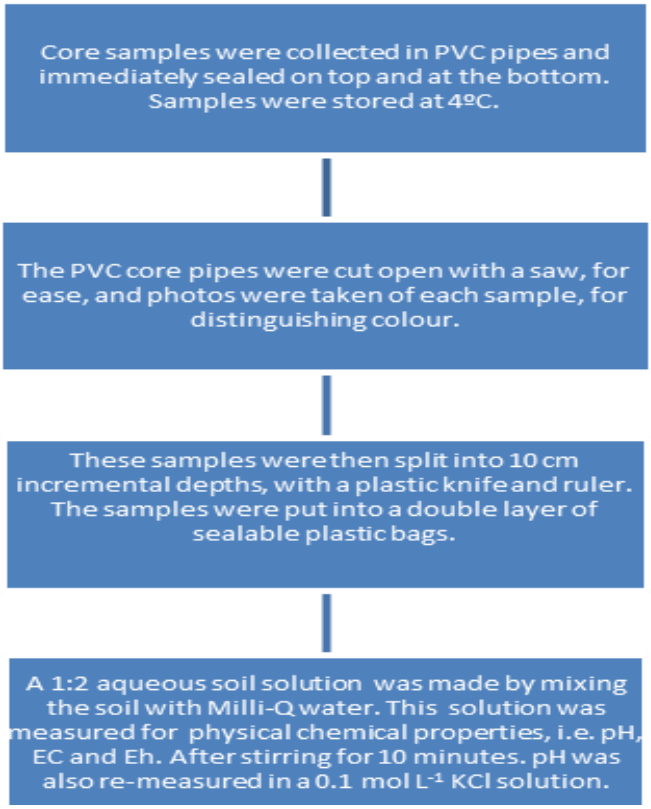

Figure 5.11 A flow diagram showing sample preparation for soil core samples from point of collection

In terms of sample preparation, soil core samples were collected on site in poly vinyl chloride (PVC) pipes and immediately sealed on top and at the bottom with plastic. Samples were then stored at 4ºC. PVC cores were cut open with a saw, for ease of opening. Photos were taken upon opening and samples were split into various depths with a plastic knife and ruler. The samples were then put into double plastic sealable bags. These samples represent soil in the undisturbed state, as the soil was not exposed to light or air before being analysed. Physical-chemical soil solution

measurements for pH, EC and Eh were done on the soil core samples, immediately after they were split.

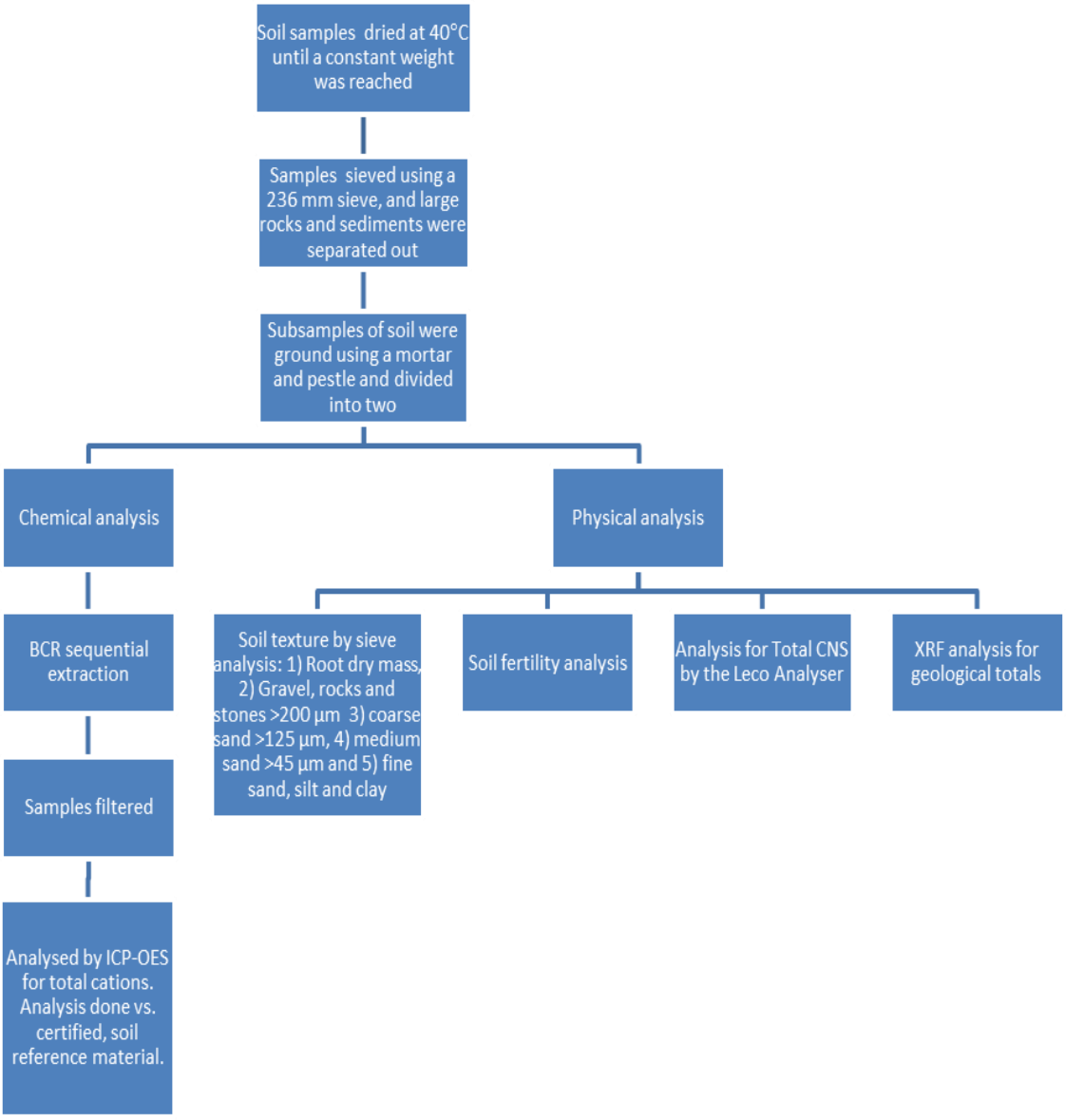

Figure 5.12 A flow diagram showing sample preparation and sample analysis schemes for soil core samples

In terms of analysis the samples were first dried at 40ºC until a constant mass was reached. The fresh mass was noted before drying and the dry mass was noted after constant mass was reached. The sample was then sieved using a 236 mm diameter sand sieve. The large rocks and sediments were separated out and put into separate plastic bags. A subsample of the sieved sample was ground using a mortar and pestle. This sample was then split into two.

The first half of the sample underwent chemical analysis; which involved the BCR sequential extraction procedure. The BCR extracts were filtered and then analysed by ICP-OES for cations. Extractions and analysis was done versus certified soil reference material (CRM).

The second half underwent physical analysis, which included soil texture analysis, which was be done by sieve analysis, soil fertility analysis, carbon, hydrogen, nitrogen and sulphur and lastly, the soil was sent for XRF determination of elemental concentration.

5.4 Analysis of soil samples

The soil analysis included both chemical analysis, and physical analysis. Details of these analyses are described below.

5.4.1 Chemical analysis

Chemical analysis included the initial soil solution measurements; the sequential extraction of the soil using the BCR sequential extraction method, and analysis of the BCR extracts using ICP-OES.

Physical-chemical soil solution measurements (pH, EC, Eh)

An aqueous solution of soil and Milli-Q water was made up in a ratio of 1:2 to make up an aqueous soil saturated paste. This paste was stirred for 10 minutes and measured for the following physical-chemical properties, i.e. pH, electrical conductivity (EC) and redox potential (Eh). The Eh values obtained were not representative of the *in situ* conditions due to disturbances, stirring and the addition of water. It is not possible to measure *in situ* Eh without buried soil probes. The pH was also re-measured in a 0.1 mol L^{-1} KCl solution. This pH is also called the buffer pH, and is used to decrease fluctuation in pH readings (Tan, 2005). The use of KCl decreases the dispersion of soil, and equalizes the salt content of soils; this affects the ionic activity in the soil, which may cause the reading to change considerably (Tan, 2005). In KCl the readings will produce more constant pH values, and usually the buffer pH is lower than the value of pH in water (Tan, 2005).

The Multiline F/Set3 field meter of WTW (Germany) was used to measure the pH and Eh, equipped with a pH cell, Sentix-41, and an oxidation-reduction potential probe, Sentix-ORP. The Windaus Winlab dataline conductivity meter was used to measure the EC, using a standard conductivity electrode. The pH electrode was calibrated using 2 buffer solutions of pH 4 and pH 7, and was checked with a buffer solution of pH 10. The Eh electrode was checked using a standard buffer solution. The conductivity electrode was calibrated using a standard conductivity buffer solution.

BCR sequential leaching procedure

The determination of elemental concentration in soils is often carried out using single or sequential extractions (Tokalioglu *et al.*, 2003). The European Community Bureau of Reference (BCR) devised a three-stage sequential extraction procedure to extract metals from soil or sediment samples (Tokalioglu *et al.*, 2003). The procedure assesses the mobility and potential bioavailability of metals which are readily exchangeable, bound to oxides and are bound to organics (Rauret *et al.*, 2000). The first step involves the liberation of weak acid extractable metals with 0.11 mol L^{-1} acetic

acid; the second step involves the solubilisation of metals associated with the reducible phases by 0.1 mol L^{-1} hydroxylamine hydrochloride and the last step involves the extraction of metals oxidised by 8.8 mol L^{-1} hydrogen peroxide, using 1.0 mol L^{-1} ammonium acetate (Rauret *et al.*, 2000). Table 5.2 shows the BCR sequential extraction scheme with the nominal target phases removed in each step (Rauret *et al.*, 2000). The procedure has shown success in various different matrices (Sahuqillo *et al.*, 1999).

Sequential extraction procedures, such as the BCR sequential extraction procedure (Rauret *et al.*, 2000), are important in the investigation of mobility and environmental toxicity of metals in complex matrices such as soil (Sulkowski *et al.*, 2006). It is accepted practice, that instead of the total concentration, it is rather the mobile fractions removed by sequential extraction procedures that relates to the ecological effects of metals, i.e. bioavailability, eco-toxicology, and risk of ground water contamination (Hlavay *et al.*, 2004).

Generally the most mobile metals are removed in the first fraction, and then continue in order of decreased mobility (Zimmerman *et al.,* 2010). Usually metals coming from anthropogenic sources reside in the first three fractions, while metals of natural sources from parent rock are found in the residual fraction of the sequential extraction procedure (Zimmerman *et al.*, 2010).

Figure 5.13 shows a typical BCR sequential extraction curve for manganese (Mn) in sediments of a mine pan (Cukrowska, Weiersbye and Tutu, 2006). Each curve represents the Mn extractant from each step: BCR 1 represents the Mn ions which are highly available and extracted with acetic acid; BCR 2 represents the Mn ions which are bound to oxides, and extracted with hydroxylamine hydrochloride; BCR 3 represents the Mn ions bound to organics, which were oxidised with hydrogen peroxide and extracted with ammonium acetate; and Total represents the total Mn ions.

Table 5.2 The three stage BCR sequential extraction procedure extraction scheme (Rauret *et al.*, 2000)

Extraction step	**Reagent(s) / Concentration / pH / Reaction conditions**	**Nominal target phases**
1	0.11 mol L^{-1} Acetic acid (CH_3COOH), pH 2.6, 16 hours of shaking	**Exchangeable / acid extractable metals** (Soil solution, carbonates, and sulphates)
2	0.1 mol L^{-1} Hydroxylamine hydrochloride ($NH_2OH.HCl$), pH 2, 16 hours of shaking	**Reducible metals / bound to oxides** (Iron / Manganese oxyhydroxides)
3	8.8 mol L^{-1} Hydrogen peroxide (H_2O_2) then 1.0 mol L^{-1} Ammonium acetate (CH_3COONH_4), pH 2, 16 hours of shaking.	**Oxidisable metals / bound to organic matter** (organic and sulphides)

The fractions investigated in this research was (1) exchangeable, carbonate bound, (2) reducible, Fe- and Mn-oxide bound, (3) organic matter bound, and (4) the residual. The major nutrient and trace metal contents of the three extracts were then determined by inductively coupled plasma – optical emission spectroscopy (ICP-OES) for cations. The total metal concentration was determined using XRF and the residual concentration was determined by subtracting all the other fractions from the total. Sequential extraction does have its limitations as the extracts do not represent *in situ* conditions, however it does provide an estimate to amounts of mobilisable metals and metalloids under various environmental conditions (Tutu, 2005).

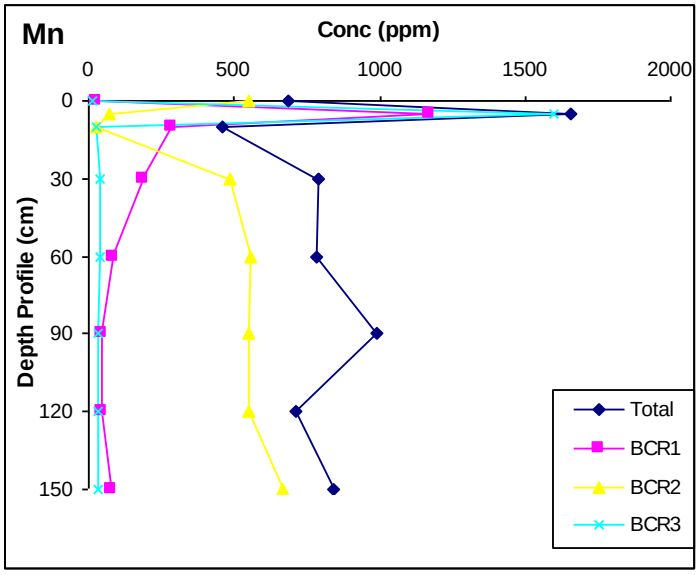

Figure 5.13 A typical BCR sequential extraction curve for Mn in sediments of a mine pan (Cukrowska *et al.*, 2006)

ICP-OES

BCR extracts were filtered and then analysed using the Spectro Genesis end-on-plasma Inductively coupled plasma-Optical emission spectrometer (ICP-OES) for total metal cations. The following major nutrients were analysed: Calcium (Ca), magnesium (Mg), phosphorous (P), potassium (K), and sulphur (S). The following trace elements were analysed: aluminium (Al), arsenic (As), chromium (Cr), copper (Cu), iron (Fe), lead (Pb), manganese (Mn), mercury (Hg), nickel (Ni), titanium (Ti), uranium (U), vanadium (V) and zinc (Zn).

5.4.2 Physical analysis

Physical analysis was done on the original soil samples, after being dried, sieved and ground. These included soil photos to check colour, CHNS analysis, XRF analysis for geochemical totals, soil texture, and soil fertility of the soil samples.

Soil photos

The soil photos were taken right after the soil cores were cut open. The complete set of soil photos is presented in Appendix A. Colour is one of the most obvious characteristics of a soil and is influenced by one of four factors (State of Victoria, 2011):

1. Parent material from which the soil generated – Rocks get broken down to form soil and these rocks can sometimes give colour to the resultant soil.
2. Organic matter – Usually gives a black colour to soil, due to the presence of humus, i.e. the final stage of organic matter breakdown.
3. Iron content – Iron in soil can give a yellow, red or bluish-grey colour depending on its various forms, i.e. under conditions of air and moisture iron forms a yellow oxide, when soil is well drained or dry iron forms red oxides, and in waterlogged soil with a lack of air, iron forms in a reduced state giving a bluish-grey colour to soil.
4. Moisture in the soil – Poorly drained soils are characterised by blue-grey colours, while well drained soils have bright uniform colours; soil colour is also darker when it is moist.

CHNS analyser

Ground soil samples were analysed using the LECO CHNS-932 CHNS elemental analyser. The samples were weighed in tin capsules, and introduced into the sample-loading chamber for analysis.

The CHNS data was used to calculate the $\frac{Top\ depth}{Bottom\ depth}$ elemental ratios, which gives an idea of the spatial concentration of these elements within the soil. Graphs were drawn for the $\frac{10cm}{30cm}$ ratios at the Vaal River West Complex and for the $\frac{10cm}{50cm}$ ratios at the Vaal River Mispah.

XRF

Ground soil samples were sent to the Analytical Facility (Spectrau) at the University of Johannesburg for XRF analysis. XRF analysis was done via the borate fusion method, for the set of major elements, including the LOI, i.e. loss on ignition.

Percentage distribution curves were drawn using the XRF data for the residuals and the ICP-OES data for the extractions. The residual was calculated from the XRF totals data, and the ICP-OES sequential extraction results. These percentage distribution curves gave an idea where the major fractions of each element were. The metals coming from anthropogenic sources would reside in the first three fractions, while metals of natural sources are found in the residual fraction of the sequential extraction procedure (Zimmerman *et al.*, 2010). Curves were drawn for the following elements: aluminium, calcium, chromium, iron, magnesium, manganese, nickel, phosphorous, potassium, titanium and vanadium through the three BCR fractions and the extraction residual at the two depths

Soil texture

The soil texture describes the proportion of different grain sizes of mineral particles in soil (FAO/IIASA/ISRIC/ISS-CAS/JRC, 2009). The soil texture triangle, originally developed by U.S. Department of Agriculture in 1951, shown in Figure 5.14, is a graphical representation of soil texture classes, and is dependent on the percentage distribution of sand, silt and clay within a soil sample. The bulk density relates to the space between particles (FAO/IIASA/ISRIC/ISS-CAS/JRC, 2009).

Soil samples that were ground using a mortar and pestle were sent to the Kwazulu-Natal Department of Agriculture and Environmental Affairs (Cedara) for soil texture analyses. Sand fractions, i.e. very fine sand (0.05 – 0.10 mm), fine sand (0.10 – 0.25 mm), medium sand (0.25 – 0.50 mm) and coarse sand (0.50 – 2.0 mm), were determined by sieve analysis (Manson *et. al*, 2000).

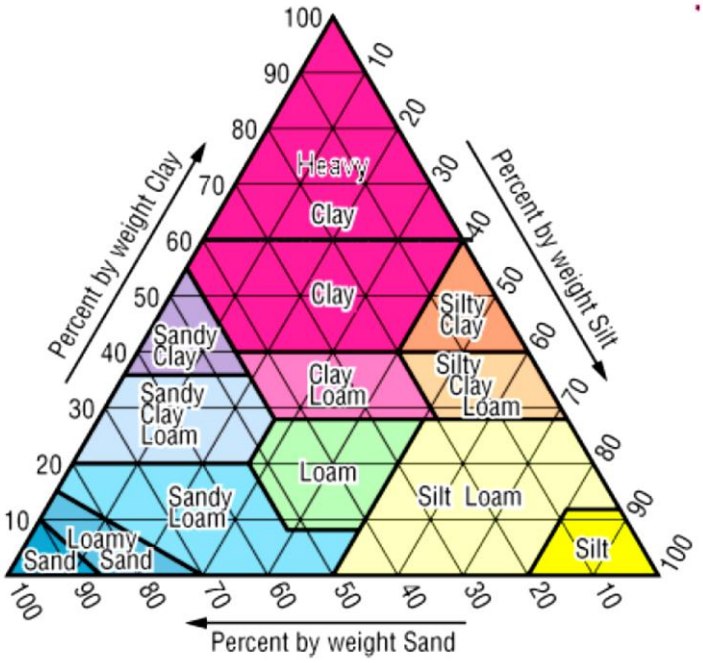

Figure 5.14 The soil texture triangle representing the various soil texture classes (FAO/IIASA/ISRIC/ISS-CAS/JRC, 2009)

Suspended clay and fine silt were determined by dispersion which involved treating a 20 g soil sample with hydrogen peroxide to oxidise the organic matter (Manson *et. al*, 2000). This sample was then made up to 400 mL, and was left to stand overnight (Manson *et. al*, 2000). The clear supernatant was siphoned off and the sample was puddled (Manson *et. al*, 2000). More deionised water was added, the sample was stirred, left overnight and the clear supernatant was siphoned off (Manson *et. al*, 2000). Dispersion agents, i.e. sodium hydroxide and sodium hexametaphosphate, were added and the sample was stirred on Hamilton Beach stirrers to form a suspension (Manson *et. al*, 2000). This suspension was made up to 1 L in a measuring cylinder (Manson *et. al*, 2000).

The clay (<0.002 mm) and fine silt (0.002 – 0.02 mm) fractions were measured with a pipette after sedimentation (Manson *et. al*, 2000). Fine silt plus clay was measured after 4 – 5 minutes at 100 mm, and clay after 5 – 6 hours at a depth of 75 mm; the time depended on the temperature (Manson *et. al*, 2000). Sand fractions were measured by sieving, and coarse silt (0.02 – 0.05 mm) was determined by difference.

From these results, soil texture characterisation and bulk density values were determined on the following webpage, by entering the relevant sand and clay percentages (Pedosphere.com, 2009):

http://www.pedosphere.com/resources/bulkdensity/worktable_us.cfm

Soil fertility

Soil fertility relates to the potential of a soil for the sustainable production of plants and animals (Amberger, 2006). Soil fertility is directly linked to plant nutrient availability, as plants need elements to grow. Table 5.3 shows a summary of all the important soil fertility parameters, and the guideline limits and ratings. Table 5.4 shows the soil characteristics within each rating.

Plant nutrients are characterised as (Hodges, 2010):

1. primary nutrients, which include nitrogen, phosphorous and potassium, are required in large amounts by plants,
2. secondary nutrients, including sulphur, calcium and magnesium, which are needed in smaller amounts, and
3. micro-nutrients, such as boron, copper, chlorine, iron, manganese, molybdenum, and zinc, which occur and are needed in very small amounts.

If any of these nutrients are lacking, it could affect plant growth negatively.

Table 5.3 Typical soil fertility parameters, their range and ratings (FAO/IIASA/ISRIC/ISS-CAS/JRC, 2009; Yara Analytical Services, 2011; Mitchell *et al.*, 1995; Hill Laboratories, 2015; Coulter *et al.*, 2008; Espinoza *et al.*, 2006)

Rating	CEC	Org C	P	K	N	Ca	Mg
	cmol kg^{-1}	**%**	**mg kg^{-1}**	**mg kg^{-1}**	**%**	**mg kg^{-1}**	**mg kg^{-1}**
Very low	<4	<0.2	0-3	0-5	0.1-0.2		0-25
Low	4-10	0.2-0.6	3.1-6.0	5.1-100	0.2-0.5	<400	26-50
Medium	10-20	0.6-1.2	6.1-10.0	101-150	0.5-1.0		51-100
High	20-40	1.2-2.0	>10	>150	>1.0		>100
Very high	>40	>2.0					

Table 5.4 Characterisation of the soil within each rating (FAO/IIASA/ISRIC/ISS-CAS/JRC, 2009; Yara Analytical Services, 2011; Mitchell *et al.*, 1995)

Rating	Characterisation
Very low	Very low nutrient retention, little or no organic matter and clay. Sandy soils.
Low	Slight nutrient retention, low organic matter and clay. Sandy soils.
Normal	Adequate nutrient retention for most plants, satisfactory organic matter and clay. Loamy silt soils.
High	High nutrient retention, increasing organic matter and clay content. Clay loam.
Very high	Very high nutrient retention, indicative of heavy soils with high organic matter and high clay content. Nutrients bound very tightly and thus availability is restricted. Clay soils.

Another important factor in soil fertility is the cation exchange capacity, i.e. CEC (Amberger, 2006). The CEC is a measure of the negative charges in the soil, and gives an indication of ability of soil to retain essential plant nutrients (Camberato, 2001; Hodges, 2010). The retention capacity of soil for cations, increases with increasing negative charge, i.e. the negative charges attract positive cations, most of which are

the essential plant nutrients needed for growth, i.e. potassium (K^+), calcium (Ca^{2+}), magnesium (Mg^{2+}), etc. (Camberato, 2001; Hodges, 2010). Soils with low CEC values cannot hold onto plant nutrients, while soils with high CEC values have the ability to build up stores of nutrients, and are less susceptible to rapid changes in soil solution levels (FAO/IIASA/ISRIC/ISS-CAS/JRC, 2009; Hodge, 2010). The CEC is dependent on organic matter, clay content and clay type within the soil (FAO/IIASA/ISRIC/ISS-CAS/JRC, 2009).

Organic carbon, another soil fertility determinant, gives an indication of the organic matter in the soil (Mitchell *et al.*, 1995). The amount of organic carbon relates to the productive health status of the soil (FAO/IIASA/ISRIC/ISS-CAS/JRC, 2009). Soils with very low organic carbon, i.e. values of <0.2%, are not very productive, and will require additional fertiliser to be productive (FAO/IIASA/ISRIC/ISS-CAS/JRC, 2009). Fertile soils are linked to medium to high amounts of organic carbon in soil, it is sensible to relate an organic carbon value of 2% for optimal soil structure (FAO/IIASA/ISRIC/ISS-CAS/JRC, 2009; Fisher *et al.*, 2007).

Ground soil samples were sent to the Kwazulu-Natal Department of Agriculture and Environmental Affairs (Cedara) for soil fertility analyses. Soil samples were air dried at room temperature, by spreading them across drying trays and forcing air over them (Manson *et. al*, 2000). Once dry the soil samples were crushed between rubber belts on a soil crusher and sieved through a 1 mm sieve (Manson *et. al*, 2000).

Sample density was determined based on a volume basis; and was converted to a mass basis by taking into account the dried mass of a 10 mL sample of soil (Manson *et. al*, 2000). The buffer pH (KCl pH) was determined by adding 25 mL of 1 mol L^{-1} KCl to 10 mL of soil in a sample cup, stirring for 5 minutes at 400 rpm using a multiple stirrer, the suspension was allowed to stand for 30 minutes, and the pH was measured using a gel-filled glass electrode while stirring (Manson, *et. al*, 2000).

The extractable calcium, magnesium and acidity was determined by adding 25 mL of 1 mol L^{-1} KCl to 2.5 mL of soil, the suspension was stirred at 400 rpm for 10 minutes using a multiple stirrer, the extracts were filtered through Whatman No. 1 filter paper, 5 mL was diluted with 20 mL of 0.0356 mol L^{-1} $SrCl_2$, then Mg and Ca were determined using atomic absorption (Manson *et. al*, 2000). The extractable acidity on the hand was determined by diluting 10 mL of the filtrate with 10 mL of deionised water, containing 2-4 drops of phenolphthalein, and the solution was titrated with 0.005 mol L^{-1} NaOH (Manson *et. al*, 2000).

Extractable phosphorus, potassium, zinc, copper and manganese was determined using the Ambic-2 extracting solution, which consisted of 0.25 mol L^{-1} NH_4CO_3 + 0.01 mol L^{-1} Na_2EDTA + 0.01 mol L^{-1} NH_4F + 0.05 g L^{-1} Superfloc (N100), which had been adjusted to pH 8 with a concentrated ammonia solution (Manson *et. al*, 2000). 25 mL of this solution was added to 2.5 mL of soil, the suspension was stirred for 10 minutes at 400 rpm, using a multiple stirrer, and the extracts were filtered using Whatman No. 1 filter paper (Manson *et. al*, 2000). Zinc, copper and manganese were determined by atomic absorption of the undiluted filtrate, potassium was determined by atomic absorption of 5 mL of filtrate diluted with 20 mL deionised water, and phosphorus was determined on a 2 mL aliquot of filtrate using the Murphy and Riley (1962) molybdenum blue procedure (Manson *et. al*, 2000).

The effective CEC (ECEC) was calculated as the sum of KCl-extractable Ca, Mg and acidity and Ambic-2 extractable K. The percentage acid saturation of the ECEC was calculated as extractable acidity x 100/ECEC (Manson *et. al*, 2000). Clay content was estimated using a combination of near-infrared reflectance and the measured sample density (Manson *et. al*, 2000). Total Carbon and Nitrogen were analysed by the Automated Dumas dry combustion method using a LECO CNS 2000 analyser (Manson *et. al*, 2000).

5.5 Certified reference material

As mentioned, all the BCR extractions and analysis of the extractants were done versus two certified reference material (CRMs). It should be noted here that there were no CRMs found that matched the soil (largely tailings) under study. Thus, the extraction protocol was validated using the stream sediment CRMs NCS DC 73315 (China National Analysis Centre for Iron and Steel) and the BCR 701. The detailed CRM information has been provided in Appendix B.

The XRF elemental totals analysis of CRM NCS DC 73315 is shown in Table 5.5, including the calculated error, and the percentage errors. The maximum percentage error was observed for Na_2O (10.26%). Table 5.6 shows the calculated elemental concentrations versus the reference value for the certified reference material. Chromium and nickel were found to have high percentage errors, i.e. 43% and 131% respectively. Table 5.7 shows the BCR 701 CRM certified values compared to the experimental values obtained after analysing the BCR sequential extractants. Standard deviations and standard errors were calculated for the triplicate experimental values. The highest standard deviations were seen for zinc (BCR 3), and for lead (BCR 2).

Table 5.5 The NCS DC 73315 certified elemental totals reference values versus the experimental values

	Units	Measured value	Reference Value	Error	% Error
Al_2O_3	mass %	15.62	15.37	0.25	1.63
CaO	mass %	5.51	5.34	0.17	3.18
Fe_2O_3	mass %	5.89	5.84	0.05	0.86
K_2O	mass %	2.16	2.11	0.05	2.37
MgO	mass %	0.93	0.98	-0.05	-5.10
Na_2O	mass %	0.35	0.39	-0.04	-10.26
SiO_2	mass %	56.09	56.44	-0.35	-0.62

Table 5.6 The NCS DS 73315 certified elemental concentrations versus the experimental values

	Units	CRM	Reference Value	Error	% Error
Cr	ppm	40	70	-29.96	-42.80
Mn	ppm	1161	1160	1.71	0.15
Ni	ppm	78	34	44.59	131
P	ppm	610	630	-19.02	-3.02
Ti	ppm	5275	5370	-94.54	-1.76
V	ppm	112	109	3.03	2.78

Table 5.7 The BCR 701 CRM certified reference values compared to experimental values

	Cd	Cr	Cu	Ni	Pb	Zn
Units	mg kg^{-1}	mg kg^{-1}	mg kg^{-1}	mg kg^{-1}	mg kg^{-1}	mg kg^{-1}
BCR Step 1						
Reference value	7.3	2.26	49.3	15.4	3.18	205
Measured value	5.0	3.70	46.4	16	1.7	198
Standard deviation	1	0.6	0.76	6.6	0.6	13
Standard error	0.6	0.3	0.44	3.8	0.4	7.5
BCR Step 2						
Reference value	3.77	45.7	125	26.6	126	114
Measured value	1.5	52	108.9	29.2	214.3	99.8
Standard deviation	0.1	9.3	2.7	4.9	15.9	9.2
Standard error	0.06	5.4	1.5	2.8	9.2	5.3
BCR Step 3						
Reference value	0.27	143	55	15.3	9.3	46
Measured value	0.0	134	36	14.2	10.3	57.4
Standard deviation	0.0	2.1	7.2	2.7	1.7	23.7
Standard error	0.0	1.2	4.1	1.6	1.0	13.7

5.6 Statistical analysis

The experiment had a multifactor experimental design, with the following factors, i.e. site, tree type, treatment, i.e. woodland or grassland substrate, depth and BCR sequential extraction step (for the major nutrients and trace metal data). The statistical analysis was performed using Statistical Package for Social Sciences (SPSS) version 15. The Principal Component Analysis (PCA) tables, histograms, analysis of variance (ANOVA) tables, and linear regression analysis (LRA) tables and plots can be found in Appendix C.

The statistical analysis was used to confirm whether the results observed where statistically significant. Statistical analysis was done on the initial soil solution measurements, the physical analysis of the soil, i.e. soil texture, soil fertility and CHNS data, and the chemical analysis, i.e. the ICP-OES elemental data on the major nutrients and the trace elements.

The descriptive statistics analysis included the sample size, mean, median, standard deviation and range, and the two sites were treated together since they were in the same geographical location. The descriptive statistics was looked at in terms of site, treatment, tree type and depth for the initial and the physical analysis. For the chemical analysis the descriptive statistics was looked at in terms of site, treatment, tree type, depth and sequential extraction step. The descriptive statistics was done on a composite sample, i.e. for the two sites, the comparison was done by comparing a composite of all depths of both treatments for each site separately; for treatment, a composite all depths of the grassland treatment were compared to the woodland treatment for both sites combined; for tree type, a composite of all depths at both sites combined were compared for *Tamarix usneoides* versus *Rhus lancea*; and for sequential extraction step, the comparison was done using a composite of all depths at both sites combined for carbonates versus oxides versus organics. The depth descriptive statistics tables were the only tables that looked at each depth separately.

For this study the composite samples were more important than the individual depth samples, as the tree roots could be at varying depths.

Significance testing using one-way ANOVA was used to determine whether there was a significant difference between the means of the sites (VRWC and VRMB), the treatment (grassland and woodland) and the tree type (*Tamarix usneoides* and *Rhus lancea*). A few ANOVA were done to compare the depths, however this was not pursued further because the composite of all the depth samples were more important. The ANOVA tests were done within a 95% confidence interval.

The percentage difference between the means of significantly different parameters across site (VRWC and VRMB), treatment (grassland and woodland) and tree (*Tamarix usneoides* and *Rhus lancea*) was calculated using formula (1); where V_1 and V_2 represent Value 1 and Value 2. A positive percentage error indicated that V_1 was greater than V_2, while a negative value indicated that V_2 was greater than V_1.

$$Percentage\ Difference = \frac{V_1 - V_2}{\frac{(V_1 + V_2)}{2}} \times 100\% \qquad (1)$$

PCA was used to represent the data in fewer variables. PCA is a descriptive method with a goal of reducing the number of variables of interest into a smaller set of components. The components were formed as linear combinations of correlated measured variables. These components were then used for further analysis.

Histograms were drawn for each component of the PCA to check for normal distribution. If data was distributed evenly around the mean then it was considered to be normally distributed; if it was distributed around a value either less than or more than the mean then the data was considered to be skew. If the data was normal then parametric tests such as analysis of variance (ANOVA), could be performed, if the data was not normally distributed then non-parametric tests were performed.

ANOVA was performed on the principal components of the major nutrients and trace elements sequential extraction data, to check whether the means of the components differed. One-way ANOVA studied the following factors: site, treatment, and types of tree. Two-way and three-way ANOVA tests were excluded from this study, as the *p-values* could not be calculated as the means were not estimable, which was due an insufficient amount of data. For components which were not normally distributed, one-way non-parametric tests were used. These included the Mann-Whitney U test, for two independent groups, or the Kruskal Wallis test, which is an extension of the Mann-Whitney U test for three or more groups. These ANOVA tests were also done within a 95% confidence interval, thus a *p-value* less than 0.05 indicated that there was a significant difference between groups within a factor. All the ANOVA tests performed were two-tailed.

LRA was performed, to determine the relationship between elemental concentrations with depth. LRA involves plotting the correlation between a dependant variable and an independent variable. Usually the dependant variable can be predicted based on the value of the independent variable. LRA was done for each of the principal components of the major nutrients and the trace elements, versus depth. The independent variable was depth, and the dependant variable was the elemental concentration of the major nutrients and trace elements. The results included the following:

- Correlation – The linear relationship between the independent and dependant could either be positive, negative or there is no correlation. If the linear relationship is weak, the correlation could possibly also be polynomial (quadratic, or cubic), or hyperbolic.
- R – Correlation coefficient indicates the degree of correlation between the independent and the dependant variables, i.e. how strong the relationship between the two variables is.
- R^2 – Variability indicates how much of the dependant variable can be explained by the independent variable.

- *p-value* – The statistical significance of the regression model between the independent and dependant variables.
- Equation – The resultant regression equation, from which the dependant variable can be predicted based on the independent variable, i.e. the value of the elemental mobility in each component could be predicted based on the depth.

The results and discussions are presented in the following chapters, namely six, seven and eight. The chapters cover initial soil analysis (Chapter six), soil texture and soil fertility (Chapter seven), and sequential extraction results (Chapter eight).

CHAPTER SIX – INITIAL SOIL ANALYSIS

The initial soil analysis is divided into three sections. The first section presents the soil core photos from the two sites, and compares colour differences. The second section presents the physical-chemical soil solution measurements for pH, pH in 0.1 mol L^{-1} KCl, conductivity, redox potential and moisture content, which was done on the soil samples immediately after the soil was split into the respective depths. All graphs in this section are plotted with standard error bars. The last section presents the statistical analysis to assess whether the trees have improved the physical-chemical quality of the soil.

6.1 Soil colour

This section presents a selection of the soil photos immediately after the cores were cut open. Figures 6.1 and 6.2 show control soil core samples taken at the VRWC and VRMP respectively.

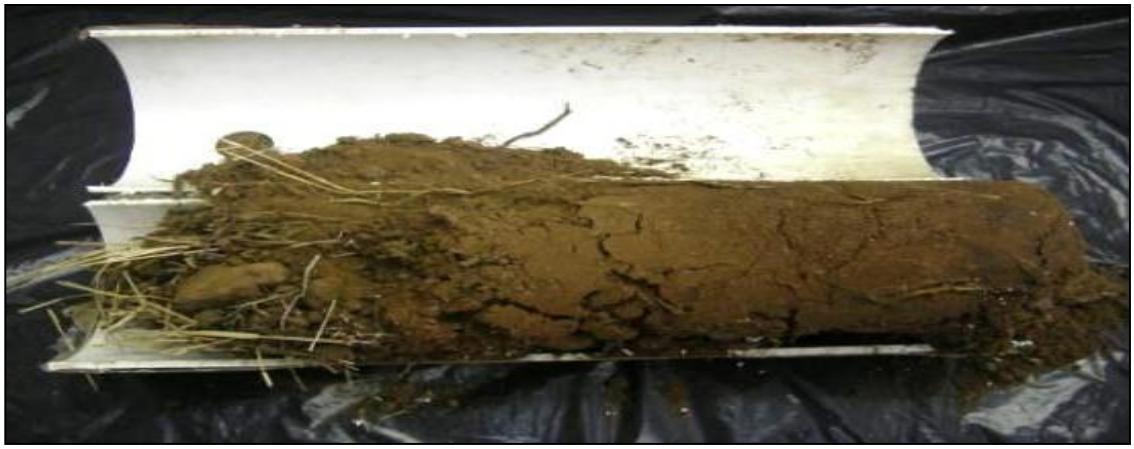

Figure 6.1 A control soil core sample taken at the Vaal River West Complex

As described in Section 5, the VRWC was characterised by dolomitic, high clay soils, while VRMP was characterised by well-drained, sandy, red Hutton soil (Wanenge, 2009). The soil at the VRMP was distinctly redder than that at VRWC. The soil at the VRMP was also more uniform and brighter in colour.

Figure 6.2 A control soil core sample taken at the Vaal River Mispah

6.2 Physical-chemical soil solution measurements

Each of the physical-chemical soil solution measurements were drawn on graphs versus depth. The graphs compared the control soil samples (CT) versus soil samples taken in the rooting zone of *Rhus lancea* (RL) and *Tamarix usneoides* (TX) trees.

Figures 6.3, 6.4, 6.5 and 6.6 show the aqueous soil solution measurements with depth of pH, and pH in 0.1 mol L^{-1} KCl for soil core samples from the VRWC and VRMP. The pH values of the control decreased with depth at both sites. The pH and pH in 0.1 mol L^{-1} KCl values show the alkalinising effect of *Tamarix usneoides* and to a lesser extent that of *Rhus lancea* compared to the control.

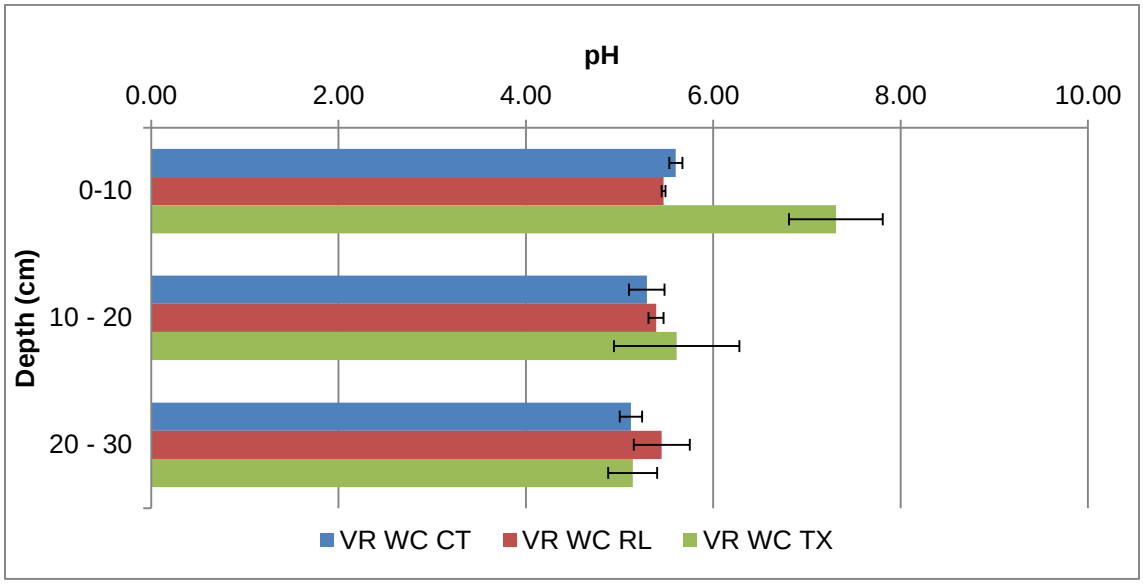

Figure 6.3 pH results with depth for soil at the Vaal River West Complex

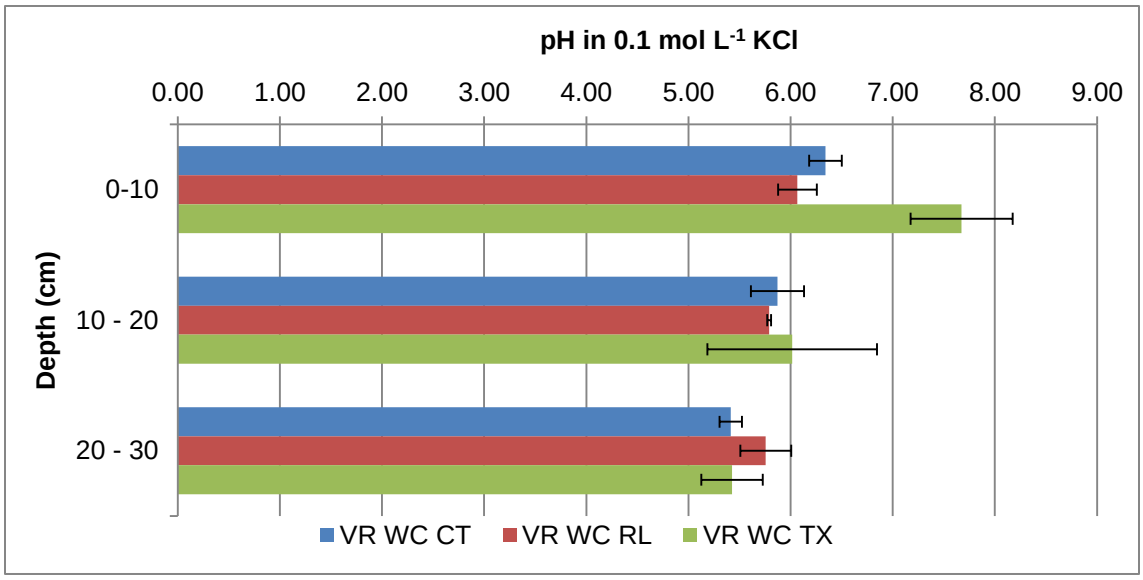

Figure 6.4 pH in 0.1 mol L^{-1} KCl results with depth for soil at the Vaal River West Complex

The conductivity measurements with depth are shown in Figures 6.7 and 6.8 for VRWC and VRMP, respectively. The conductivity values of the soils surrounding the trees

were higher than that of the control site, highlighting the salt hyperaccumulation capabilities from the soil and ground water by *Tamarix usneoides* and, to a lesser extent, that of *Rhus lancea*. The increased cations and anions in the rooting zone of the trees, as indicated by the conductivity, relate to the ability of trees to accumulate high concentrations of micro- and macro-nutrients and metals from the surrounding polluted soils and groundwater.

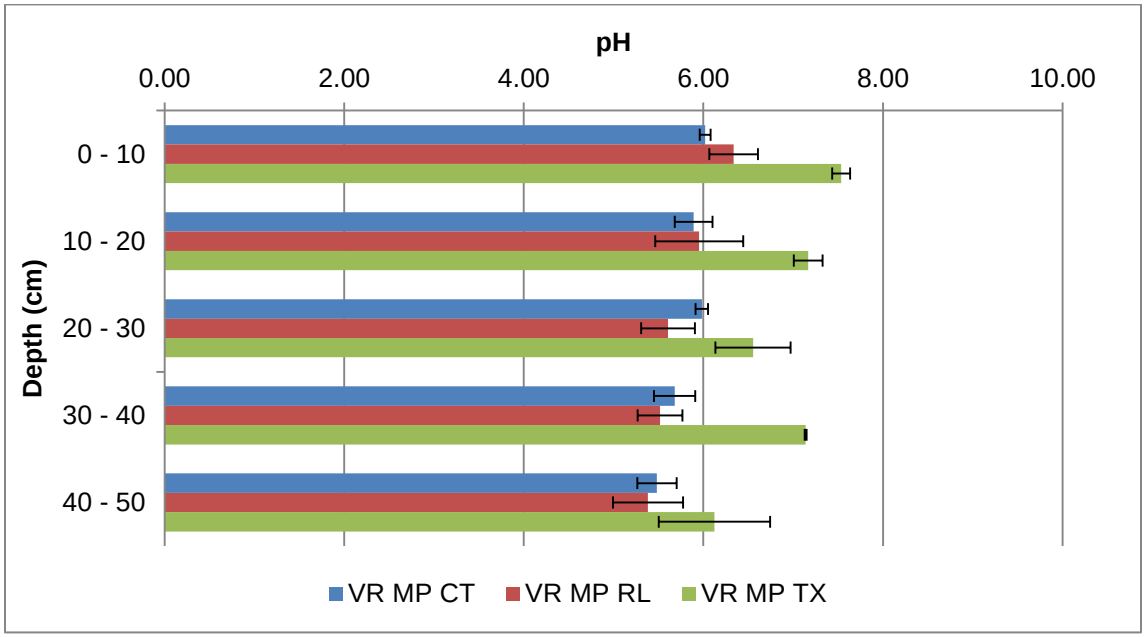

Figure 6.5 pH results with depth for soil at the Vaal River Mispah

The redox potential measurements with depth are shown in Figures 6.9 and 6.10 for the VRWC and VRMP, respectively. The redox potential in the control increased with depth. The redox potential of the soil surrounding the trees was lower than the control sample. The presence of *Rhus lancea* and *Tamarix usneoides* decreased the oxidation potential of the soil; hence the soils have become more reducing.

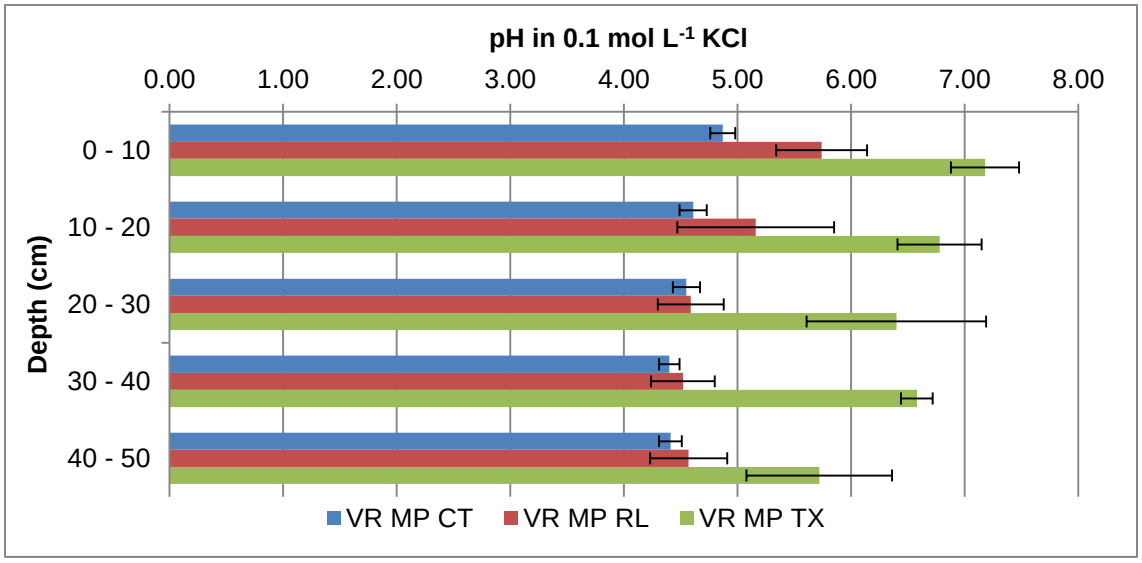

Figure 6.6 pH in 0.1 mol L^{-1} KCl results with depth for soil at the Vaal River Mispah

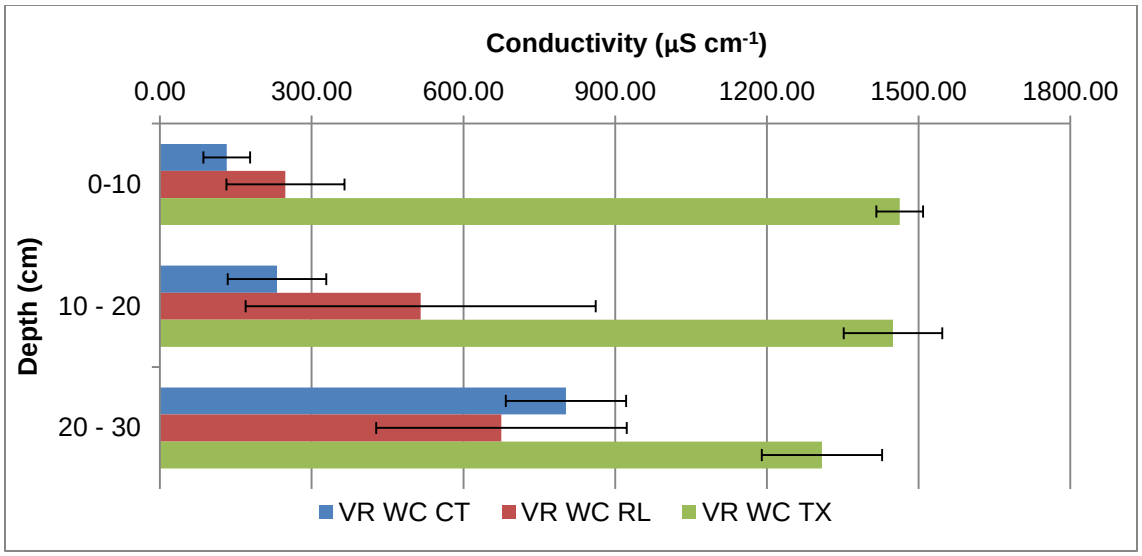

Figure 6.7 Conductivity results with depth for soil at the Vaal River West Complex

The moisture content at the VRWC and VRMP is shown in Figures 6.11 and 6.12, respectively. At the VRWC, the moisture content of the control increased with depth. This was synonymous with the fact that the site has shallow, polluted ground water (Wanenge, 2009). The soil at the VRMP were well-draining soils (Wanenge, 2009),

thus the moisture content of the control did not increase drastically with depth, even though these samples had a deeper sample depth.

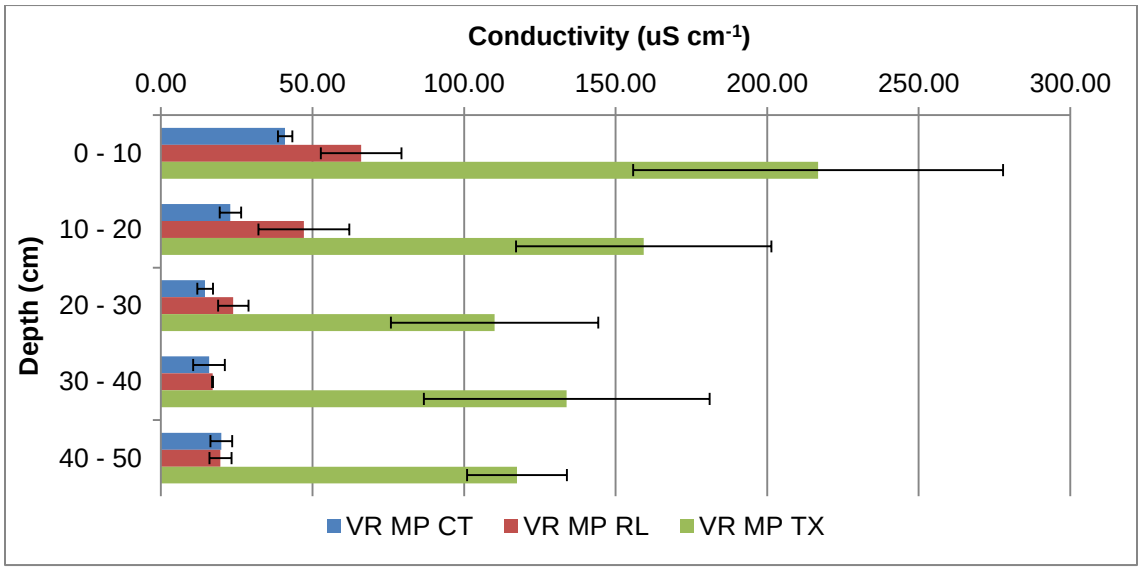

Figure 6.8 Conductivity results with depth for soil at the Vaal River Mispah

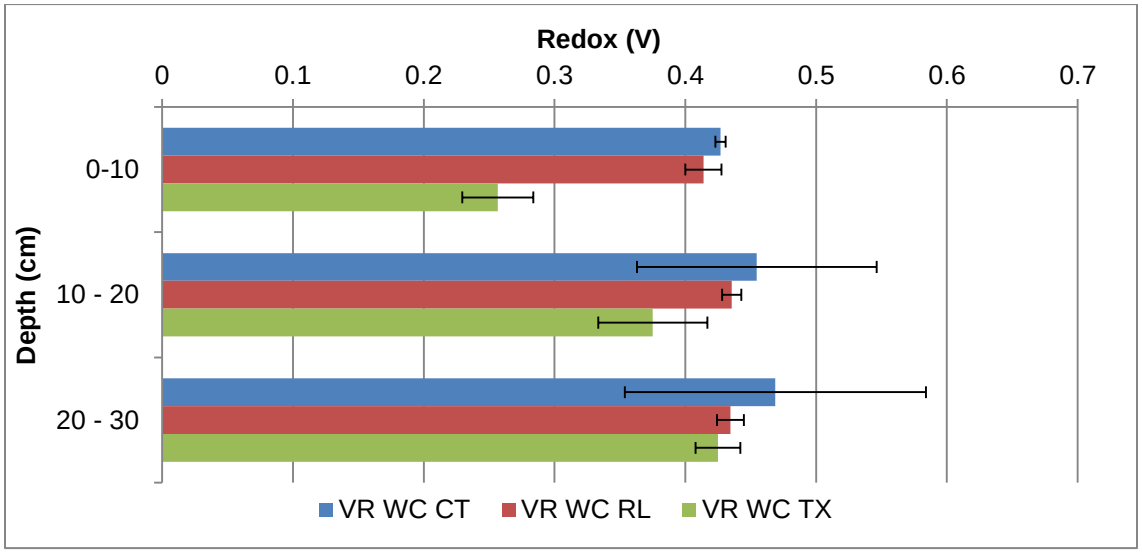

Figure 6.9 Redox potential results with depth for soil at the Vaal River West Complex

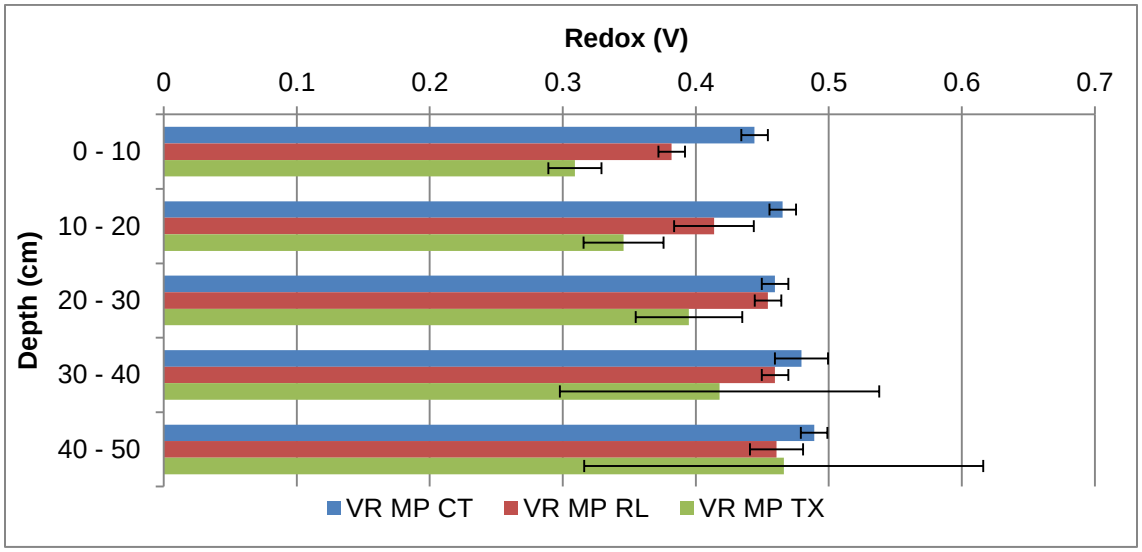

Figure 6.10 Redox potential results with depth for soil at the Vaal River Mispah

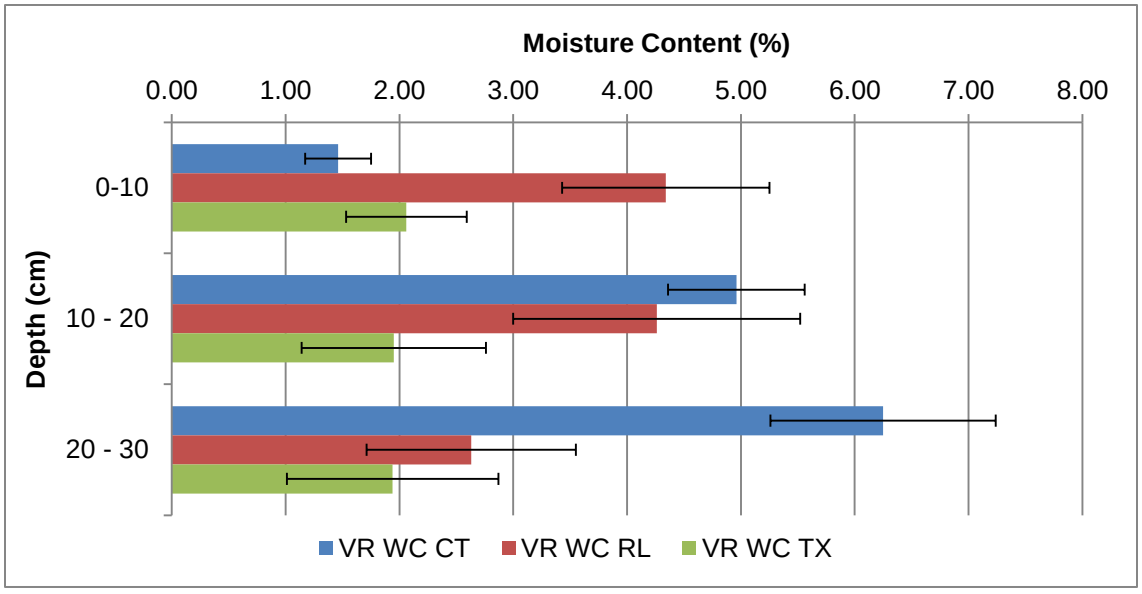

Figure 6.11 Moisture content results with depth for soil at the Vaal River West Complex

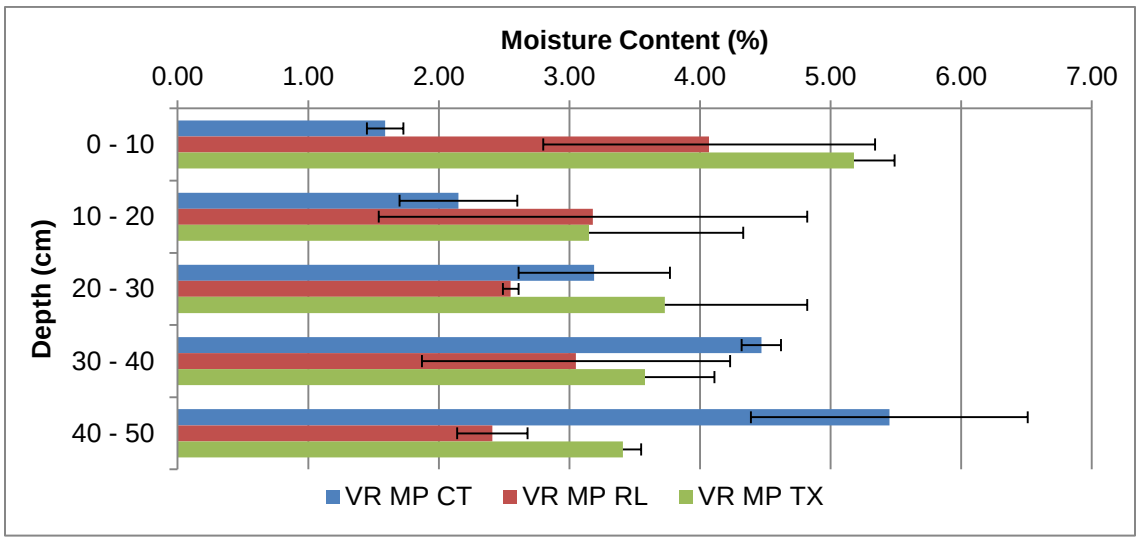

Figure 6.12 Moisture content results with depth for soil at the Vaal River Mispah

The trees have had drying effects on the soil, as the moisture content of the soil taken from the rooting zone of the trees decreased with depth. *Tamarix usneoides* was more effective than *Rhus lancea* in decreasing the soil moisture. By decreasing the soil moisture content, the trees have aided in the remediation of acid rock drainage, as the recharge rate of the ground water levels has decreased, due to the trees taking up water for photosynthesis and for growth.

6.3 Statistical analysis

The descriptive statistics for the samples across the sites, treatment, type of tree, and by depth for the two Vaal River sites are shown in Tables 6.1, 6.2, 6.3, and 6.4. Tables 6.1, 6.2 and 6.3 represent the composite sample at all depths. The tables include the mean, median and standard deviation for the initial soil solution determinants.

The p-values in Table 6.1 indicated that soil pH (p = 0.31), pH in KCl (p = 0.82), redox potential (p = 0.62) and moisture content (p = 0.19) were statistically similar at the two

sites. The conductivity was significantly different at the two sites, as the *p-value* was less than 0.05 (p = 3.12E-9); the conductivity was 168% higher at VRWC than at VRMP. The standard deviation for conductivity at the VRWC site was high, indicating that there was a large variability in the conductivity at this site, while the variability at VRMP was small. This variability is due to the descriptive statistics being a representation of the composite sample for the site, for the control, *Tamarix usneoides* and *Rhus lancea* at all depths.

Table 6.1 Descriptive statistics of initial soil solution measurements by site

Determinant	Units	Site	Mean	Median	Standard Deviation	*p-value*
Soil pH	-	VRWC	6.03	5.76	0.99	0.31
		VRMP	6.25	6.07	0.78	
pH in KCl	-	VRWC	5.57	5.25	0.97	0.82
		VRMP	5.52	5.17	0.94	
Conductivity	µS cm^{-1}	VRWC	834.97	563.00	766.13	3.12E-9
		VRMP	61.87	38.36	46.06	
Redox potential	V	VRWC	0.41	0.43	0.08	0.62
		VRMP	0.42	0.45	0.07	
Moisture content	%	VRWC	3.41	3.11	2.28	0.19
		VRMP	2.86	2.57	1.25	

Table 6.2 Descriptive statistics of initial soil solution measurements by treatment

Determinant	Units	Treatment	Mean	Median	Standard Deviation	*p-value*
Soil pH	-	Grassland	5.76	5.67	0.62	0.01
		Woodland	6.30	6.14	0.92	
pH in KCl	-	Grassland	4.90	4.75	0.55	1.00E-5
		Woodland	5.86	5.38	0.93	
Conductivity	µS cm^{-1}	Grassland	114.37	32.70	179.06	0.02
		Woodland	470.49	118.80	694.56	
Redox potential	V	Grassland	0.4700	0.4777	0.0327	0.00
		Woodland	0.3946	0.4179	0.0678	
Moisture content	%	Grassland	3.46	2.76	2.32	0.18
		Woodland	2.87	2.93	1.30	

In Table 6.2, the grassland and woodland treatments were significantly different in terms of pH (p = 0.01), pH in KCl (p = 1.00E-5), conductivity (p = 0.02) and redox potential (p = 0.00). The pH was 7% higher, redox potential 15% lower and conductivity 88% higher in the woodland substrate. This highlights the alkalinising, salt hyperaccumulating and reducing effects of the trees. The standard deviations for conductivity were high for the woodland substrate, showing the large variability in the composite sample. The soil moisture showed no significant difference between the two treatment substrates.

The difference in the soil solution measurements between the trees is highlighted in Table 6.3. There was a significant difference between the trees in terms of pH in KCl (p = 0.03), conductivity (p = 3.46E-3) and redox potential (p = 0.01). The pH in KCl was 10% higher, redox potential 18% lower and conductivity 107% higher for *Tamarix usneoides* than *Rhus lancea*. *Tamarix usneoides* seemed more effective in alkalinising the buffer pH, salt hyperaccumulation in decreasing the oxidation potential in the soil. The standard deviation of the conductivity for the composite sample for *Tamarix usneoides* indicated that the variability was large, likely due to the tree's known salt hyperaccumulation capabilities.

Table 6.3 Descriptive statistics of initial soil solution measurements by type of tree

Determinant	Units	Tree	Mean	Median	Standard Deviation	*p-value*
Soil pH	-	*Tamarix usneoides*	6.59	7.17	1.15	0.11
		Rhus lancea	6.17	6.11	0.49	
pH in KCl	-	*Tamarix usneoides*	6.16	6.48	1.12	0.03
		Rhus lancea	5.57	5.25	0.58	
Conductivity	µS cm^{-1}	*Tamarix usneoides*	754.92	153.60	856.67	3.46E-3
		Rhus lancea	186.05	79.20	288.24	
Redox potential	V	*Tamarix usneoides*	0.37	0.36	0.08	0.01
		Rhus lancea	0.42	0.43	0.04	
Moisture content	%	*Tamarix usneoides*	3.09	3.10	1.44	0.25
		Rhus lancea	2.66	2.67	1.14	

Tables 6.4 (a) and (b) indicated that the pH and pH in KCl decreased with depth at both sites, the conductivity increased with depth at the VRWC, and decreased with depth at the VRMP, and the redox potential increased with depth at both sites. The soil moisture did not follow a distinct trend. The standard deviations for conductivity at VRWC were once again high for each depth, indicating that the variability in the conductivity values was high across various depths as well.

Table 6.4 (a) Descriptive statistics of initial soil solution measurements; soil pH and pH in KCl, by depth

Determinant	Units	Site	Depth	Mean	Median	Standard Deviation
Soil pH	-	VRWC	0-10	6.70	6.56	0.87
			10-20	5.89	5.76	0.78
			20-30	5.53	5.46	0.39
		VRMP	0-10	6.63	6.12	0.71
			10-20	6.34	6.12	0.76
			20-30	6.05	5.99	0.59
			30-40	5.98	5.88	0.74
			40-50	5.61	5.51	0.63
pH in KCl	-	VRWC	0-10	6.15	5.77	0.94
			10-20	5.41	5.25	0.63
			20-30	5.24	5.08	0.39
		VRMP	0-10	5.93	5.36	1.06
			10-20	5.52	4.85	1.15
			20-30	5.18	4.78	1.13
			30-40	4.99	4.45	0.98
			40-50	4.80	4.51	0.75

On comparing the significant difference between the soil pH at VRWC at depths 0-10 cm and 20-30 cm in table 6.4 (a) and (b), there was a significant difference (p = 3.00E-5) between the pH at the two depths. At VRWC the conductivity showed no significant difference (p = 0.19) between depths 0-10 cm and 20-30 cm. At VRMP, the pH (p = 4.10E-4) and the conductivity (p = 0.05) showed a significant difference between depths 0-10 cm and 40-50 cm. These *p-values* indicated how the spatial characteristics of each site differ in terms of depth. The in-depth analysis in terms of depth however

was not pursued further as the focus of this study was on 3 factors: site, treatment and tree type, and not on depth, as the tree roots could be at any depth, since tree roots do not grow in a uniform, lateral direction.

Table 6.4 (b) Descriptive statistics of initial soil solution measurements; conductivity, redox potential and moisture content by depth

Determinant	Units	Site	Depth	Mean	Median	Standard Deviation
Conductivity	µS cm^{-1}	VRWC	0-10	605.90	180.80	697.60
			10-20	753.26	545.00	672.09
			20-30	928.96	914.00	425.46
		VRMP	0-10	107.96	77.30	94.77
			10-20	76.45	35.42	71.11
			20-30	49.50	19.70	52.46
			30-40	45.79	17.07	59.91
			40-50	44.20	22.58	44.68
Redox potential	V	VRWC	0-10	0.36	0.41	0.08
			10-20	0.42	0.43	005
			20-30	0.44	0.45	0.03
		VRMP	0-10	0.38	0.39	59.60
			10-20	0.41	0.44	59.37
			20-30	0.44	0.46	45.77
			30-40	0.44	0.45	50.19
			40-50	0.44	0.48	40.64
Moisture content	%	VRWC	0-10	2.69	2.34	1.52
			10-20	3.85	4.38	2.02
			20-30	3.61	3.60	2.46
		VRMP	0-10	3.61	4.56	1.88
			10-20	2.83	2.28	1.79
			20-30	3.16	2.65	1.14
			30-40	3.59	4.15	1.31
			40-50	3.62	2.81	1.75

The initial soil solution measurements were represented by two components via PCA (Table C1, Appendix C); soil pH, pH in KCl and the redox potential in Component 1, and conductivity and soil moisture in Component 2, as described in Table 6.5, with a

variance of 77.5%. Histograms (Figures C1, C2, Appendix C) indicated that both components were not normally distributed.

Table 6.5 The PCA of the initial soil solution measurements

Data set	Component	Parameters included	Normally distributed
Initial soil solution measurements	1	Soil pH, pH in KCl, redox potential	No
Initial soil solution measurements	2	Conductivity, soil moisture content	No

6.4 Summary and conclusions

The soil at the VRMP had a distinct red colour, and the soil was more uniform and brighter in colour than that of the VRWC, due to it being better drained.

pH decreased with depth at both sites. The alkalinising effect of trees was highlighted by increased in the pH values compared to the control. This was further confirmed by the statistical analysis where the pH values in the woodland substrate were found to be significantly different from those in the grassland substrate as the *p-values* were 0.01 for pH and 1.00E-5 for pH in KCl. The pH values were 7% higher for the woodland treatment compared to the grassland substrate. There was a significant difference (p = 0.03) between the buffer pH for *Tamarix usneoides* and *Rhus lancea,* hence *Tamarix usneoides* was more effective in alkalinising the buffer pH; the buffer pH was 10% higher. By improving the pH, the trees have aided in the remediation of acid rock drainage, as the process is directly dependant on pH; in fact the process is aggravated by low pH values.

The conductivity values were 168% higher at the VRWC than at the VRMP, and the *p* of 3.12E-9, indicated that the conductivity was significantly different at the two sites. The conductivity at the VRWC was found to increase with depth while at the VRMP it decreased with depth. The salt hyperaccumulation capabilities of the trees were highlighted by the high conductivity values in the soil of the tree samples, which was confirmed by the statistical data, as there was a significant difference (p = 0.02) between the conductivity of the woodland substrate compared to the grassland substrate; the woodland samples had conductivity values 88% higher. Increased conductivity indicates increased cation and anion concentrations in the soil. This increase was related to the trees' ability to accumulate high concentrations of micro- and macro-nutrients, and metals from the surrounding polluted soils and groundwater. The soil around *Tamarix usneoides* had 107% higher conductivity values than that for *Rhus lancea*, indicating that *Tamarix usneoides* had greater hyperaccumulation capabilities; the *p-value* (p = 3.46E-3) indicated that there was a significant difference between the trees. The standard deviations indicated that there was a large variability in the conductivity values at the VRWC site, and a small variability at the VRMP site. The high variability was due to a composite sample being considered for the site.

The redox potential increased with depth at both sites. The statistical analysis indicated that there was a significant difference between the redox potential of the woodland and grassland substrates (p = 0.00); further the redox potential was 15% lower in the presence of the trees. These results indicated that the trees have made the soil environment more reducing, i.e. the oxidation potential in the soil has been lessened. The *p-value* comparing the significance difference between the two trees was found to be 0.01, hence *Tamarix usneoides* was more effective in reducing the soil environment than *Rhus lancea;* the redox was 18% lower for *Tamarix usneoides*.

Even though the trees seem to have minor drying effects on the soil, the statistical analysis did not prove this, as the soil moisture content was not significantly different between site, treatment and tree. Hence no formal conclusions can be made with regards to the soil moisture improvement in terms of the trees.

A similar trend was observed at a landfill site where the same trees have been planted to remediate the soil; the trees have had significant alkalinising effects, salt hyperaccumulation (measured by conductivity) and a decrease in the oxidation potential of the landfill soil as well. To be noted the conductivity at the landfill site also showed extremely high standard deviations for the conductivity; again indicating the high variability. The high standard deviations at both the site included in this study and the landfill site could be due to the large salt hyperaccumulation capabilities of both trees, which is affecting the variability of the data (Arendze, unpublished).

PCA extracted the initial soil solution analysis into two components, i.e. Component 1 comprised of soil pH, pH in KCl and the redox potential, and Component 2 consisted of conductivity and soil moisture.

These results gave a positive indication of the use of the two trees for the remediation of mine polluted soils as there were definite improvements in the physical-chemical characteristics of the soil, in terms of pH, conductivity and redox potential. These determinants are all dependent factors in the ARD process.

CHAPTER SEVEN – PHYSICAL SOIL ANALYSIS

Physical soil analysis is important as it relates to the condition of the soil, in terms of mineral composition and plant nutrient availability. This chapter describes the soil texture, soil fertility and CHNS results, and focuses on whether there were any improvements in the physical soil quality as a result of the trees. Each section includes the relevant statistical analysis. All graphs in this section are plotted with standard error bars.

7.1 Soil texture

This section presents soil class in terms of percentage clay, silt, and sand content, and the statistical analysis to check whether the presence of the trees had significantly caused a change in the soil texture at the two sites.

7.1.1 Soil class

The changes in soil texture class and bulk density with depth for soil core samples at the Vaal River West Complex and the Vaal River Mispah are shown in Tables 7.1 and 7.2, respectively. The soil texture class and bulk density were determined based on the percentage of clay, sand and silt in the soil. The tables compare the control samples (CT) with that of samples taken from the rooting zones of *Rhus lancea* (RL) and *Tamarix usneoides* (TX) trees.

The soil texture of the soil in the control samples at both sites was characterised as loamy sand, which consists mainly of coarse, grainy sand particles. Due to sand particles being grainy, the pore spaces in between the particles was moderately high, hence it is expected that the water retention of the soil in the control samples was low.

Table 7.1 Changes in soil texture and bulk density values with depth for soil at the Vaal River West Complex

Sample	Depth	Soil texture	Bulk density
	cm	-	g cm^{-3}
VRWC CT	0-10	Loamy sand	1.62
VRWC CT	10-20	Sandy loam	1.59
VRWC CT	20-30	Loamy sand	1.61
VRWC RL	0-10	Sandy loam	1.53
VRWC RL	10-20	Sandy loam	1.59
VRWC RL	20-30	Loamy sand	1.61
VRWC TX	0-10	Sandy loam	1.61
VRWC TX	10-20	Sandy loam	1.61
VRWC TX	20-30	Sandy loam	1.59

At the VRWC the soil texture changed from loamy sand to sandy loam from 0-20 cm depth for *Rhus lancea*, and from 0-30 cm depth for *Tamarix usneoides*. At VRMP the soil texture changed from loamy sand to sandy loam at depths from 30-50 cm for *Rhus lancea*, and from 0-20 cm for *Tamarix usneoides*.

The trees increased the silt and clay fractions in the soil, thus making the soil more central in the soil texture triangle. The silt and clay particles are smaller and finer, thus

the water retention and plant nutrient retention are expected to have increased. The bulk density at both sites decreased in the top layers of soil, implying that the space between the soil particles has decreased; hence an increase in the plant nutrient and water retention capabilities of the soil is likely.

Table 7.2 Changes in soil texture and bulk density values with depth for soil at the Vaal River Mispah

Sample	Depth	Soil texture	Bulk density
	cm	-	g cm^{-3}
VRMP CT	0-10	Loamy sand	1.6
VRMP CT	10-20	Loamy sand	1.58
VRMP CT	20-30	Loamy sand	-*
VRMP CT	30-40	Loamy sand	1.57
VRMP CT	40-50	Sandy loam	1.53
VRMP RL	0-10	Loamy sand	1.58
VRMP RL	10-20	Loamy sand	1.57
VRMP RL	20-30	Loamy sand	1.56
VRMP RL	30-40	Sandy loam	1.55
VRMP RL	40-50	Sandy loam	1.52
VRMP TX	0-10	Sandy loam	1.52
VRMP TX	10-20	Sandy loam	1.53
VRMP TX	20-30	Loamy sand	1.57
VRMP TX	30-40	Loamy sand	1.58
VRMP TX	40-50	Loamy sand	1.57

* Result could not be calculated.

7.1.2 Statistical analysis

The descriptive statistics for the soil texture analysis across sites, treatment, type of tree and by depth for the Vaal River sites are shown in Tables 7.3, 7.4, 7.5, and 7.6. Tables 7.1, 7.2 and 7.3 represent the composite sample at all depths. The tables include the mean, median and standard deviation.

In Table 7.3, the VRMP had higher percentages of clay (26%), silt (15%) and sand (6%) in the soil than the VRWC, and the *p-values* indicated that there was a significant difference between the clay (p = 5.10E-6), silt (p = 4.75E-19), and sand (p = 2.49E-9) at the two sites. The bulk density showed no significant difference at the two sites (p = 0.31). The results indicate the differences between the soil characteristics at the two sites.

Table 7.3 Descriptive statistics of soil texture measurements by site

Determinant	Units	Site	Mean	Median	Standard Deviation	*p-value*
Clay	%	VRWC	9.08	9.09	1.47	5.10E-6
		VRMP	11.84	11.82	2.32	
Silt	%	VRWC	13.29	14.09	2.79	4.75E-19
		VRMP	5.83	5.36	3.49	
Sand	%	VRWC	77.09	77.37	3.38	2.49E-9
		VRMP	81.97	82.88	2.62	
Bulk density	g cm^{-3}	VRWC	1.60	1.61	0.03	0.31
		VRMP	1.56	1.57	0.02	

The woodland treatment, in Table 7.4, showed a significant difference to the grassland treatment in terms of clay (p = 2.74E-3) and bulk density (p = 0.03). The woodland treatment had 18% higher clay content, and 1% lower bulk density than the grassland treatment as indicated in Table 7.4. The trees increased the clay fraction in the soil;

suggesting increased water plant-nutrient retention. The decreased bulk density would imply smaller spaces between the particles, hence higher water retention.

Table 7.4 Descriptive statistics of soil texture measurements by treatment

Determinant	Units	Treatment	Mean	Median	Standard Deviation	*p-value*
Clay	%	Grassland	9.52	9.41	2.99	2.74E-3
		Woodland	11.45	11.68	2.21	
Silt	%	Grassland	9.86	9.99	4.53	0.09
		Woodland	8.01	6.02	4.25	
Sand	%	Grassland	81.15	81.07	3.35	0.11
		Woodland	79.64	80.08	3.88	
Bulk density	$g\ cm^{-3}$	Grassland	1.59	1.59	0.03	0.03
		Woodland	1.57	1.57	0.03	

Table 7.5 indicated that *Tamarix usneoides* and *Rhus lancea* showed no significant difference between soil texture components, as the *p-values* were all greater than 0.05.

Table 7.5 Descriptive statistics of soil texture measurements by type of tree

Determinant	Units	Tree	Mean	Median	Standard Deviation	*p-value*
Clay	%	*Tamarix usneoides*	11.11	11.28	2.57	0.29
		Rhus lancea	11.79	11.90	1.78	
Silt	%	*Tamarix usneoides*	8.47	6.25	4.61	0.47
		Rhus lancea	7.56	5.73	3.92	
Sand	%	*Tamarix usneoides*	79.16	77.58	3.71	0.40
		Rhus lancea	80.11	81.27	4.06	
Bulk density	$g\ cm^{-3}$	*Tamarix usneoides*	1.57	1.58	0.03	0.32
		Rhus lancea	1.56	1.57	0.03	

Descriptive statistics for the soil texture determinants with depth can be found in Table 7.6.

Table 7.6 Descriptive statistics of soil texture measurements by site and depth

Determinant	Units	Site	Depth	Mean	Median	Standard Deviation
Clay	%	VRWC	0-10	9.38	7.84	2.46
			10-20	9.05	9.15	0.80
			20-30	8.82	9.09	0.44
		VRMP	0-10	11.69	10.78	2.24
			10-20	12.40	11.53	1.77
			20-30	9.40	11.82	3.97
			30-40	11.83	11.53	1.10
			40-50	13.88	14.83	1.44
Silt	%	VRWC	0-10	15.93	15.89	0.56
			10-20	12.52	12.23	2.54
			20-30	11.43	11.74	2.45
		VRMP	0-10	5.26	5.80	1.18
			10-20	5.44	5.36	0.65
			20-30	7.58	4.97	4.36
			30-40	4.88	5.16	0.74
			40-50	6.00	5.64	1.80
Sand	%	VRWC	0-10	74.94	75.74	3.35
			10-20	77.53	77.37	1.59
			20-30	78.82	79.10	3.81
		VRMP	0-10	81.62	81.81	3.65
			10-20	81.86	83.86	3.05
			20-30	83.17	82.88	0.86
			30-40	82.75	82.92	1.69
			40-50	80.45	79.22	2.57
Bulk density	g cm^{-3}	VRWC	0-10	1.59	1.61	0.04
			10-20	1.60	1.59	0.01
			20-30	1.60	1.61	0.01
		VRMP	0-10	1.57	1.58	0.04
			10-20	1.56	1.57	0.02
			20-30	1.57	1.57	0.01
			30-40	1.57	1.57	0.01
			40-50	1.54	1.53	0.02

At the VRWC the clay and silt decreased and the sand increased with depth. At the VRMP the sand and silt increased, then decreased with depth, while the clay decreased the increased with depth. The bulk density at both sites did not change with depth.

PCA (Table C2, Appendix C) represented the soil texture data in two components, namely Component 1 including: clay, silt and bulk density, and Component 2 including: sand as shown in Table 7.7. The components had a total variance of 94.0%. Component 1 was normally distributed and component 2 was not (Figures C3, C4, Appendix C).

Table 7.7 The PCA of the soil texture analysis

Data set	Component	Parameters included	Normally distributed
Soil texture	1	Clay, silt, bulk density	Yes
Soil texture	2	Sand	No

7.2 Soil fertility

The soil fertility results were divided into the cation exchange capacity, organic carbon content, primary nutrients and secondary nutrients. Statistical analysis was conducted to further elucidate trends.

7.2.1 Cation exchange capacity

The changes in cation exchange capacity (CEC) of the soil samples at the Vaal River West Complex and Vaal River Mispah with depth are shown in Figures 7.1 and 7.2, respectively. The graphs compare the control samples (CT), with that of samples taken from the rooting area of *Rhus lancea* (RL) and *Tamarix usneoides* (TX) trees.

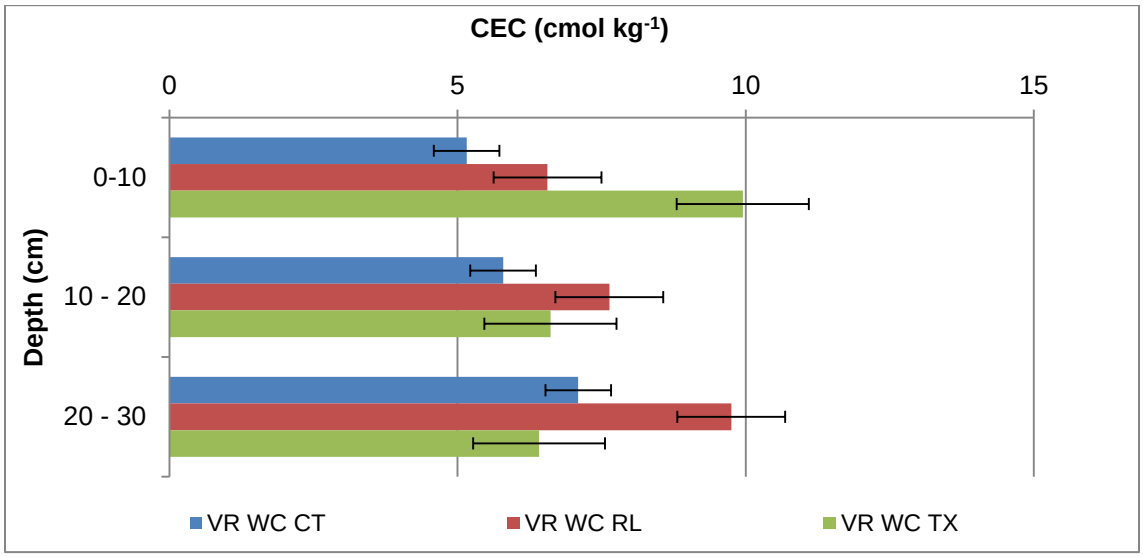

Figure 7.1 Results for cation exchange capacity with depth for soil at the Vaal River West Complex

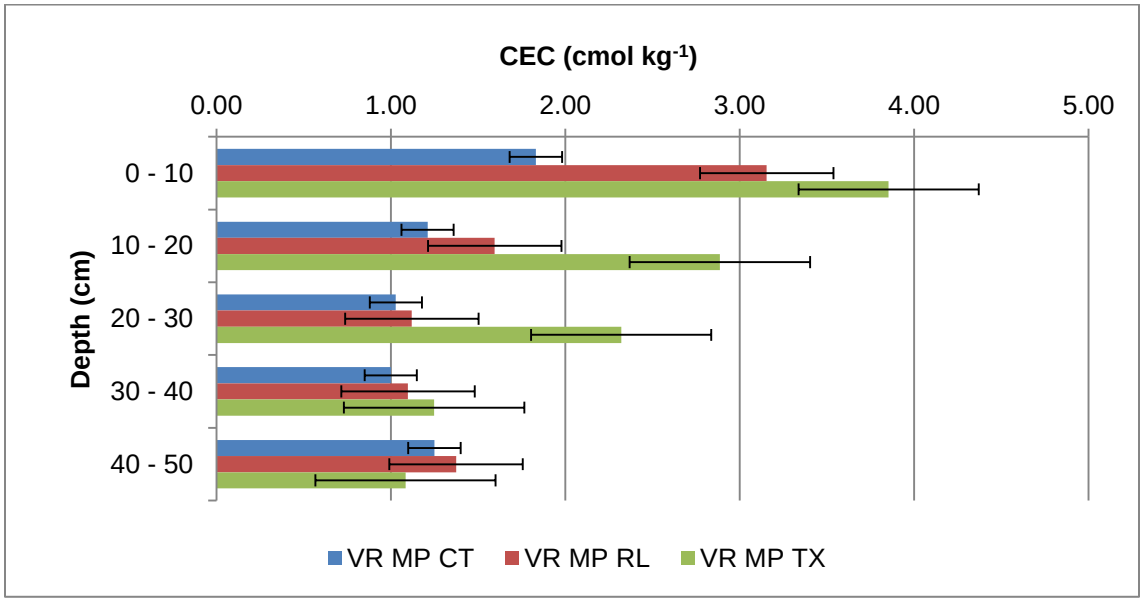

Figure 7.2 Results for cation exchange capacity with depth for soil at the Vaal River Mispah

The CEC in the control samples were much higher at the VRWC, with values above 5 cmol kg^{-1}. At the VRMP the values were below 2 cmol kg^{-1}, thus the plant nutrient retention in the soil is lower at the VRMP than at the VRWC. *Rhus lancea* increased the CEC values at both sites through the entire depth profile that was sampled. *Tamarix usneoides* increased the CEC in the top layers of the soil which were sampled, i.e. at the VRWC from 0-20 cm, and at the VRMP from 0-40 cm.

The maximum CEC at the VRWC was 9.95 cmol kg^{-1}, and at the VRMP was 3.85 cmol kg^{-1}; both at a depth of 0-10 cm in the presence of *Tamarix usneoides*. The nutrient holding capacity of the soil has thus improved in the presence of *Rhus lancea* and *Tamarix usneoides*, thus the productivity of the soil for plant growth has also improved.

7.2.2 Organic carbon content

The results for the variation of the organic carbon content with depth for the soil samples are shown in Figures 7.3 and 7.4, respectively.

The highest organic carbon values of 2.1%, 5.05% and 3.55% (at the VRWC) and 3.75%, 2.75% and 1.75% (at the VRMP) for the control, *Rhus lancea,* and *Tamarix usneoides*, respectively were recorded at the top layer of soil, i.e. 0-10 cm. At the VRWC, *Rhus lancea* and *Tamarix usneoides* increased the organic carbon values at depth 0-10 cm. This is likely due to plant litter on the soil surface.

At the VRMP the control samples' organic carbon values were higher than that of *Rhus lancea* and *Tamarix usneoides* at all depths sampled, except at 30-40 cm. This increase could possibly be due to microbial activity around the roots. However, the presence of the trees did not seem to have a major impact in increasing the organic matter in the soil at this site.

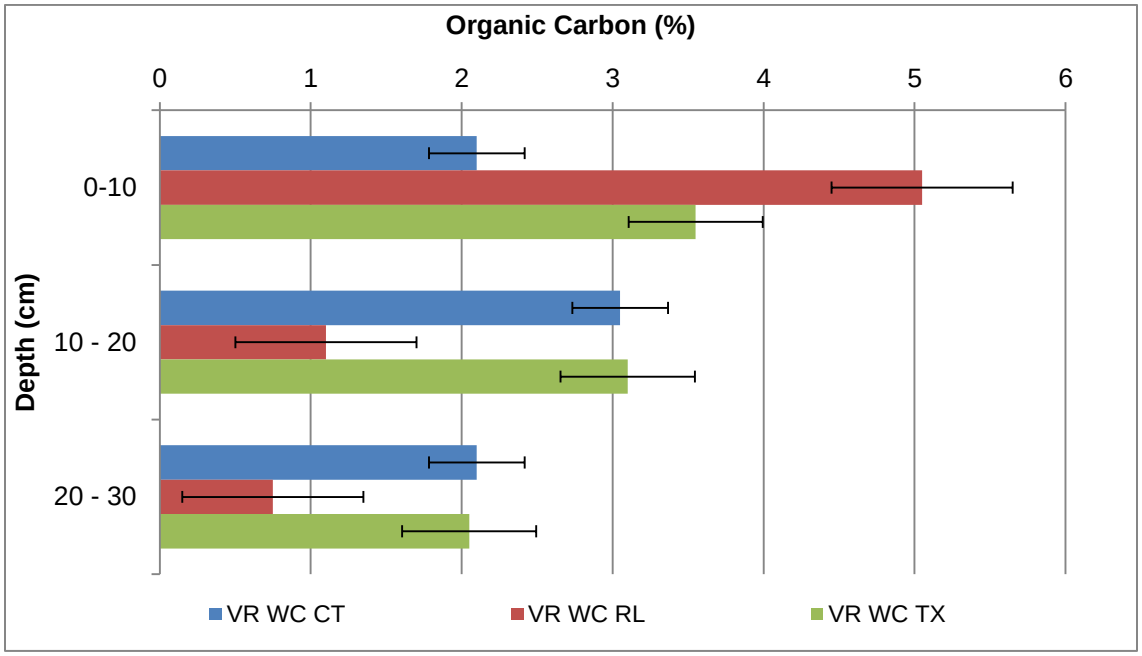

Figure 7.3 Results for variation of organic carbon content with depth for soil at the Vaal River West Complex

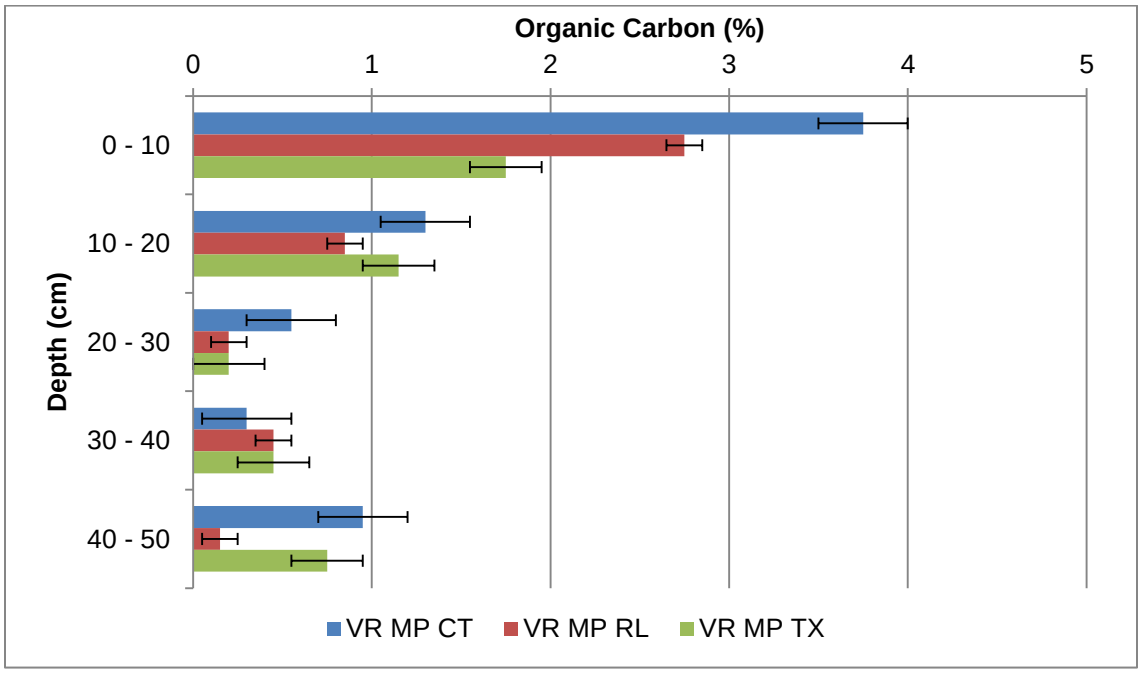

Figure 7.4 Results for variation of organic carbon content with depth for soil at the Vaal River Mispah

7.2.3 Primary nutrients

The results for the variation of primary nutrients (phosphorus, potassium and nitrogen) with depth at the sites are shown in Figures 7.5, 7.6 and 7.7.

Rhus lancea had not improved the phosphorous in the soil at both sites. At the VRWC *Tamarix usneoides* increased the phosphorous through the entire depth profile (0-30 cm). At the VRMP *Tamarix usneoides* increased the phosphorous in the deeper soil samples, from depths 20-50 cm.

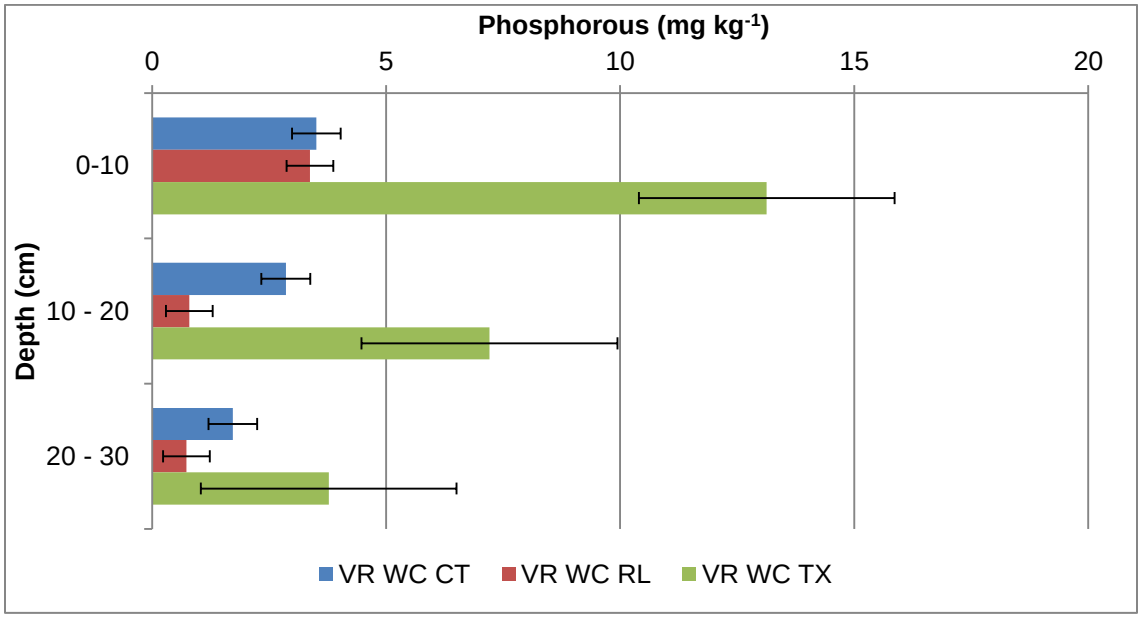

Figure 7.5 Results for phosphorous with depth, for soil at the Vaal River West Complex

At the VRWC *Rhus lancea* did not improve the potassium in the soil, however at VRMP the potassium was increased due to *Rhus lancea* in the entire depth profile that was sampled. At the VRWC *Tamarix usneoides* increased the potassium in the top layer of

soil, i.e. 0-10 cm only, while at the VRMP the potassium was increased by *Tamarix usneoides* in the entire depth profile (0-50 cm).

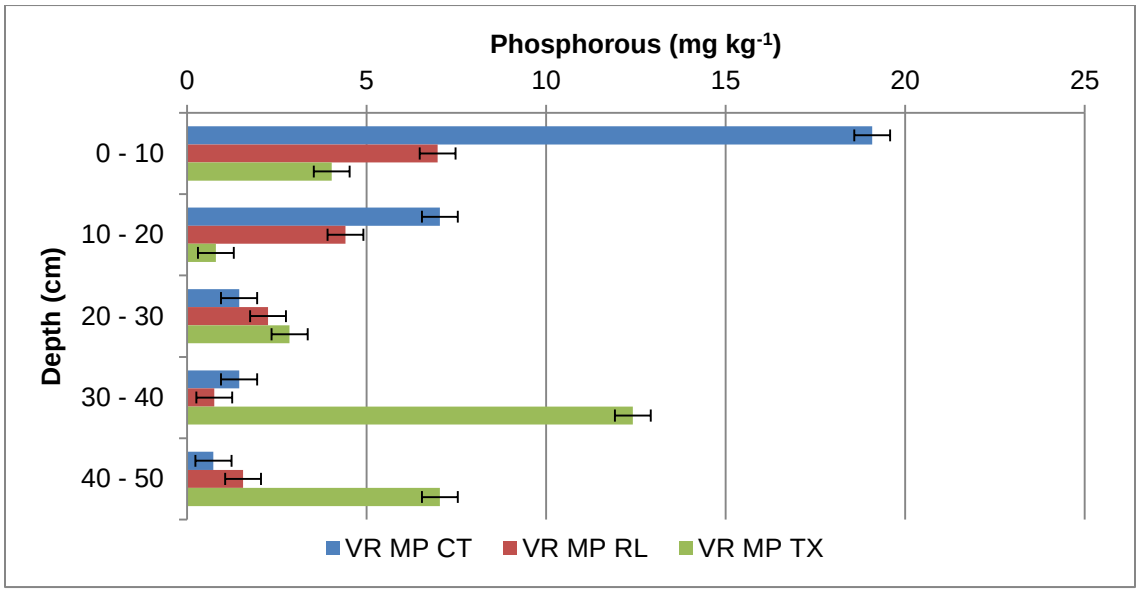

Figure 7.6 Results for phosphorous with depth for soil at the Vaal River Mispah

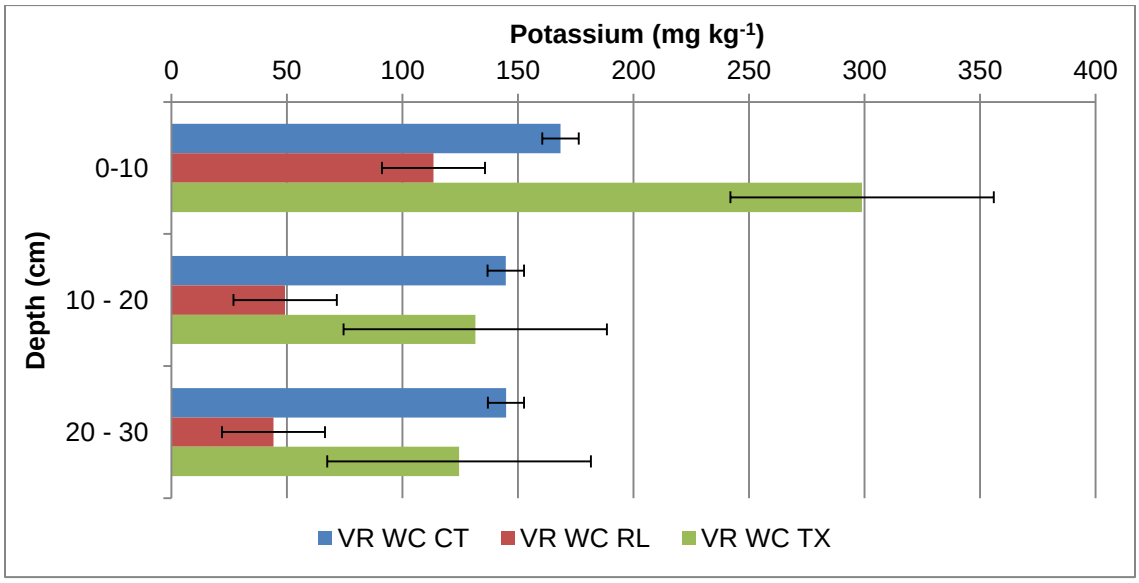

Figure 7.7 Results for potassium with depth for soil at the Vaal River West Complex

At the VRWC *Rhus lancea* increased the nitrogen values in the top layer of soil (0-10 cm), while *Tamarix usneoides* increased the nitrogen values in the entire depth profile (0-30 cm). At VRMP the presence *of Rhus lancea and Tamarix usneoides* had little effect on the nitrogen values in the soil.

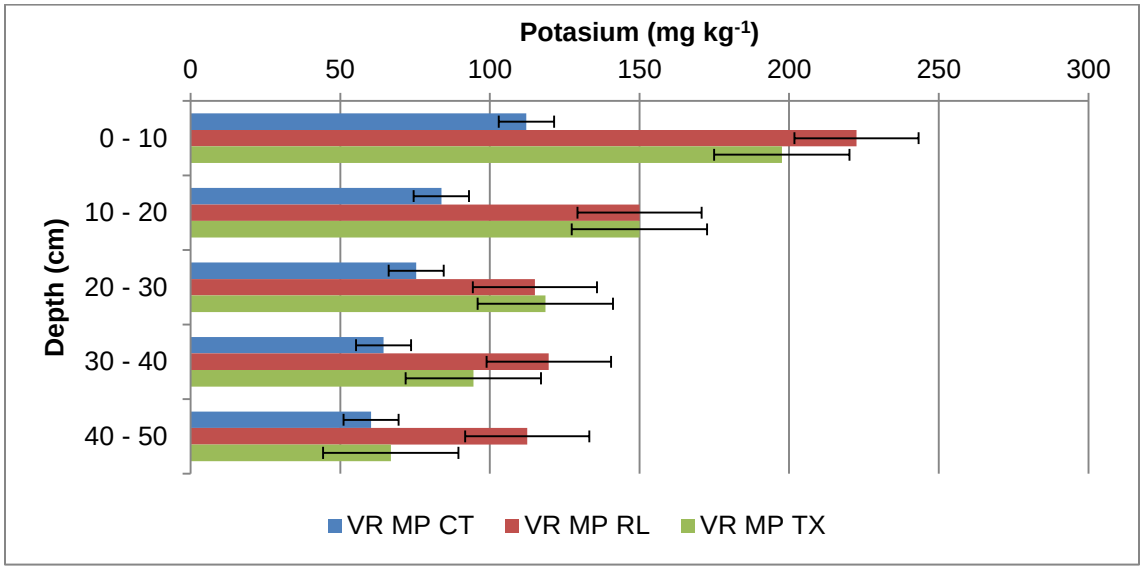

Figure 7.8 Results for potassium with depth for soil at the Vaal River Mispah

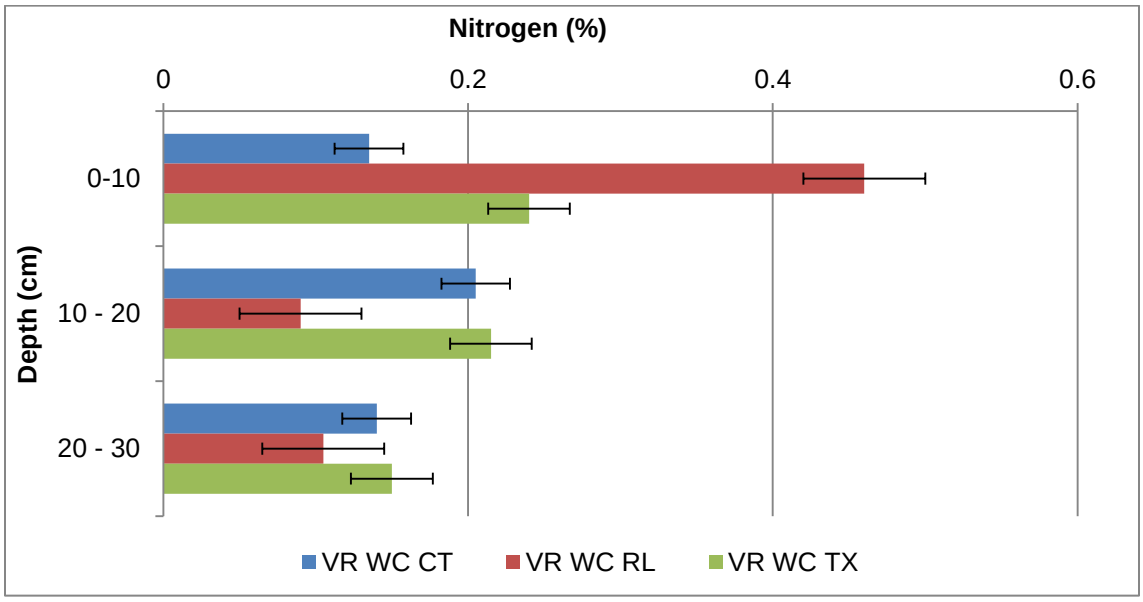

Figure 7.9 Results for nitrogen with depth for soil at the Vaal River West Complex

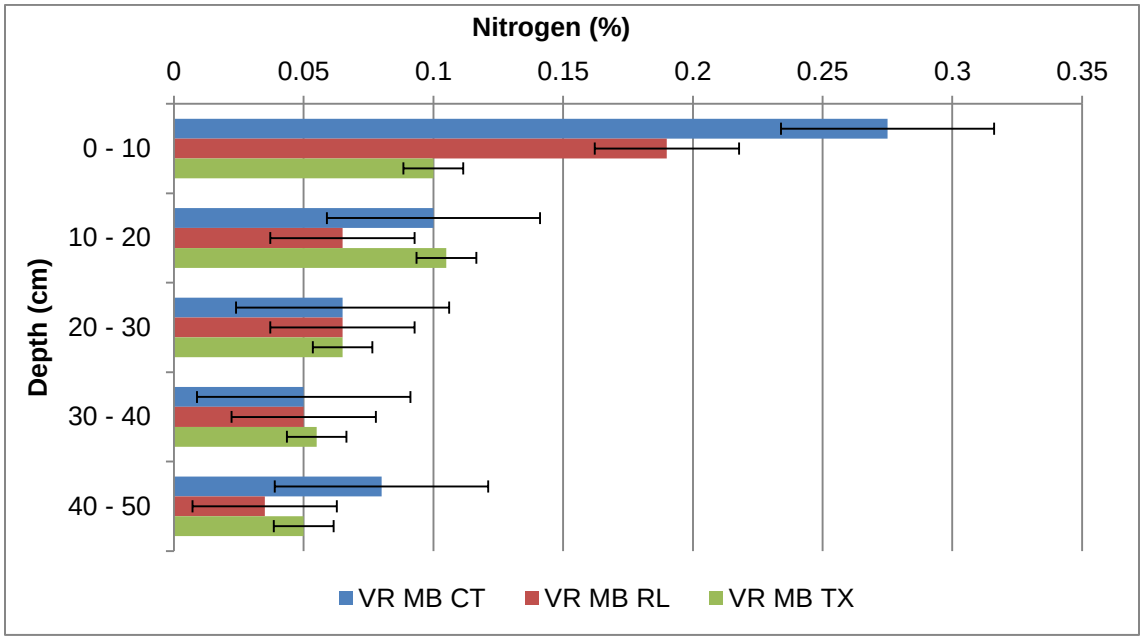

Figure 7.10 Results for nitrogen with depth for soil at the Vaal River Mispah

7.2.4 Secondary nutrients

The results for the variation of secondary nutrients (calcium and magnesium) with depth for the sites are shown in Figures 7.11 and 7.12, and 7.13 and 7.14.

The calcium values in the control soil samples at the VRWC were higher than those for the VRMP site; at the VRWC the calcium was above 700 mg/L, while at the VRMP the calcium was below 250 mg L^{-1}.

At the VRWC *Rhus lancea* increased the calcium values through the entire depth profile (0-30 cm), while *Tamarix usneoides* had little effect on the calcium values in the soil. At the VRMP *Rhus lancea* and *Tamarix usneoides* increased the calcium in the top layers of soil, i.e. 0-20 cm and 0-30 cm, respectively.

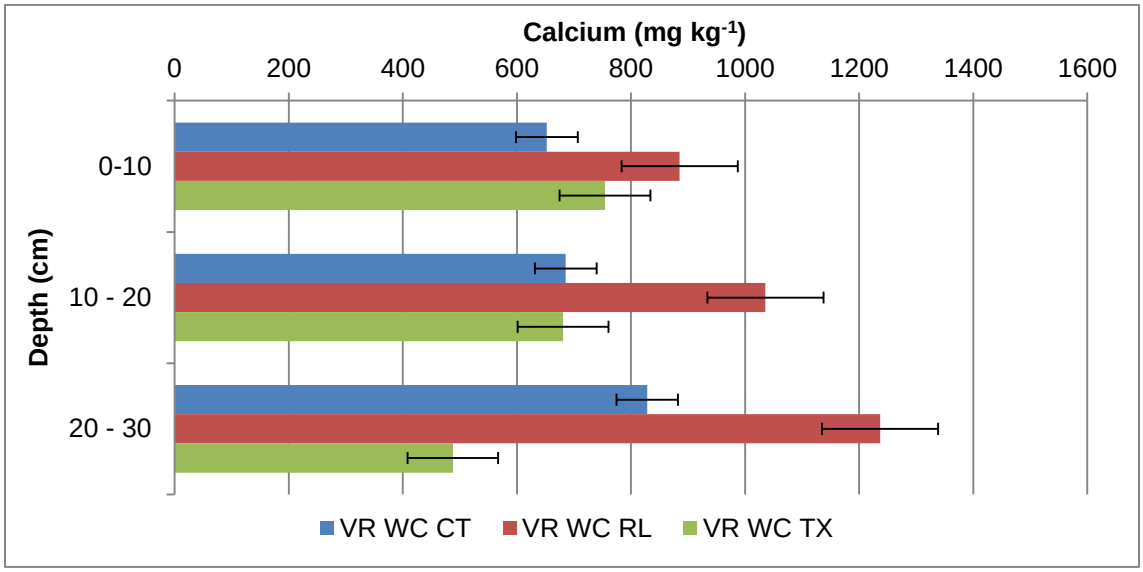

Figure 7.11 Results for calcium with depth for soil at the Vaal River West Complex

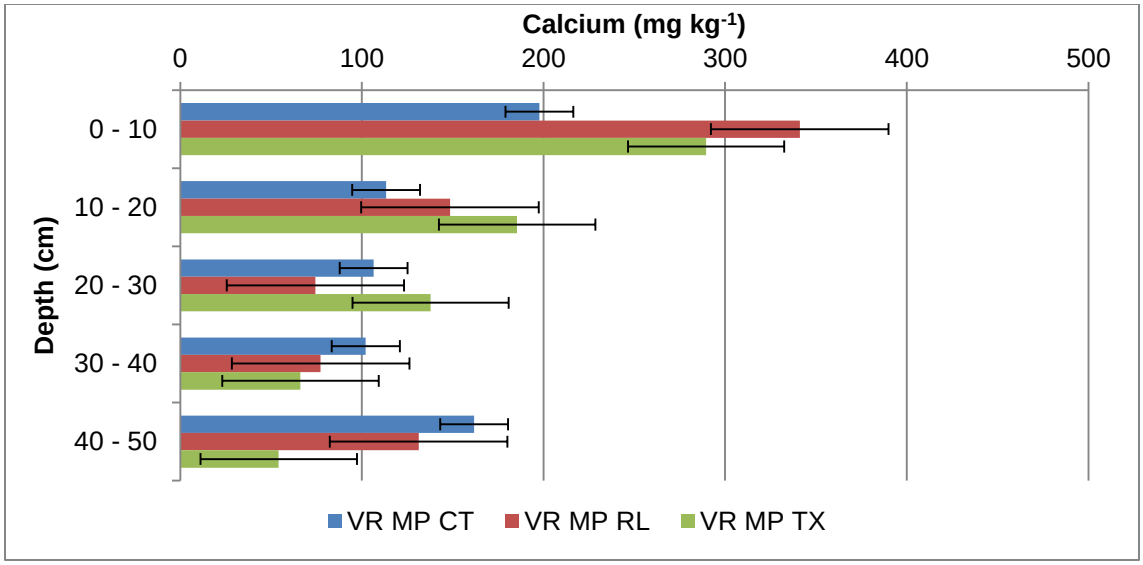

Figure 7.12 Results for calcium with depth for soil at the Vaal River Mispah

The magnesium values in the soil of the control samples at the VRWC were also much higher than that at the VRMP; at the VRWC the calcium was over 190 mg/L, while at the VRMP the calcium was below 100 mg/L.

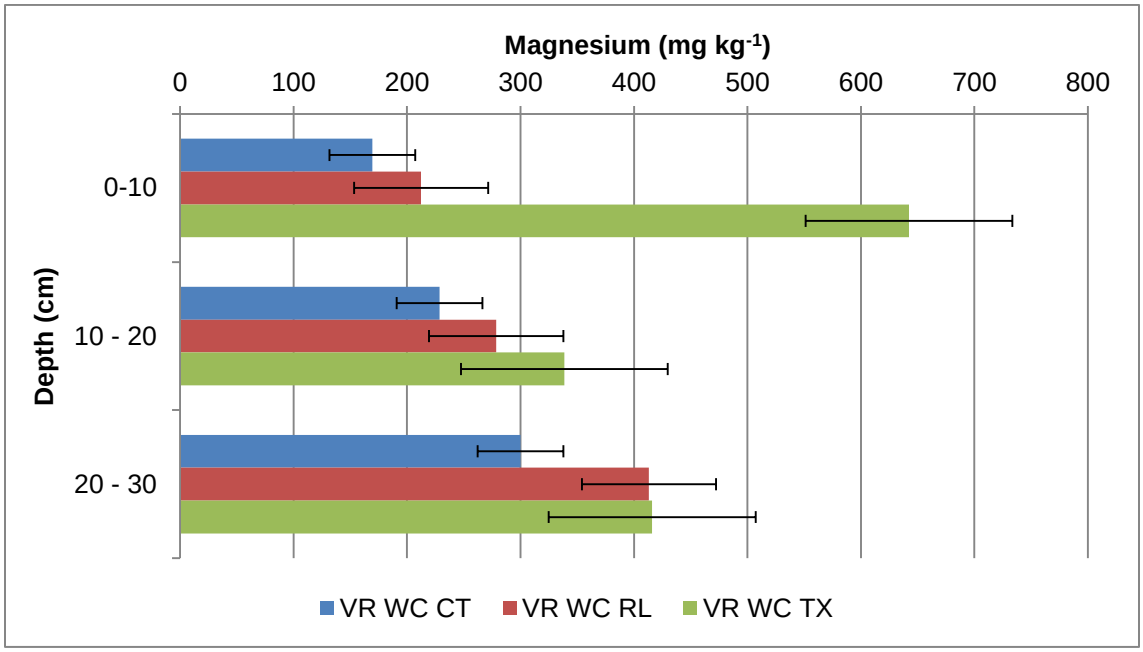

Figure 7.13 Results for magnesium with depth for soil at the Vaal River West Complex

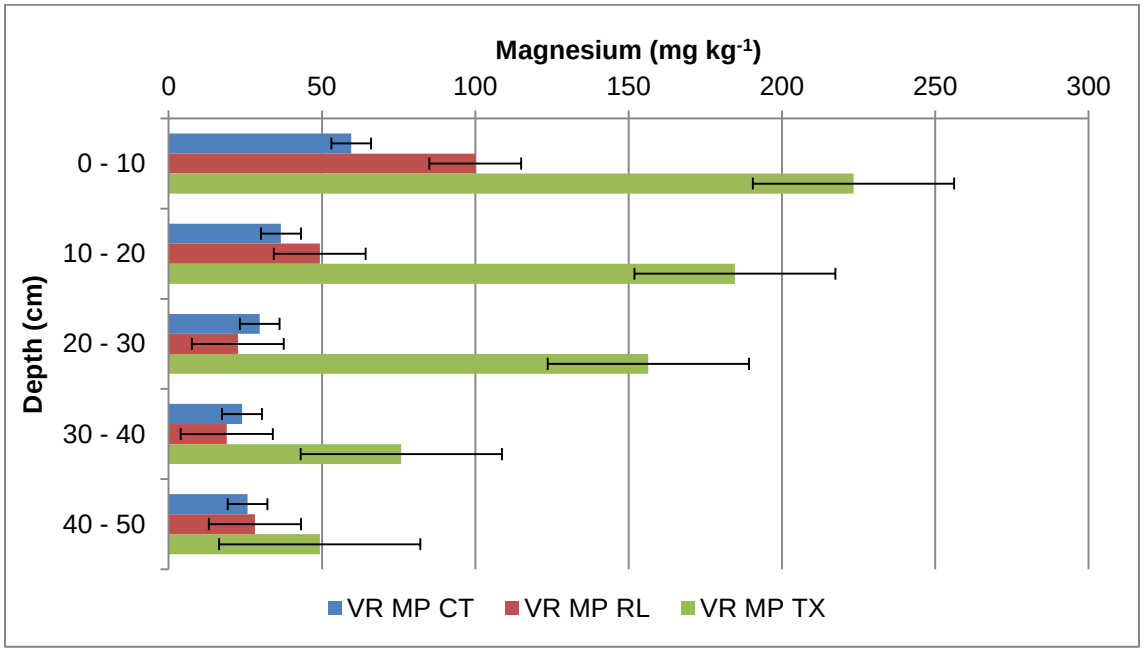

Figure 7.14 Results for magnesium with depth for soil at the Vaal River Mispah

At VRWC *Rhus lancea* increased the magnesium in the deeper soil samples (10-30 cm), while *Tamarix usneoides* improved the magnesium through the entire depth profile sampled. At VRMP *Rhus lancea* increased the magnesium in the top layers of soil (0-20 cm), while *Tamarix usneoides* increased the magnesium through the entire sampled depth (0-50 cm).

7.2.5 Statistical analysis

The descriptive statistics for the soil fertility analysis across the sites, treatment, type of tree, and by depth for the Vaal River sites are shown in Tables 7.8, 7.9, 7.10 and 7.11. Tables 7.8, 7.9 and 7.10 represent the composite sample at all depths. The tables include the mean, median and standard deviation.

Table 7.8 shows that there was a significant difference between VRWC and VRMP in terms of total cations (p = 0.00), cation exchange capacity (p = 0.00) and organic carbon (p = 4.12E-7). VRWC had 129% higher cation exchange capacity, 112% higher total cations and 89% higher organic carbon than the VRMP. Thus, the soil fertility was better at the VRWC.

Table 7.8 Descriptive statistics of soil fertility measurements by site

Determinant	Units	Site	Mean	Median	Standard Deviation	*p-value*
Total cations	cmol L^{-1}	VRWC	8.19	7.34	2.36	0.00
		VRMP	2.30	1.76	1.07	
Cation exchange capacity	cmol kg^{-1}	VRWC	7.22	6.16	1.59	0.00
		VRMP	1.74	1.25	0.88	
Organic carbon	%	VRWC	2.54	2.10	1.26	4.12E-7
		VRMP	1.04	0.75	1.00	

Statistically there was no significant difference between the total cations (p = 0.11), cation exchange capacity (p = 0.13), and organic carbon (p = 0.46) content of the woodland and grassland treatment substrates. Thus no conclusions can be made in terms of the presence of the trees and the improvement with regards to soil fertility.

Table 7.9 Descriptive statistics of soil fertility measurements by treatment

Determinant	Units	Treatment	Mean	Median	Standard Deviation	*p-value*
Total cations	cmol L^{-1}	Grassland	3.60	2.06	2.58	0.11
		Woodland	4.91	3.83	3.52	
Cation exchange capacity	cmol kg^{-1}	Grassland	3.05	1.54	2.14	0.13
		Woodland	4.17	3.03	3.10	
Organic carbon	%	Grassland	1.76	1.70	1.16	0.46
		Woodland	1.52	0.98	1.40	

Table 7.10 indicated that there was no significant difference between *Tamarix usneoides* and *Rhus lancea* with regards to soil fertility, i.e. total cations (p = 0.93), cation exchange capacity (p = 0.78) and organic carbon (p = 0.60). Thus no conclusions can be drawn in terms of improvement of soil fertility in terms of tree type.

Table 7.10 Descriptive statistics of soil fertility measurements by type of tree

Determinant	Units	Tree	Mean	Median	Standard Deviation	*p-value*
Total cations	cmol L^{-1}	*Tamarix usneoides*	4.87	4.18	2.78	0.93
		Rhus lancea	4.96	3.12	4.19	
Cation exchange capacity	cmol kg^{-1}	*Tamarix usneoides*	4.30	3.37	2.97	0.78
		Rhus lancea	4.03	2.38	3.29	
Organic carbon	%	*Tamarix usneoides*	1.63	1.45	1.17	0.60
		Rhus lancea	1.41	0.80	1.61	

The total cations, and cation exchange capacity, increased with depth at the VRWC as shown in Table 7.11 while the total cations and the cation exchange capacity decreased with depth at the VRMP. The top layer of soil always had the highest organic carbon values, and decreased at both sites with depth. The organic carbon percentage values were synonymous with top soil enrichment.

Table 7.11 Descriptive statistics of soil fertility measurements by site and depth

Determinant	Units	Site	Depth	Mean	Median	Standard Deviation
Total cations	cmol L^{-1}	VRWC	0-10	7.19	5.88	2.00
			10-20	7.68	7.34	1.55
			20-30	9.43	8.23	2.93
		VRMP	0-10	3.75	4.07	1.06
			10-20	2.49	2.17	0.84
			20-30	2.05	1.49	0.90
			30-40	1.55	1.45	0.20
			40-50	1.67	1.70	0.98
Cation exchange capacity	cmol kg^{-1}	VRWC	0-10	7.22	6.56	2.13
			10-20	6.68	6.61	0.80
			20-30	7.75	7.09	1.53
		VRMP	0-10	2.95	3.16	0.89
			10-20	1.90	1.60	0.76
			20-30	1.49	1.12	0.62
			30-40	1.12	1.10	0.11
			40-50	1.24	1.25	0.13
Organic carbon	%	VRWC	0-10	3.57	3.55	1.28
			10-20	2.42	3.05	0.99
			20-30	1.63	2.05	0.66
		VRMP	0-10	2.75	2.75	0.87
			10-20	1.10	1.15	0.20
			20-30	0.32	0.20	0.18
			30-40	0.40	0.45	0.08
			40-50	0.62	0.75	0.36

The soil fertility data was extracted into one component by PCA (Table C3, Appendix C) as indicated in Table 7.12 which included all three parameters, i.e. total cations,

cation exchange capacity and organic carbon, with a variance of 74.3%. The histogram (Figure C5, Appendix C) indicated that the component was not normally distributed.

Table 7.12 The PCA of the soil fertility measurements

Data set	Component	Parameters included	Normally distributed
Soil fertility	1	Total cations, cation exchange capacity, organic carbon	No

7.3 CHNS analysis

The CHNS analysis included the elemental ratios, and the statistical analysis, to check whether the presence of the trees has significantly caused a change.

7.3.1 Elemental ratios

Figure 7.15 shows the $\frac{10cm}{30cm}$ ratios for carbon, hydrogen, and nitrogen at the Vaal River West Complex. Figure 7.16 shows the $\frac{10cm}{50cm}$ ratios for carbon, hydrogen, and nitrogen at the Vaal River Mispah. The graphs compare the control samples (CT), with that of samples taken from the rooting area of *Rhus lancea* (RL) and *Tamarix usneoides* (TX) trees. Sulphur was undetected in the soil at both sites.

At the VRWC the control samples' carbon, hydrogen and nitrogen $\frac{10cm}{30cm}$ ratios were around 1, indicating that the carbon, nitrogen, and hydrogen concentrations were similar in the top layer and bottom layers of soil. *Rhus lancea* increased the $\frac{10cm}{30cm}$ ratios

of carbon, nitrogen and hydrogen. *Tamarix usneoides* increased the carbon $\frac{10cm}{30cm}$ ratio, and decreased the hydrogen and nitrogen $\frac{10cm}{30cm}$ ratios in the soil.

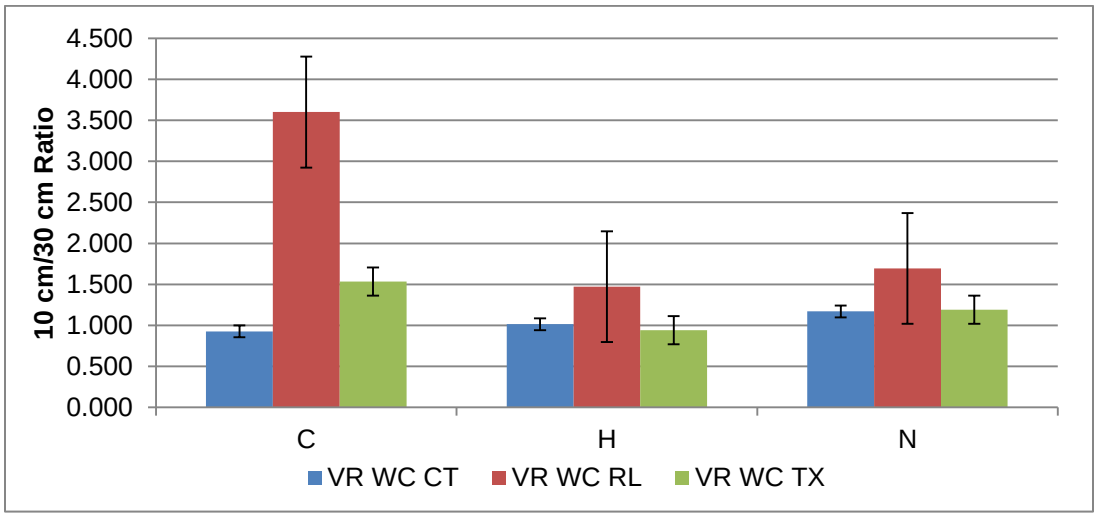

Figure 7.15 $\frac{10cm}{30cm}$ ratio curves for carbon, hydrogen, and nitrogen at the Vaal River West Complex

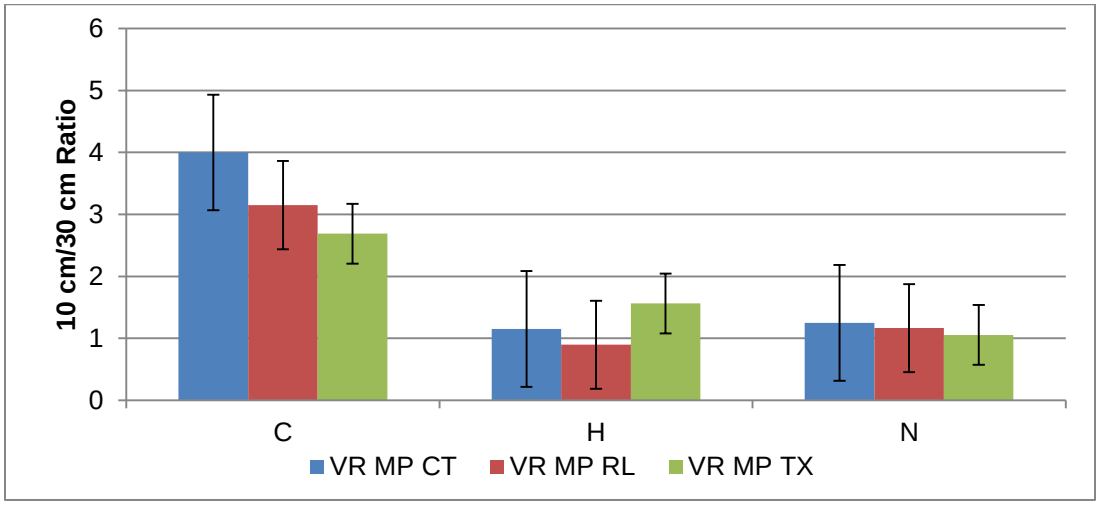

Figure 7.16 $\frac{10cm}{50cm}$ ratio curves for carbon, hydrogen and nitrogen at the Vaal River Mispah

At the VRMP the control samples' hydrogen and nitrogen $\frac{10cm}{50cm}$ ratios were around 1, indicating that the concentrations of these elements were similar in the top and bottom layers of soil sampled. However, the carbon $\frac{10cm}{50cm}$ ratio had a value of 4, which indicated that the concentration of carbon was 4 times higher in the top layer of soil compared to the bottom layer. *Rhus lancea* decreased the carbon, hydrogen and nitrogen $\frac{10cm}{50cm}$ ratios. *Tamarix usneoides* increased the carbon and nitrogen $\frac{10cm}{50cm}$ ratios, and decreased the hydrogen $\frac{10cm}{50cm}$ ratio.

An increased $\frac{Top\ depth}{Bottom\ depth}$ elemental ratio indicated that the concentration of these elements in the top layer of soil had increased, largely due to top soil enrichment. A decreased $\frac{Top\ depth}{Bottom\ depth}$ elemental ratio indicated that these elements increased in the bottom layer of soil which was sampled. Accumulation within the soil could be due to absorbance of these elements from the rooting zone, which would concentrate them in the deeper samples. The increased carbon in the top layer of soil for *Rhus lancea* related to the high leaf index of the tree, leading to top soil enrichment in terms of carbon.

7.3.2 Statistical analysis

The descriptive statistics for the CHNS analysis across the sites, treatment, type of tree, and by depth for the Vaal River sites are shown in Tables 7.13, 7.14, 7.15, and 7.16. Tables 7.13, 7.14 and 7.15 represent the composite sample at all depths. The tables include the mean, median and standard deviation.

Table 7.13 showed that the percentage of carbon (p = 0.00), and hydrogen (p = 0.00) were statistically significantly different at the two sites, while nitrogen was not

significantly different (p = 0.15). The carbon and hydrogen percentages were 121%, and 48% higher at the VRWC, compared to that of the VRMP.

Table 7.14 indicated that there was no significant difference between the woodland and the grassland substrates in terms of carbon (p = 0.89), hydrogen (p = 0.23), and nitrogen (p = 0.26), hence no conclusions can be made with respect to the improvement of the soil by the trees.

Table 7.13 Descriptive statistics of CHNS data by site

Determinant	Units	Site	Mean	Median	Standard Deviation	*p-value*
Carbon	%	VRWC	2.12	1.95	0.76	0.00
		VRMP	0.53	0.35	0.33	
Hydrogen	%	VRWC	0.55	0.51	0.07	0.00
		VRMP	0.34	0.32	0.07	
Nitrogen	%	VRWC	0.34	0.36	0.06	0.15
		VRMP	0.31	0.32	0.08	

Table 7.14 Descriptive statistics of CHNS data by treatment

Determinant	Units	Treatment	Mean	Median	Standard Deviation	*p-value*
Carbon	%	Grassland	1.15	1.00	0.84	0.89
		Woodland	1.11	0.69	0.99	
Hydrogen	%	Grassland	0.39	0.37	0.12	0.23
		Woodland	0.43	0.44	0.13	
Nitrogen	%	Grassland	0.33	0.34	0.03	026
		Woodland	0.31	0.36	0.09	

Table 7.15 showed that *Tamarix usneoides* and *Rhus lancea* showed no significant difference for carbon (p = 0.66) and hydrogen (p = 0.86), but showed a significant difference for nitrogen (p = 2.14E-14). *Tamarix usneoides* had 46% higher nitrogen compared to that of *Rhus lancea*.

Table 7.15 Descriptive statistics of CHNS data by type of tree

Determinant	Units	Tree	Mean	Median	Standard Deviation	*p-value*
Carbon	%	*Tamarix usneoides*	1.18	0.62	1.04	0.66
		Rhus lancea	1.05	0.82	0.97	
Hydrogen	%	*Tamarix usneoides*	0.43	0.46	0.11	0.86
		Rhus lancea	0.43	0.39	0.14	
Nitrogen	%	*Tamarix usneoides*	0.38	0.39	0.02	2.14E-14
		Rhus lancea	0.24	0.22	0.06	

Table 7.16(a) Descriptive statistics of carbon and hydrogen data by site and depth

Determinant	Units	Site	Depth	Mean	Median	Standard Deviation
Carbon	%	VRWC	0-10	2.70	2.88	0.70
			10-20	2.09	2.52	0.68
			20-30	1.59	1.87	0.49
		VRMP	0-10	1.07	1.17	0.29
			10-20	0.63	0.65	0.06
			20-30	0.31	0.29	0.03
			30-40	0.29	0.29	0.02
			40-50	0.32	0.34	0.05
Hydrogen	%	VRWC	0-10	0.58	0.51	0.11
			10-20	0.56	0.58	0.04
			20-30	0.51	0.50	0.02
		VRMP	0-10	0.41	0.39	0.04
			10-20	0.37	0.32	0.07
			20-30	0.29	0.30	0.03
			30-40	0.28	0.28	0.03
			40-50	0.35	0.34	0.05

Tables 7.16 (a) and (b) indicated that at the VRWC, the carbon, hydrogen, and nitrogen percentages decreased with depth. At the VRMP the carbon and nitrogen

percentages decreased with depth, while the hydrogen percentage decreased, then increased with depth.

Table 7.16(b) Descriptive statistics of nitrogen data by site and depth

Determinant	Units	Site	Depth	Mean	Median	Standard Deviation
Nitrogen	%	VRWC	0-10	0.38	0.39	0.02
			10-20	0.33	0.37	0.06
			20-30	0.29	0.31	0.05
		VRMP	0-10	0.34	0.37	0.08
			10-20	0.32	0.35	0.08
			20-30	0.30	0.32	0.08
			30-40	0.30	0.31	0.09
			40-50	0.30	0.29	0.08

The CHNS data was represented in two components by PCA (Table C4, Appendix C) as shown in Table 7.17. Component 1 included: carbon, and hydrogen, and Component 2 included: nitrogen, with an 83.40% variance. From the histograms (Figures C6, C7, Appendix C) component 1 was not normally distributed, while component 2 was normally distributed.

Table 7.17 The PCA of the CHNS data

Data set	Component	Parameters included	Normally distributed
CHNS data	1	Carbon, hydrogen	No
CHNS data	2	Nitrogen	Yes

7.4 Summary and conclusions

The results for the physical soil analysis was summarised and concluded within each set of results, i.e. soil texture, soil fertility and CHNS data.

7.4.1 Soil texture

The presence of the trees showed a minor change in the soil texture, by introducing more clay particles, into predominantly sandy soil; the soil texture has become more central in the soil texture triangle. This was substantiated by the statistical analysis where the clay (p = 2.74E-3) and bulk density (p = 0.03) were significantly different for the woodland treatment compared to the grassland treatment; 18% higher clay content, and 1% lower bulk density than the grassland treatment, hence the water retention of the soil has improved slightly.

There was a significant difference between the clay (p = 5.10E-6), silt (p = 4.75E-19), and sand (p = 2.49E-9) at the two sites; the VRMP had 26% higher clay, 15% higher silt and higher sand 6%, than VRWC, hence the soil texture differs at each site.

Tamarix usneoides and *Rhus lancea* showed no significant difference in terms of soil texture, as the *p-values* were all above 0.05, hence no conclusions can be drawn with regards to tree type and the effect on soil texture.

At a landfill site where the same trees have been planted, even though the soil texture in the control was different (sandy clay loam), the trees have introduced finer particles into the soil, and have changed the soil texture to clay loam (Arendze, unpublished).

The soil texture data could be represented by two components: Component 1 including: clay, silt and bulk density, and Component 2 including: sand.

7.4.2 Soil fertility

The presence of the trees have shown no significant difference in terms of soil fertility (p >0.05); when comparing the woodland versus the grassland treatment, hence no conclusions can be made in terms of the presence of the trees and the effect on soil fertility.

The soil at the VRWC site had better soil fertility than that at VRMP, as the total cations (112%), cation exchange capacity (129%) and organic carbon (89%) were higher at VRWC than VRMP. The statistical analysis confirmed that the difference in the soil fertility parameters at the two sites was significant (p <0.05)

When comparing the trees, there was no statistically significant difference between the soil fertility in the presence of *Tamarix usneoides* and *Rhus lancea*; thus no conclusions can be made with regards to soil fertility and tree type.

The soil fertility data was extracted into one component by PCA.

7.4.3 CHNS analysis

Sulphur was not detected in the soil at both sites. At VRWC *Rhus lancea* increased the $\frac{10cm}{30cm}$ ratios of carbon, nitrogen, and hydrogen, while *Tamarix usneoides* increased the carbon $\frac{10cm}{30cm}$ ratio, and decreased the hydrogen and nitrogen $\frac{10cm}{30cm}$ ratios in the soil. At VRMP *Rhus lancea* decreased the carbon, hydrogen and nitrogen $\frac{10cm}{50cm}$ ratio. *Tamarix*

usneoides increased the carbon and nitrogen $\frac{10cm}{50cm}$ ratios, and decreased the hydrogen $\frac{10cm}{50cm}$ ratios.

At a landfill site where the same trees were planted, *Rhus lancea* and Tamarix *usneoides* decreased the carbon, hydrogen and nitrogen $\frac{10cm}{30cm}$ ratios, so the observed trend was similar to that seen at VRMP (Arendze, unpublished).

The woodland substrate showed no significant difference in the carbon, hydrogen and nitrogen percentages (p >0.05) in the soil compared to that of the grassland substrate, thus no conclusions can be made in terms of improvement in the presence of the trees.

The carbon (p = 0.00), and hydrogen (p = 0.00) showed a significant difference in concentration at the two sites; i.e. they were 121% and 48% higher respectively at VRWC compared to VRMP. The nitrogen concentration was 46% significantly higher (p = 2.14E-14) in the presence of *Tamarix usneoides* compared to *Rhus lancea*.

The CHNS data was represented in two components by PCA, including carbon and hydrogen in the first component and nitrogen in the second component.

CHAPTER EIGHT – SEQUENTIAL EXTRACTION RESULTS

This section presents the sequential extraction results for the two sites. Results are presented major nutrients and trace elements. The BCR extraction curves with depth, and the statistical analysis are included to deduce whether the trees have affected the mobility of the major nutrients and trace elements. The last section presents the percentage distribution curves, which gave an idea where the major percentage fractions of each element were and whether there was drastic change in the presence of the trees.

8.1 Major nutrients

The major nutrients included calcium, magnesium, phosphorous, potassium, and sulphur. Firstly, the BCR extraction curves were plotted, then the major nutrient ratios were calculated and lastly the statistical analysis was done in order to ascertain whether the trees have changed the mobility of the major nutrients in the soil.

8.1.1 BCR extraction curves

BCR extraction curves were plotted for each major nutrient at each site; and compared the control samples (CT) with samples taken from the rooting zone of *Rhus lancea* (RL) and *Tamarix usneoides* (TX) trees.

If data on the BCR sequential extraction curves are not visible on the graph, then the data was likely below the detection limits for that data point.

Calcium

Calcium BCR extraction curves at the VRWC and VRMP are shown in Figures 8.1 and 8.2.

At both sites the calcium in the control was mobilised in the first fraction indicating that the calcium was mainly bound to carbonate. At the VRWC, *Rhus lancea* increased the concentration of calcium ions in the first fraction through all depths (0-30 cm) while *Tamarix usneoides* increased the calcium concentration only in the top layer (0-10 cm) of soil in the same fraction. At the VRMP, *Rhus lancea* increased calcium concentrations in the carbonate-bound fraction at all depths except at 20-30 cm while *Tamarix usneoides* increased the concentration of the first fraction through all the depths sampled (0-50 cm).

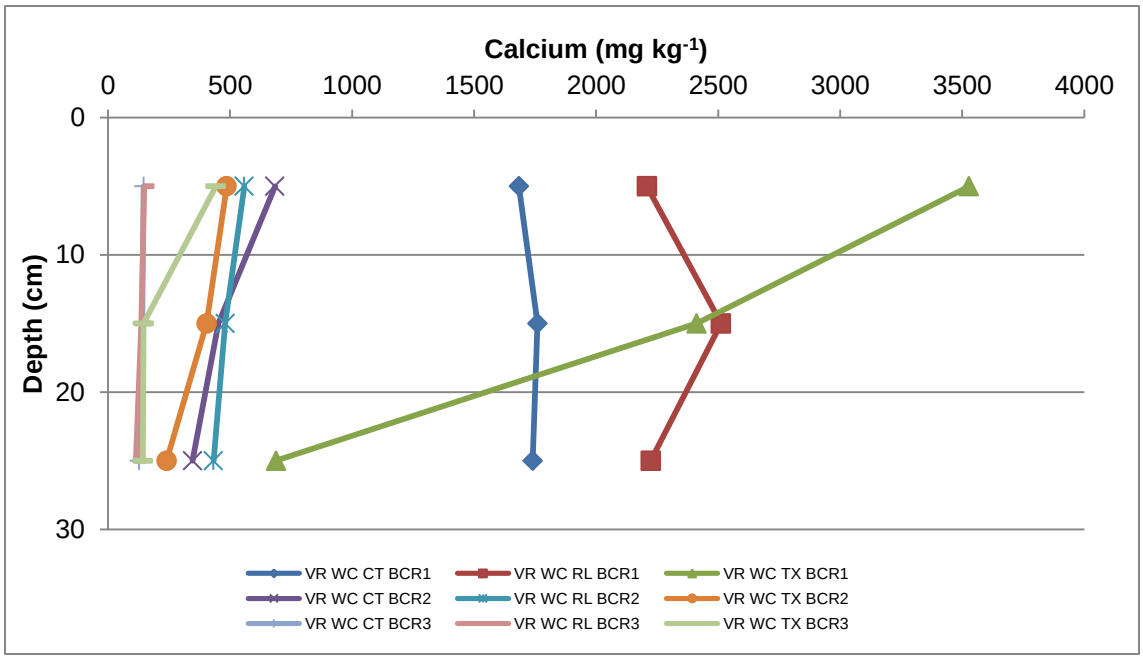

Figure 8.1 BCR sequential extraction curve with depth for calcium at the Vaal River West Complex

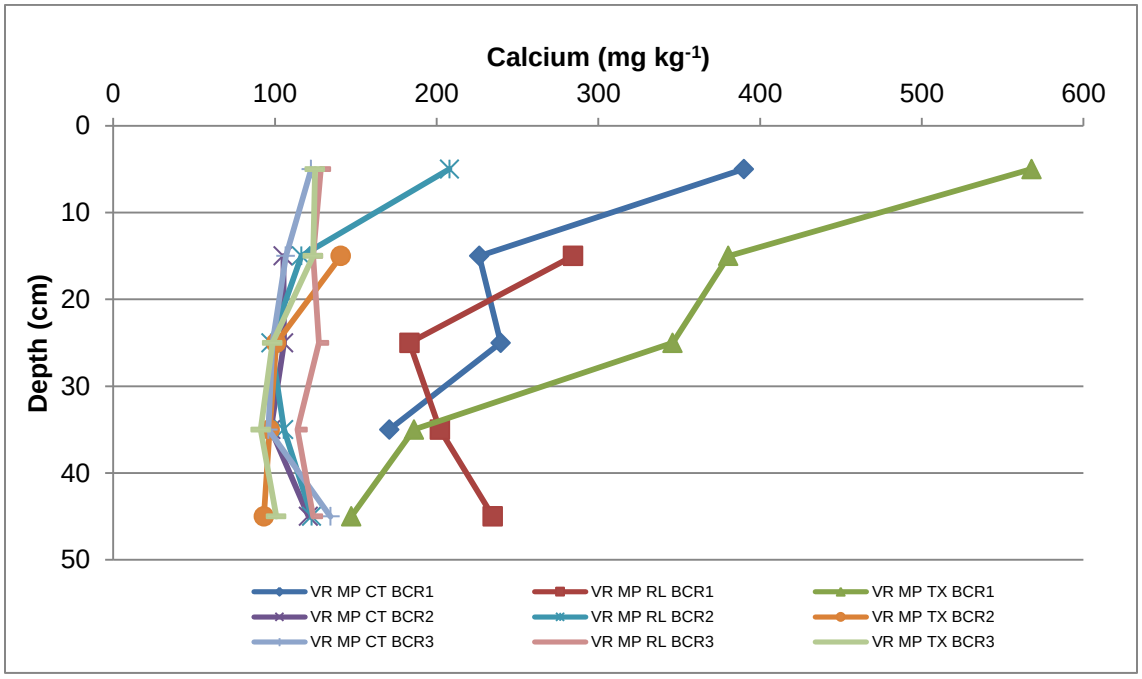

Figure 8.2 BCR sequential extraction curve with depth for calcium at the Vaal River Mispah

Magnesium

Magnesium BCR extraction curves at the VRWC and VRMP are shown in Figures 8.3 and 8.4. Magnesium in the control sample was mobile in the first fraction at both sites, indicating that it was mainly carbonate bound.

At the VRWC, *Rhus lancea* and *Tamarix usneoides* increased the magnesium concentration in the first fraction in all depths (0-30 cm). At VRMP *Rhus lancea* increased the magnesium concentration in the first fraction in the top layer (0-10 cm) of soil while *Tamarix usneoides* increased concentration through all sampled depths (0 – 50 cm).

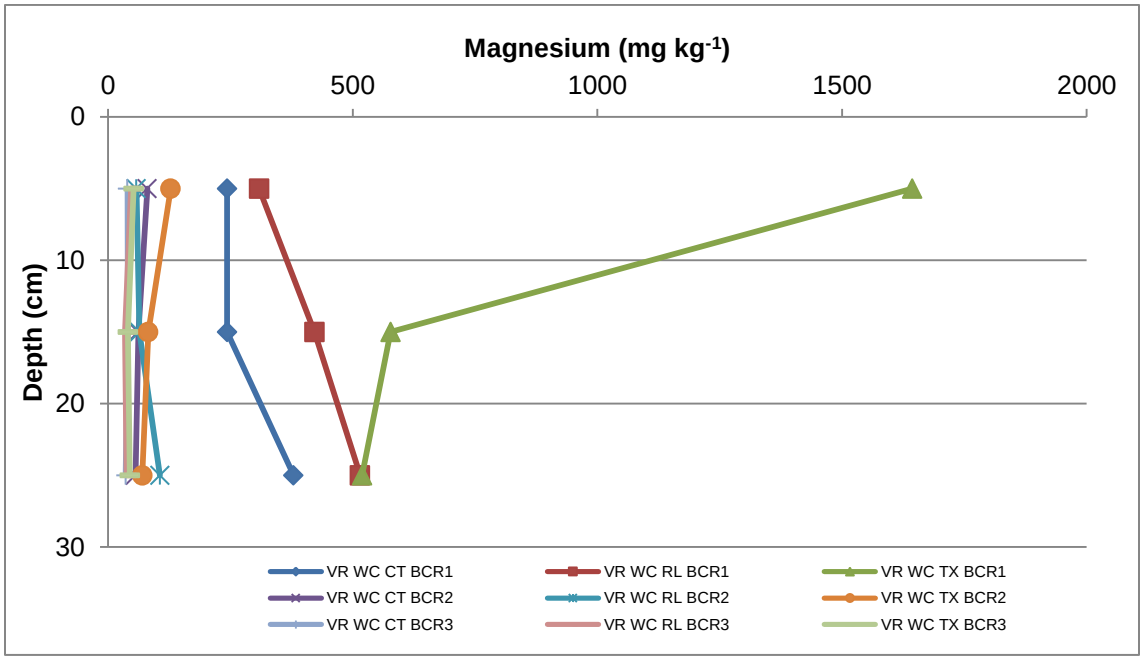

Figure 8.3 BCR sequential extraction curve with depth for magnesium at the Vaal River West Complex

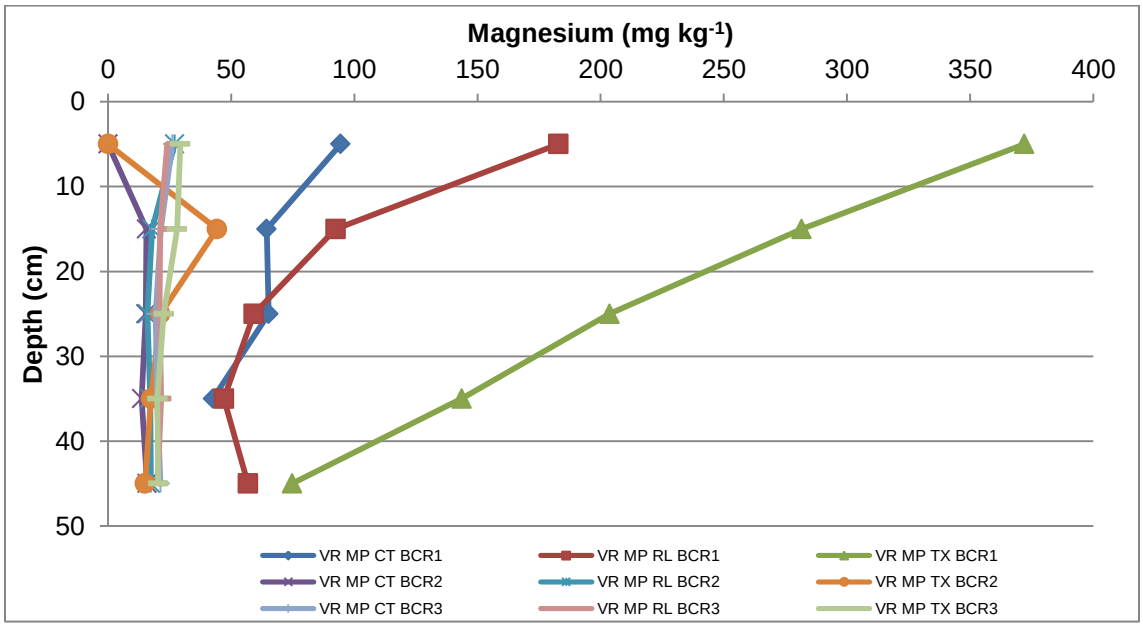

Figure 8.4 BCR sequential extraction curve with depth for magnesium at the Vaal River Mispah

Phosphorous

Phosphorous BCR extraction curves at the VRWC and VRMP are shown in Figures 8.5 and 8.6.

In the control samples phosphorous was most mobile in the third fraction which indicated that it was mainly organic bound at both sites. At the VRWC *Rhus lancea* increased organic bound phosphorous in the top layer (0-10 cm) of soil, while *Tamarix usneoides* increased the same phosphorous fraction in all depths (0-30 cm).

At VRMP *Rhus lancea* increased phosphorous concentration in the third fraction in all depths sampled (0-30 cm), while *Tamarix usneoides* increased concentration in the deeper soil samples (20-50 cm).

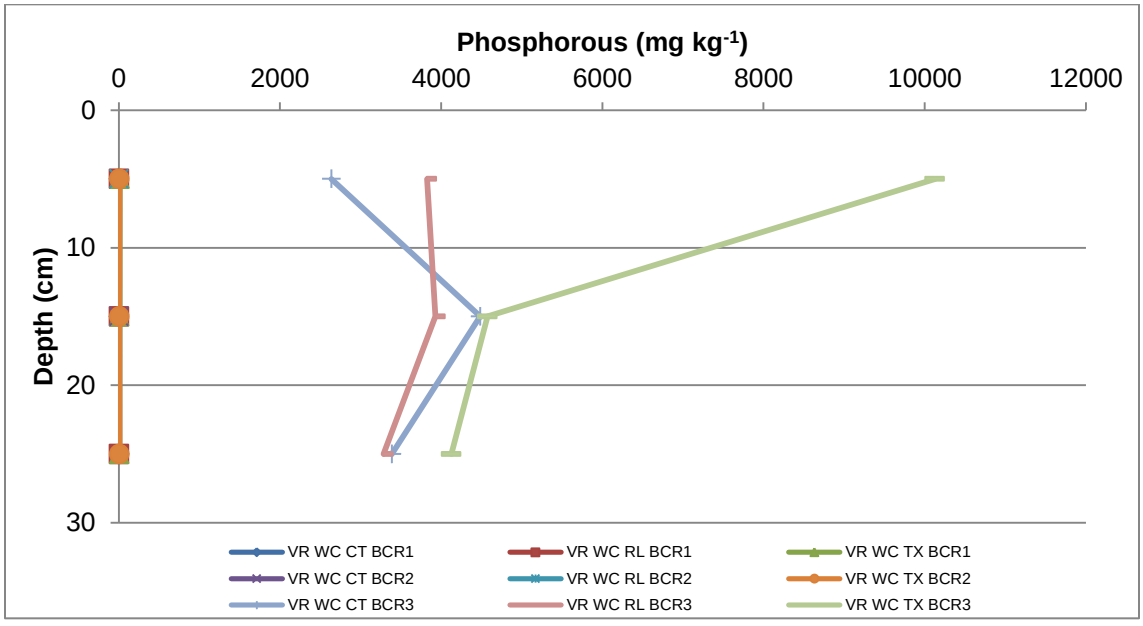

Figure 8.5 BCR sequential extraction curve with depth for phosphorous at the Vaal River West Complex

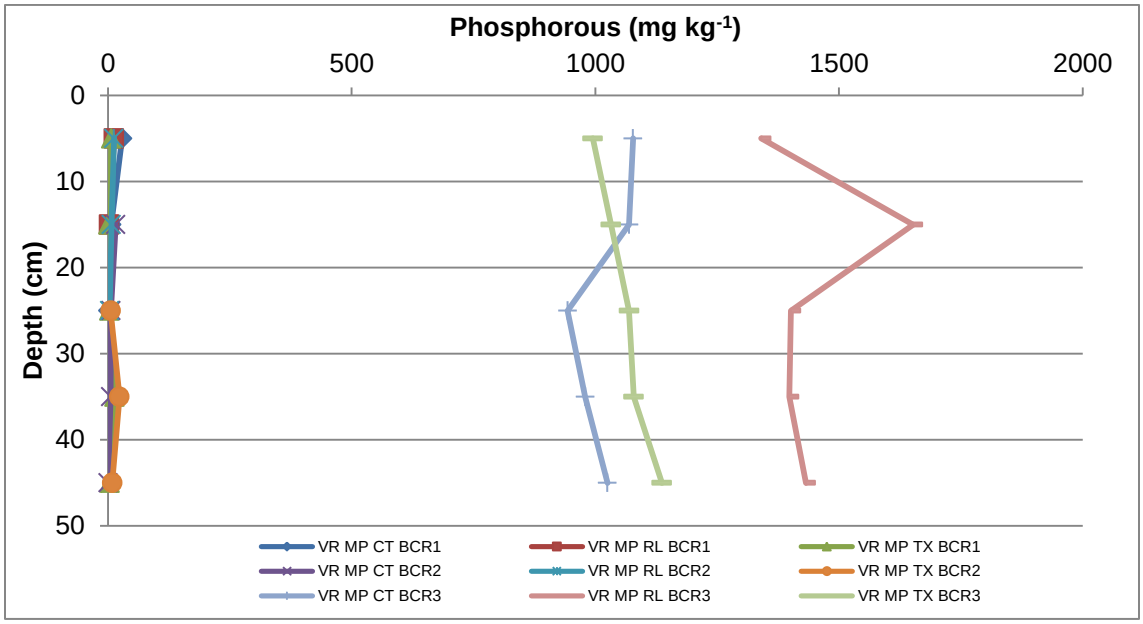

Figure 8.6 BCR sequential extraction curve with depth for phosphorous at the Vaal River Mispah

Potassium

Potassium BCR extraction curves at the VRWC and VRMP are shown in Figures 8.7 and 8.8. The control samples indicated that potassium was mobile in all three BCR fractions at the VRWC, while at the VRMP it was mobile in the carbonate fraction.

At the VRWC *Rhus lancea* increased the concentration of potassium in all three fractions in all sample depths (0-30 cm), while *Tamarix usneoides* only increased the concentration in the first fraction in all depths (0-30 cm).

At VRMP *Rhus lancea* increased the concentration of potassium in the carbonate and organic fractions in all depths (0-50 cm); generally the increase in the third fraction was greater in deeper samples, while the increase in the first fraction was greater in top layers of soil. *Tamarix usneoides* increased the concentration of carbonate bound potassium, in all sample depths (0-50 cm) at the VRMP.

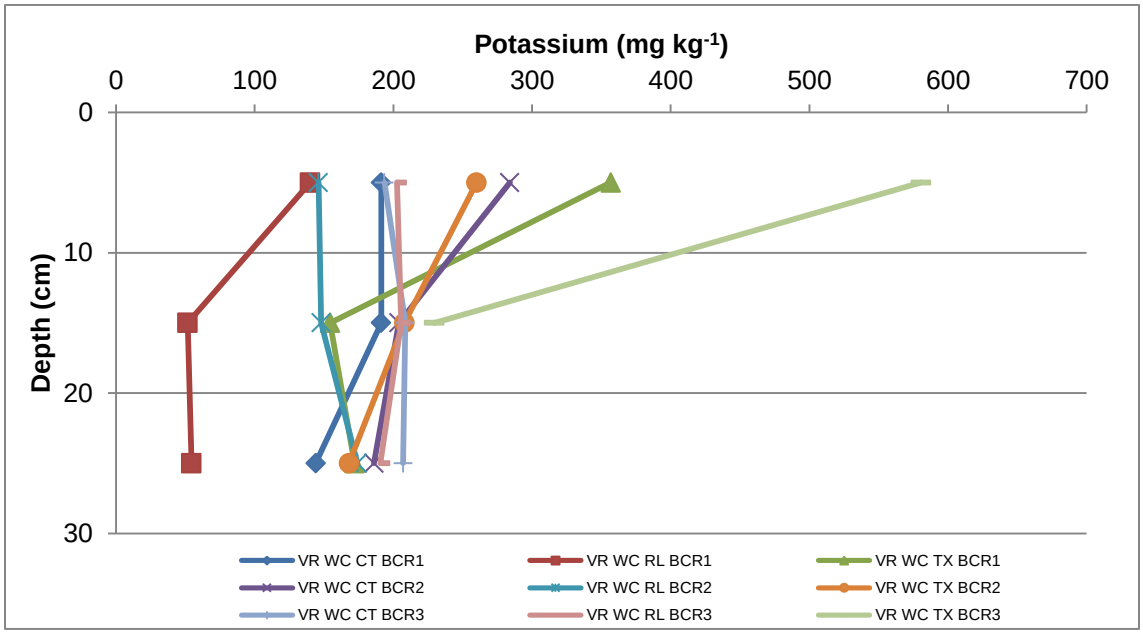

Figure 8.7 BCR sequential extraction curve with depth for potassium at the Vaal River West Complex

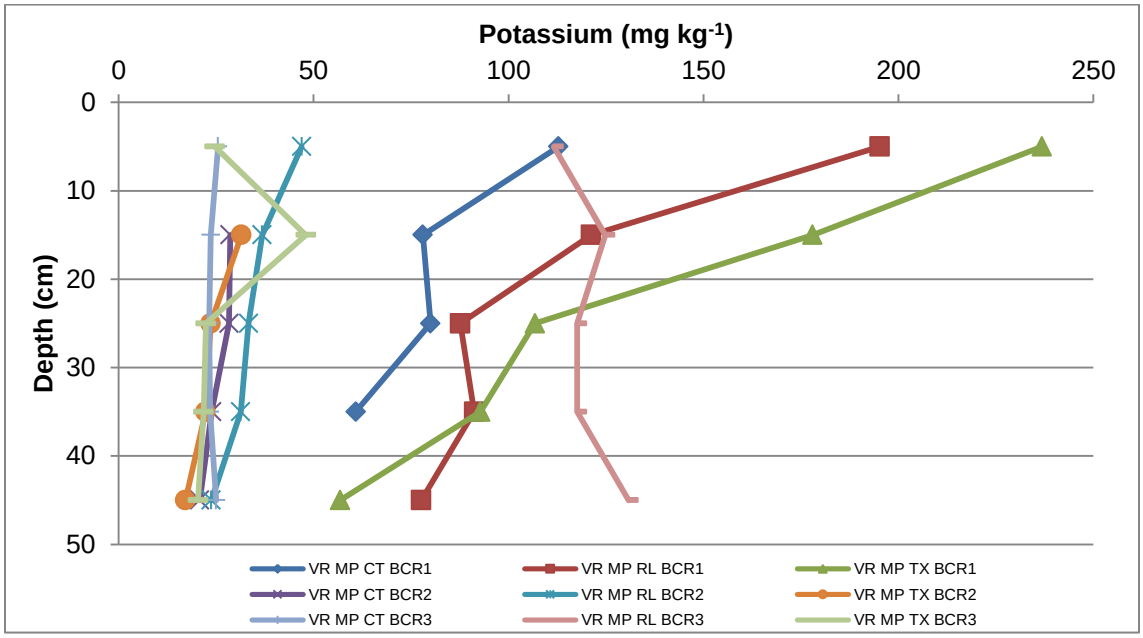

Figure 8.8 BCR sequential extraction curve with depth for potassium at the Vaal River Mispah

Sulphur

Sulphur BCR extraction curves at VRWC and VRMP are shown in Figures 8.9 and 8.10.

In the control samples, sulphur was most mobile in the first fraction at the VRWC and in all three fractions at the VRMP. At the VRWC, *Rhus lancea* and *Tamarix usneoides* increased the concentration of sulphur bound to carbonates in all depths (0-30 cm). At the VRMP, *Rhus lancea* and *Tamarix usneoides* increased the concentration of sulphur bound to organics in all sampled depths (0-50 cm). It should be noted however that this sulphur could also be from an organic source, notably decomposed plant matter. No further distinctions were made to ascertain the source and this would require further assessment in future studies.

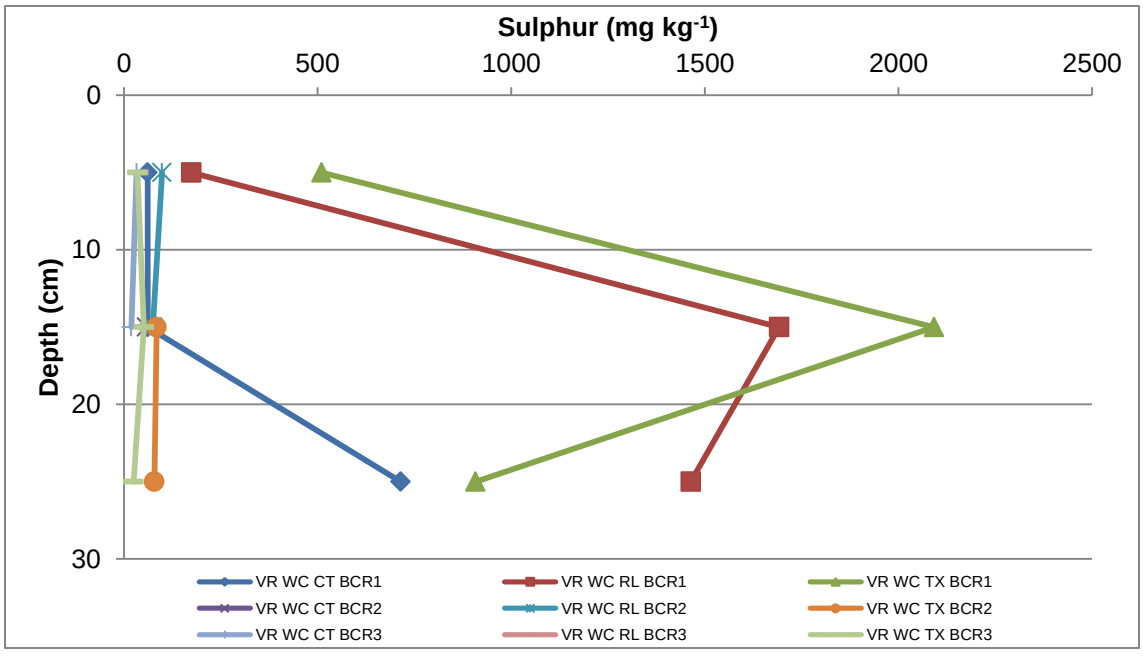

Figure 8.9 BCR sequential extraction curve with depth for sulphur at the Vaal River West Complex

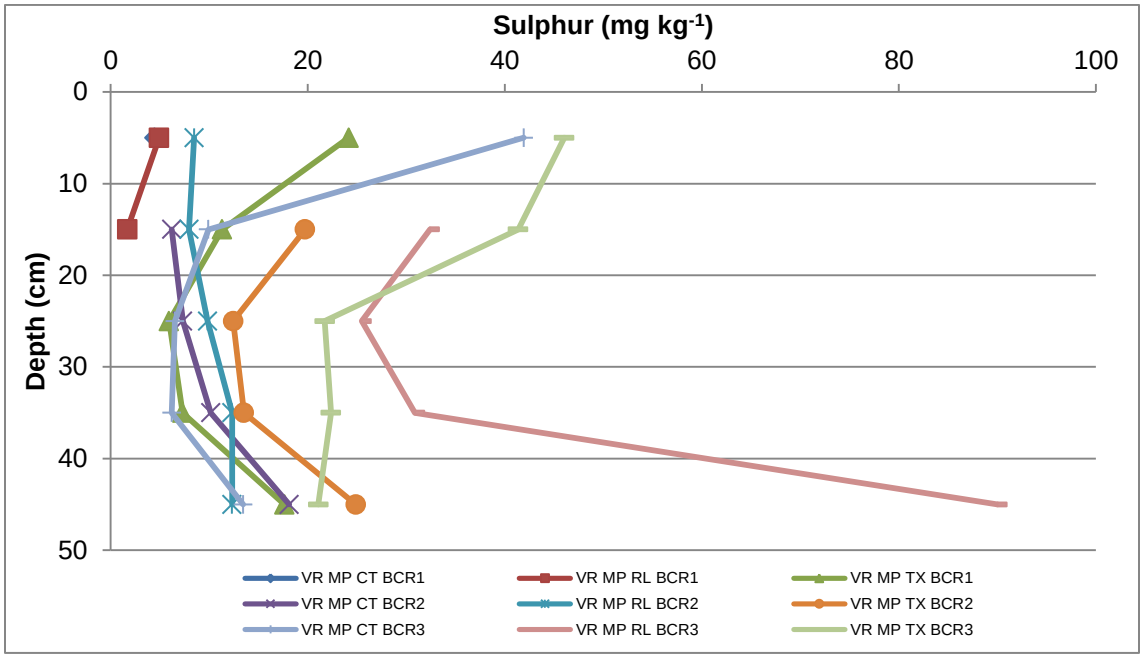

Figure 8.10 BCR sequential extraction curve with depth for sulphur at the Vaal River Mispah

8.1.2 Statistical analysis

The descriptive statistics for the major nutrients across site, treatment, type of tree, sequential extraction step and by depth for the two Vaal River sites are shown in Tables 8.1, 8.2, 8.3, 8.4, 8.5 (a) and 8.5 (b). Tables 8.1, 8.2, 8.3 and 8.4 represent the composite sample at all depths. The tables include the mean, median and standard deviation for the initial soil solution determinants.

Of the major nutrients, phosphorous had the highest concentrations as shown in Table 8.1. The *p-values* indicated that all the major nutrients were significantly different (p <0.05) at the two sites; higher concentrations were observed at the VRWC compared to the VRMP (Calcium 133%, magnesium 120%, phosphorous 126%, potassium 96% and sulphur 183%, higher).

Table 8.1 Descriptive statistics of major nutrients by site

Determinant	Units	Site	Mean	Median	Standard Deviation	*p-value*
Calcium	mg kg^{-1}	VRWC	890.22	429.50	944.26	1.18E-14
		VRMP	175.92	151.50	95.69	
Magnesium	mg kg^{-1}	VRWC	233.54	43.40	379.98	1.15E-6
		VRMP	583.00	27.05	74.53	
Phosphorous	mg kg^{-1}	VRWC	1641.72	8.80	2521.50	2.10E-4
		VRMP	646.61	16.08	747.68	
Potassium	mg kg^{-1}	VRWC	198.99	190.50	95.48	0.00
		VRMP	70.16	36.26	56.42	
Sulphur	mg kg^{-1}	VRWC	437.49	86.00	62.49	9.38E-8
		VRMP	18.76	14.64	13.66	

In Table 8.2 calcium showed a significant difference in concentration (p = 0.01) between the woodland and grassland treatment; the calcium was 14% higher in the woodland treatment, while magnesium, phosphorous, potassium and sulphur showed no significant difference (p >0.05). The presence of the trees changed the soil substrate by increasing the calcium concentration in the soil, which is beneficial for plant growth.

Table 8.2 Descriptive statistics of major nutrients by treatment

Determinant	Units	Treatment	Mean	Median	Standard Deviation	*p-value*
Calcium	mg kg^{-1}	Grassland	415.84	159.00	535.17	0.01
		Woodland	743.81	388.60	926.11	
Magnesium	mg kg^{-1}	Grassland	78.38	33.98	113.14	0.06
		Woodland	150.23	38.90	302.09	
Phosphorous	mg kg^{-1}	Grassland	936.17	28.92	1146.24	0.37
		Woodland	1180.30	76.00	1718.28	
Potassium	mg kg^{-1}	Grassland	108.16	78.80	82.71	0.17
		Woodland	128.03	120.00	103.62	
Sulphur	mg kg^{-1}	Grassland	143.49	30.60	320.76	0.18
		Woodland	260.01	32.55	543.47	

Table 8.3 indicated that magnesium concentrations was significantly different (p = 0.03) in the presence of *Tamarix usneoides* compared to that of *Rhus lancea*; the magnesium was 71% higher for *Tamarix usneoides*). Thus *Tamarix usneoides* was more effective in increasing the magnesium concentrations in the soil.

Calcium, magnesium and sulphur were mainly present in the carbonate bound fraction, while phosphorous was mainly present in the organic bound fraction as shown in Table 8.4. Potassium was equally present in all three fractions BCR fractions, which was confirmed by the *p-value* (p = 0.05), which indicated that for potassium there was no significant difference between the fractions.

Table 8.3 Descriptive statistics of major nutrients by type of tree

Determinant	Units	Tree	Mean	Median	Standard Deviation	*p-value*
Calcium	mg kg^{-1}	*Tamarix usneoides*	483.84	156.00	799.18	0.96
		Rhus lancea	477.04	162.00	718.76	
Magnesium	mg kg^{-1}	*Tamarix usneoides*	204.95	43.40	397.04	0.03
		Rhus lancea	97.06	35.20	149.19	
Phosphorous	mg kg^{-1}	*Tamarix usneoides*	1105.22	39.96	2016.19	0.59
		Rhus lancea	1295.79	1668.00	1131.48	
Potassium	mg kg^{-1}	*Tamarix usneoides*	138.91	103.50	134.09	0.22
		Rhus lancea	117.30	138.00	59.35	
Sulphur	mg kg^{-1}	*Tamarix usneoides*	186.83	26.83	46.71	0.72
		Rhus lancea	218.66	37.75	49.40	

In Tables 8.5 (a) and (b) calcium, magnesium, and potassium were found to be more concentrated in the top layers of soil (0-10 cm), while sulphur was found to be more concentrated in the deepest soil sample at both sites, i.e. 20-30 cm for VRWC and 40-50 cm for VRMP. Phosphorous was most concentrated in the top layer (0-10 cm) of

soil at VRWC, and was most concentrated in the deeper soil samples (40-50 cm) at VRMP.

Table 8.4 Descriptive statistics of major nutrients by sequential extraction step

Determinant	Units	Sequential extraction	Mean	Median	Standard Deviation	*p-value*
Calcium	mg kg^{-1}	Carbonates	1005.50	383.40	1004.66	2.22E-16
		Oxides	248.87	131.80	179.32	
		Organics	152.15	142.50	60.27	
Magnesium	mg kg^{-1}	Carbonates	321.55	204.20	384.13	3.89E-15
		Oxides	30.07	24.02	19.38	
		Organics	32.71	31.50	7.50	
Phosphorous	mg kg^{-1}	Carbonates	7.08	6.00	6.15	0.00
		Oxides	7.92	6.40	5.45	
		Organics	2601.46	1750.50	1972.57	
Potassium	mg kg^{-1}	Carbonates	132.73	112.00	69.40	0.05
		Oxides	97.43	35.04	88.80	
		Organics	133.66	140.25	123.71	
Sulphur	mg kg^{-1}	Carbonates	407.98	61.60	664.77	2.29E-8
		Oxides	79.59	14.20	255.34	
		Organics	35.53	31.80	23.18	

The standard deviations across site, treatment, tree, sequential extraction step and depth were found to be extremely high, due to a composite sample at all depths being statistically analysed; the high values indicate that there was great variability in the data either across site, treatment, tree, sequential extraction step and depth. In Table 8.1 calcium, magnesium, phosphorous, potassium and sulphur showed larger standard deviations at the VRWC, which indicated that the variability in the concentration of the major nutrients was higher at the VRWC and lower at the VRMB. In Table 8.2 the standard deviations were higher for the woodland treatment compared to the grassland treatment, hence there was a greater variability in the major nutrient concentration in the woodland treatment. In Table 8.3, calcium, magnesium, phosphorous and potassium showed greater variability in concentration in the presence of *Tamarix usneoides* than *Rhus lancea*, while sulphur showed greater variability in the presence of *Rhus lancea*. In Table 8.4, calcium, magnesium and sulphur showed greater variability in the carbonate bound fraction, while phosphorous showed greater

variability in the organic bound fraction. In Tables 8.5 (a) and 8.5 (b) the highest variability was seen for calcium, magnesium, phosphorous and potassium in the shallow depth samples, while sulphur showed greater variability in the deeper soil samples.

Table 8.5(a) Descriptive statistics of the major nutrients, calcium, magnesium and phosphorous, by site and depth

Determinant	Units	Site	Depth	Mean	Median	Standard Deviation
Calcium	mg kg^{-1}	VRWC	0-10	1085.78	550.00	1094.61
			10-20	919.48	402.00	954.55
			20-30	665.39	342.00	735.54
		VRMP	0-10	272.77	183.60	160.21
			10-20	188.48	154.50	88.06
			20-30	164.03	123.00	79.30
			30-40	137.30	121.50	38.40
			40-50	145.99	137.50	40.90
Magnesium	mg kg^{-1}	VRWC	0-10	309.97	50.90	571.66
			10-20	186.63	39.10	228.62
			20-30	204.04	43.40	236.50
		VRMP	0-10	110.81	37.70	121.74
			10-20	67.15	35.05	80.75
			20-30	50.98	26.30	57.59
			30-40	39.78	25.30	38.86
			40-50	30.32	25.15	19.78
Phosphorous	mg kg^{-1}	VRWC	0-10	1848.87	8.90	3288.99
			10-20	1628.48	7.70	2158.46
			20-30	1412.36	9.50	1824.35
		VRMP	0-10	617.83	28.88	724.05
			10-20	590.46	11.34	801.47
			20-30	535.82	5.76	717.74
			30-40	688.71	23.92	748.97
			40-50	727.75	10.20	1087.28

Table 8.5(b) Descriptive statistics of the major nutrients, potassium and sulphur by site and depth

Potassium	mg kg^{-1}	VRWC	0-10	261.71	202.50	132.53
			10-20	176.13	198.00	52.39
			20-30	159.14	172.00	38.26
		VRMP	0-10	113.38	112.00	77.99
			10-20	80.72	58.90	56.77
			20-30	62.70	33.08	43.01
			30-40	47.37	30.40	28.79
			40-50	52.09	28.08	47.46
Sulphur	mg kg^{-1}	VRWC	0-10	247.23	74.00	402.25
			10-20	541.46	78.00	806.62
			20-30	541.97	397.00	551.92
		VRMP	0-10	25.32	15.42	22.68
			10-20	18.93	12.03	17.03
			20-30	14.66	9.84	9.91
			30-40	16.80	12.56	11.31
			40-50	32.73	18.56	33.95

The major nutrients were summarised into two components by PCA (Table C5, Appendix C) as shown in Table 8.6. Calcium, magnesium and sulphur were highly correlated in Component 1 and phosphorous and potassium was highly correlated in Component 2 with a variance of 83.2%. The histograms (Figures C8, C9, Appendix C) indicated that both components were not normally distributed.

Table 8.6 The PCA of the major nutrients

Data set	**Component**	**Parameters included**	**Normally distributed**
Major nutrients	1	Calcium, magnesium, sulphur	No
Major nutrients	2	Phosphorous, potassium	No

Table 8.7 shows a summary of the results obtained from the one-way ANOVA tests for the major nutrient components (Tables C7, C8, C9, C10, C11, C12, Appendix C).

Table 8.7 A summary of the one-way ANOVA results for the components of the major nutrients

Component	Factor	Test used	*p-value*
1	Site	Mann-Whitney	0.00
	Treatment	Mann-Whitney	0.39
	Tree	Kruskal-Wallis	0.67
2	Site	Mann-Whitney	0.00
	Treatment	Mann-Whitney	0.41
	Tree	Kruskal-Wallis	0.12

The *p-values*, i.e. 0.39 and 0.41, indicated that statistically, there was no significant difference between the grassland and the woodland treatment substrates. The *p-values*, i.e. 0.67 and 0.12, indicated that there was also no significant difference between the tree species. There was however a significant difference between the sites as the p-*values* was 0.00 and 0.00 for both components. Thus the concentration of the major nutrients at the different sites, VRWC and VRMP, were significantly different in both components.

A summary of the LRA for the components of the major nutrients (Figures C13, C14, Tables C22, C23, C24, C25, C26, C27, Appendix C) is shown in Table 8.8. The *p-values* were both less than 0.05 (0.00 for Component 1 and 0.00 for Component 2), thus the regression model equations were significant in being able to predict the concentration of major nutrients based on the depth. Both components of the major nutrients had a negative, linear correlation with depth.

The correlation coefficients had values of 0.287 and 0.396 respectively for Component 1 and 2, implying that the relationship between concentrations of the major nutrients in both components versus depth was not very strong. This was further highlighted by the variability, i.e. only 8.2% of the major nutrient concentrations in Component 1 could be explained by depth, and only 15.7% of the major nutrient concentrations in Component 2.

Table 8.8 A summary of the LRA for the components of the major nutrients

Component	Correlation	R	R^2	*p-value*	Equation
1	Linear - negative	0.287	0.082	0.00	$y = 0.583 - 0.23(Depth)$
2	Linear - negative	0.396	0.157	0.00	$y = 0.805 - 0.31(Depth)$

8.2 Trace elements

Trace elements included aluminium, arsenic, chromium, copper, iron, lead manganese, mercury, nickel, titanium, uranium, vanadium, and zinc. The BCR extraction curves were first plotted, then the trace metal ratios were studied, and lastly the statistical analysis was presented to determine whether the trees changed the mobility of the trace elements in the soil.

8.2.1 BCR extraction curves

A BCR extraction curve was drawn for each trace element at each site and compared the control samples (CT) with that of samples taken from the rooting area of *Rhus lancea* (RL) and *Tamarix usneoides* (TX) trees.

Aluminium

Aluminium BCR extraction curves at the VRWC and VRMP are shown in Figures 8.11 and 8.12. In the control samples, aluminium was most mobile in the second fraction and to a lesser extent in the third fraction at the VRWC and VRMP; at the VRMP aluminium was also slightly mobile in the first fraction. At the VRWC *Rhus lancea* and *Tamarix usneoides* decreased the concentration of oxide bound aluminium in the top layers (0-30 cm) of soil and also decreased the concentration of organic bound aluminium in the deeper samples (20-30 cm).

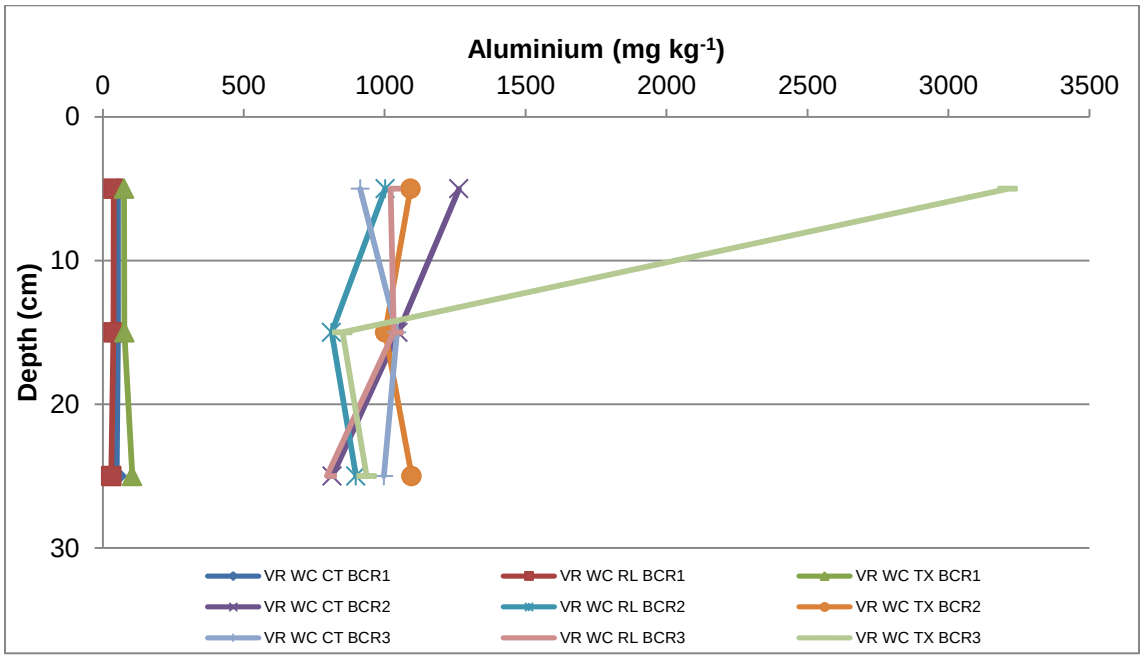

Figure 8.11 BCR sequential extraction curve with depth for aluminium at the Vaal River West Complex

At the VRMP *Rhus lancea* decreased the concentration of carbonate and oxide bound aluminium in the entire depth profile sampled (0-50 cm), but increased the organic bound aluminium in all depths 0-50 cm). *Tamarix usneoides* decreased the carbonate bound aluminium in the top layers (0-10 cm) of soil, and oxide and organic bound aluminium in the deeper soil samples (20- 50 cm).

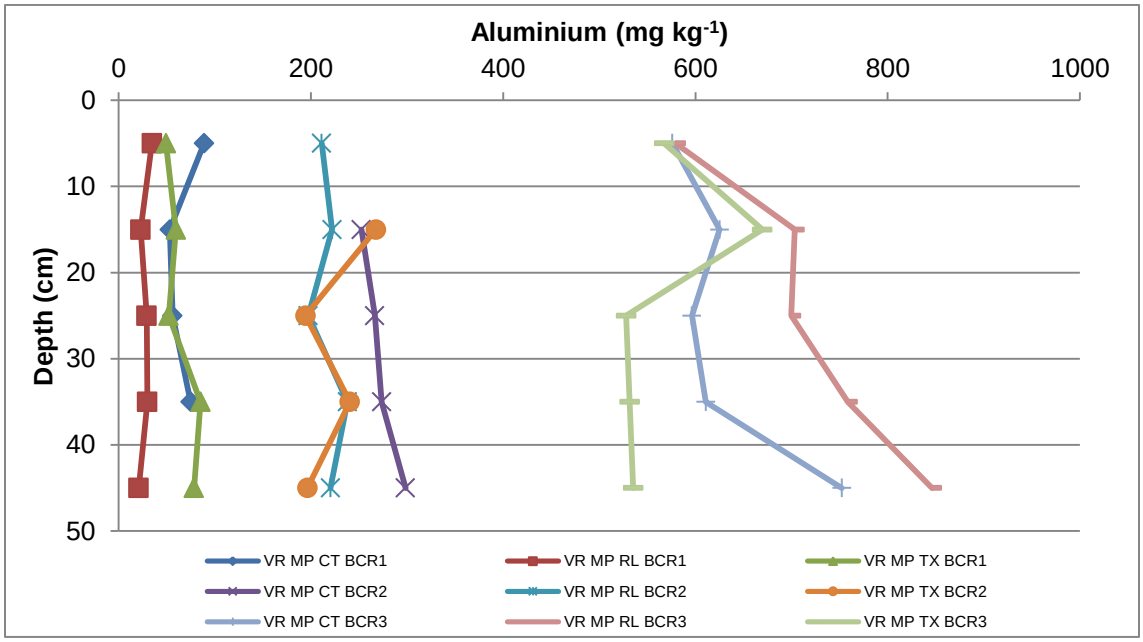

Figure 8.12 BCR sequential extraction curve with depth for aluminium at the Vaal River Mispah

Arsenic

Arsenic BCR extraction curves at VRWC and VRMP are shown in Figures 8.13 and 8.14.

In the control samples at the VRWC, arsenic was bound to all three fractions, with the most mobile fraction being the organic fraction (third fraction), then the iron oxide fraction (second fraction), and lastly the carbonate, leachable fraction (first fraction). *Rhus lancea* and *Tamarix usneoides* showed similar carbonate-bound arsenic concentrations as the control, and both trees increased the oxide bound arsenic concentrations in all depths (0-30 cm) at the VRWC. *Rhus lancea* decreased the concentration of organic bound arsenic in the middle depth, i.e. 10-20 cm; while *Tamarix usneoides* decreased the concentration in the deeper sample depths at the VRWC.

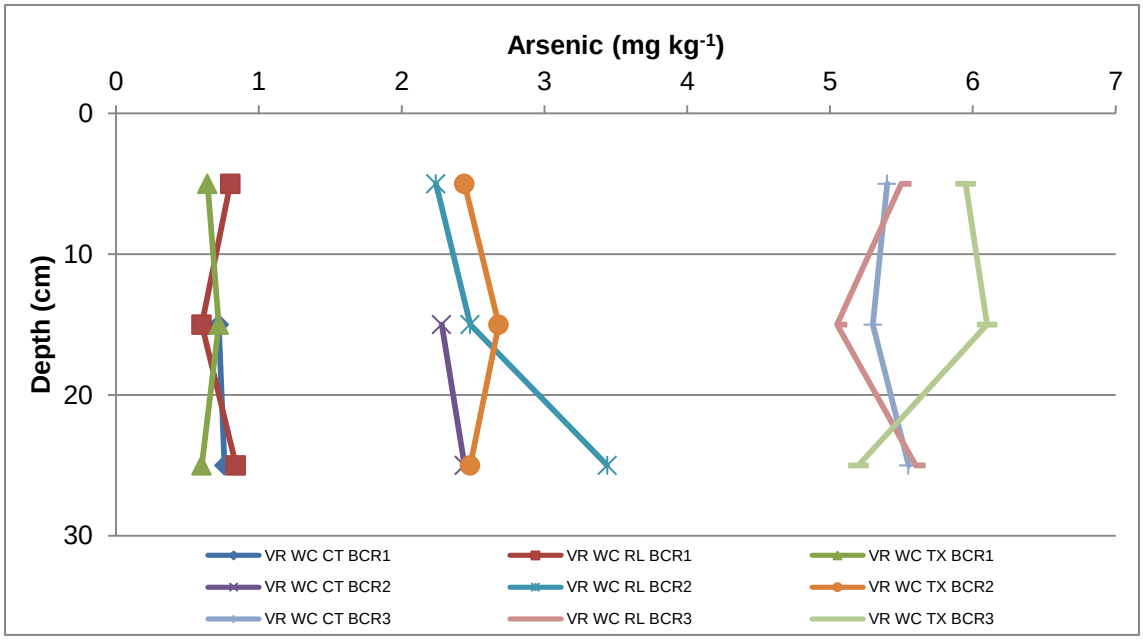

Figure 8.13 BCR sequential extraction curve with depth for arsenic at the Vaal River West Complex

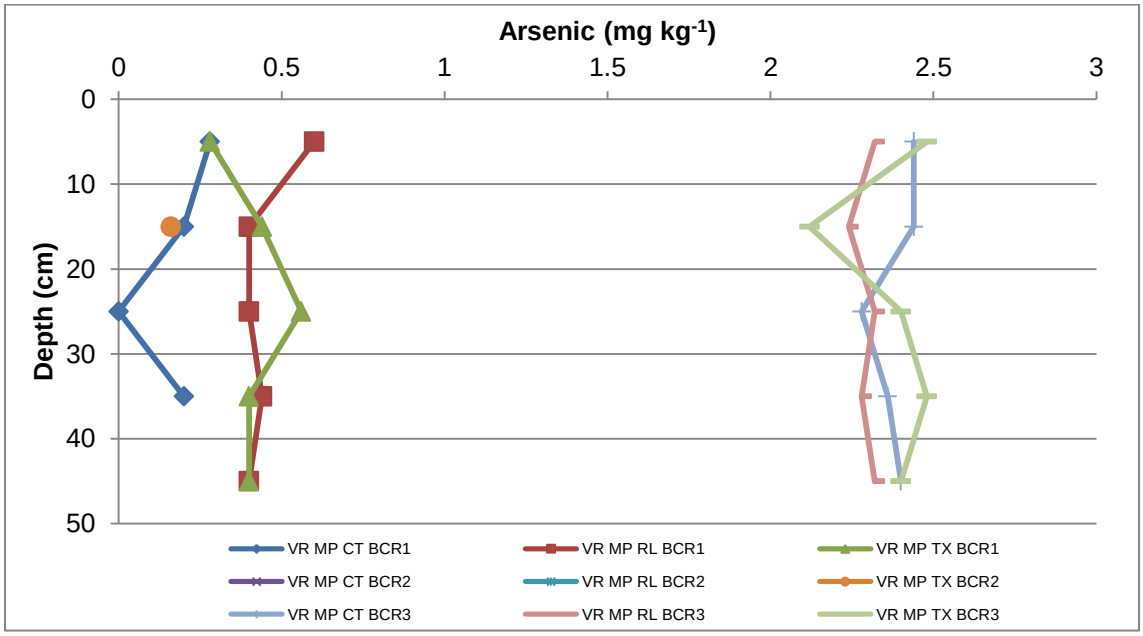

Figure 8.14 BCR sequential extraction curve with depth for arsenic at the Vaal River Mispah

At the VRMP the arsenic in the control samples was most mobile in the third fraction and to a lesser extent in the first fraction. *Rhus lancea* and *Tamarix usneoides* both decreased the concentration of the arsenic ions bound to organics in the top layers (0-10 cm) of soil, and increased the carbonate bound arsenic mobility in the entire depth profile sampled (0-50 cm) at the VRMP.

Chromium

Chromium BCR extraction curves at the VRWC and VRMP are shown in Figures 8.15 and 8.16.

In the control samples at the VRWC and VRMP chromium was most readily mobilised in the third (organic bound) fraction. At both sites *Rhus lancea* decreased the concentration of the organic bound chromium in the top layer (0-10 cm) of soil, while *Tamarix usneoides* decreased organic bound chromium concentration in the deeper soil samples (20-30 cm at the VRWC and 40-50 cm at the VRMP).

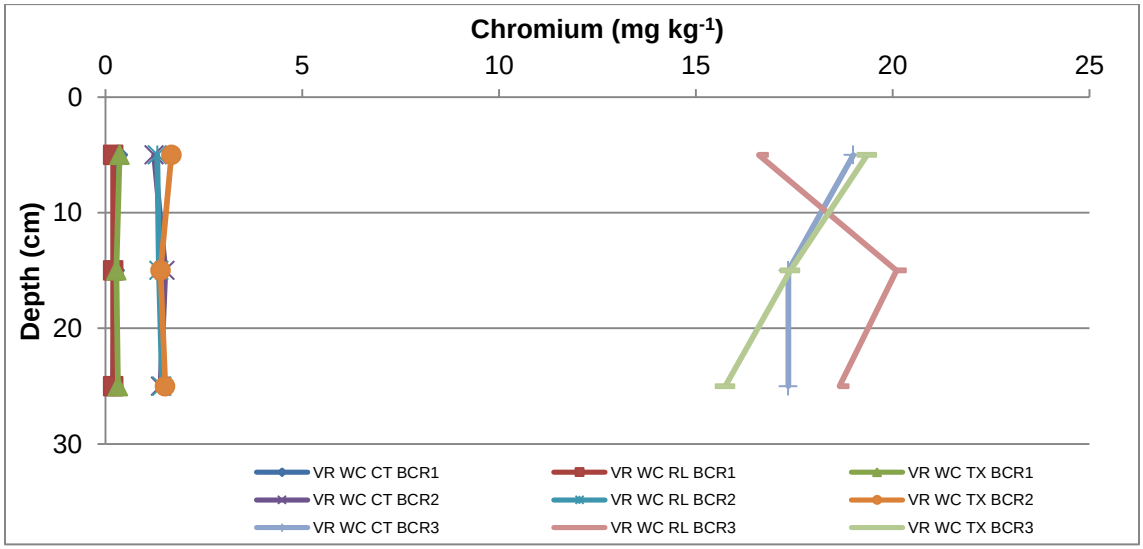

Figure 8.15 BCR sequential extraction curve with depth for chromium at the Vaal River West Complex

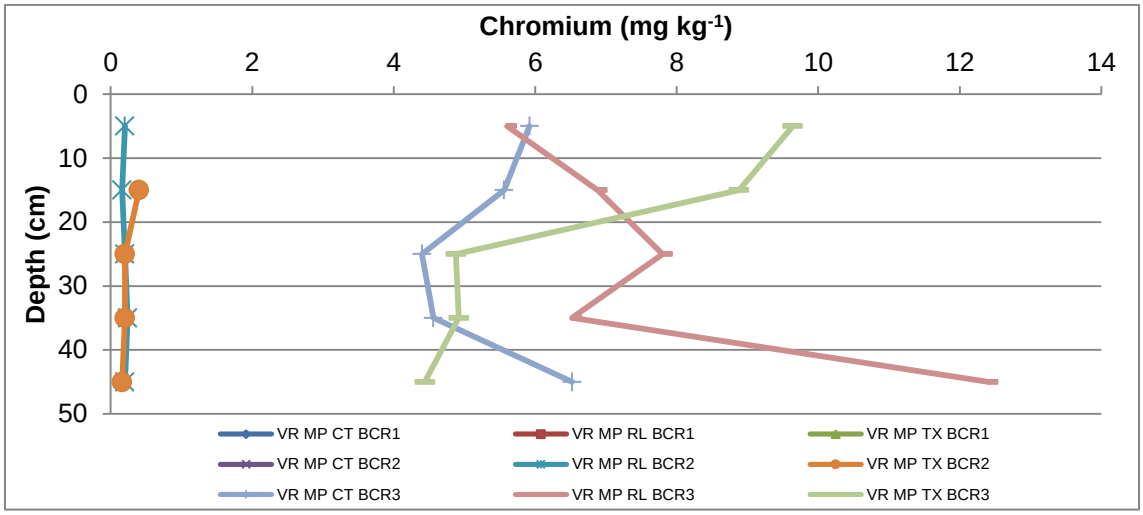

Figure 8.16 BCR sequential extraction curve with depth for chromium at the Vaal River Mispah

Copper

Copper BCR extraction curves at the VRWC and VRMP are shown in Figures 8.17 and 8.18.

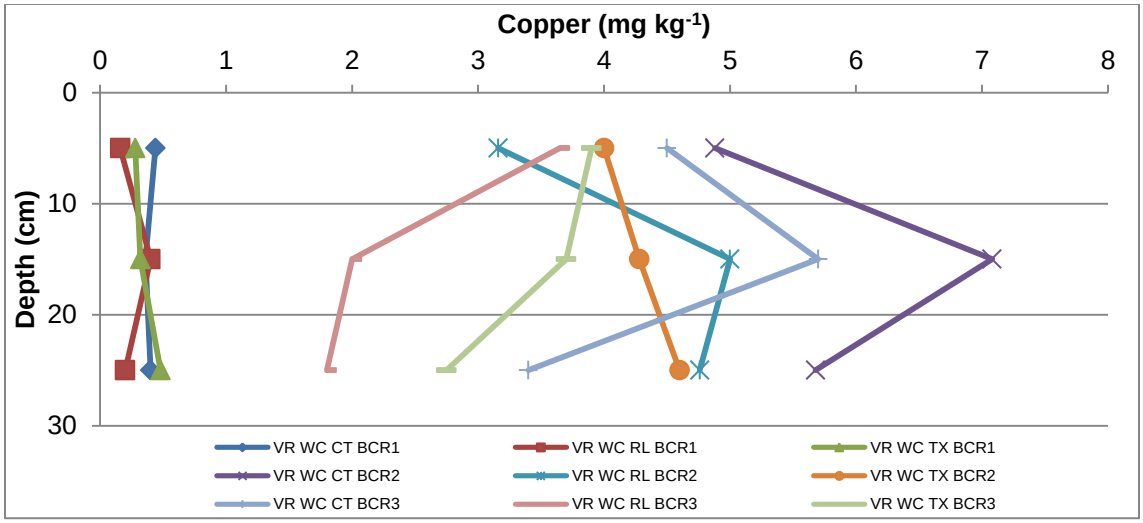

Figure 8.17 BCR sequential extraction curve with depth for copper at the Vaal River West Complex

The control samples at the VRWC showed that copper was most mobile in the second fraction and to a lesser extent in the third fraction. *Rhus lancea* and *Tamarix usneoides* decreased the concentrations of oxide and organic bound copper in all depths (0-30 cm) at the VRWC.

At the VRMP copper in the control sample was mobile in all three fractions, with the oxide bound fraction being the most mobile, followed by the third fraction and then the first fraction. *Rhus lancea* did not change the concentration of copper in the first and second fractions, but did increase the organic bound copper in all depths (0-50 cm) at the VRMP. *Tamarix usneoides* did not change the copper concentration in the first fraction, but increased the oxide bound copper in the top layers (0-10 cm) of soil, and the organic bound copper in the deeper soil samples (10 – 50 cm) at the VRMP.

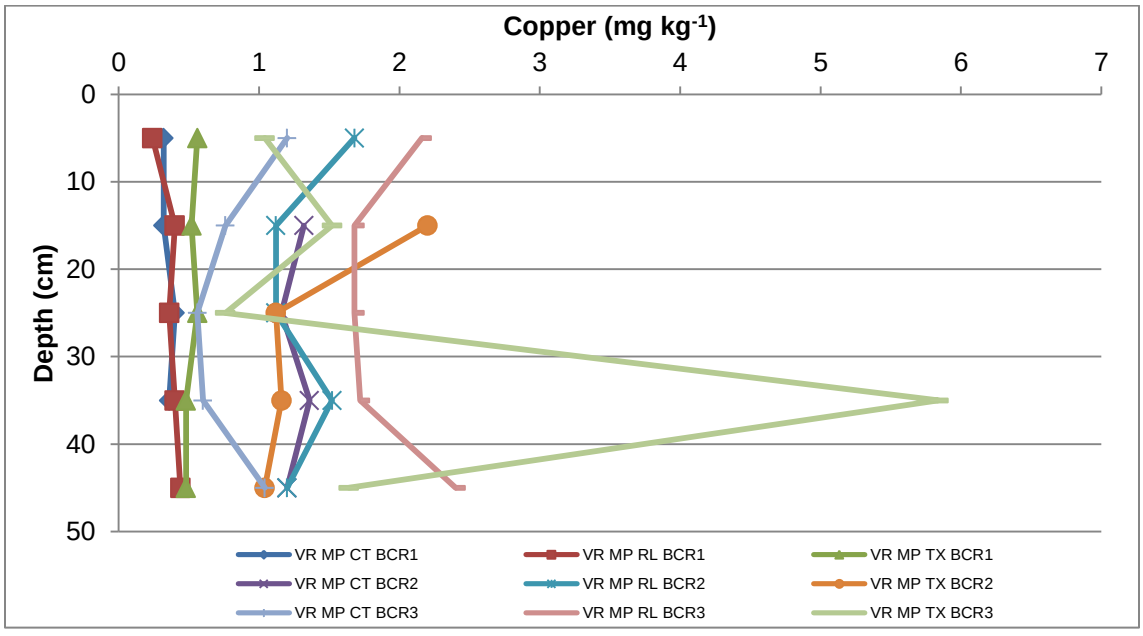

Figure 8.18 BCR sequential extraction curve with depth for copper at the Vaal River Mispah

Iron

Iron BCR extraction curves at the VRWC and VRMP are shown in Figures 8.19 and 8.20. At the VRWC iron was most mobile in the second fraction in the control sample, i.e. oxide bound. *Rhus lancea* decreased the concentration of oxide bound iron in the middle sample depth, i.e. 10-20 cm, while *Tamarix usneoides* decreased the concentration in all sampled depths (0-30 cm).

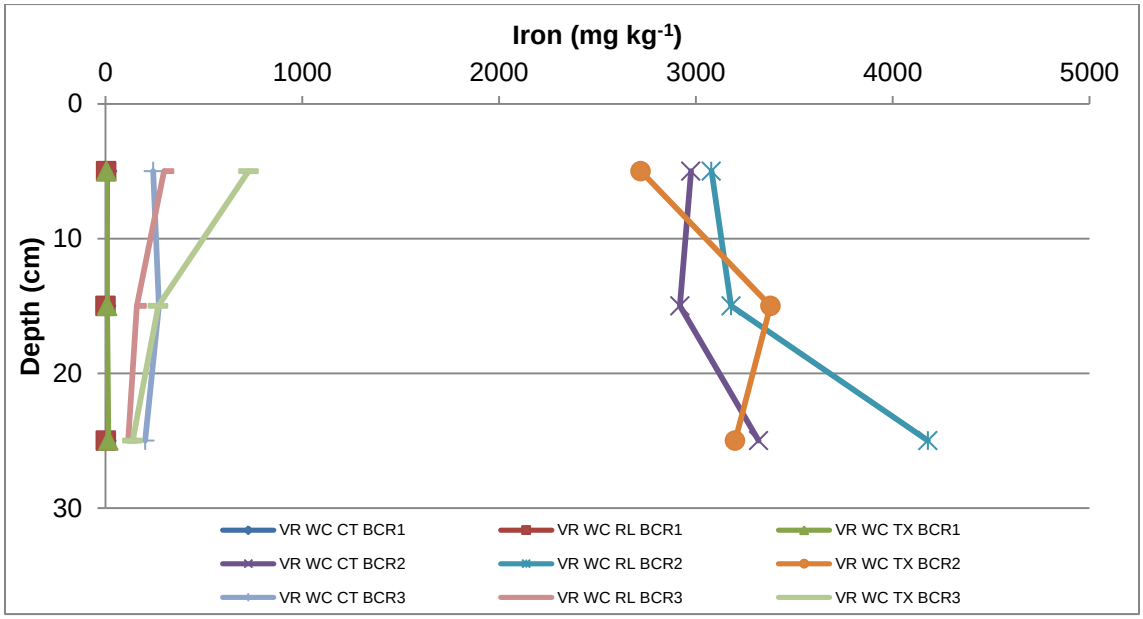

Figure 8.19 BCR sequential extraction curve with depth for iron at the Vaal River West Complex

At the VRMP the control samples indicated that iron was most readily mobile in the second fraction followed to a lesser extent by the third fraction. *Rhus lancea* increased oxide bound iron concentration in the top layers (0-10 cm) of soil, and organic bound iron in all depths sampled (0-50 cm) at the VRMP. *Tamarix usneoides* decreased the oxide bound iron concentrations in the deeper samples (40-50 cm), and increased the organic bound iron in the top layers (0-10 cm) of soil at the VRMP.

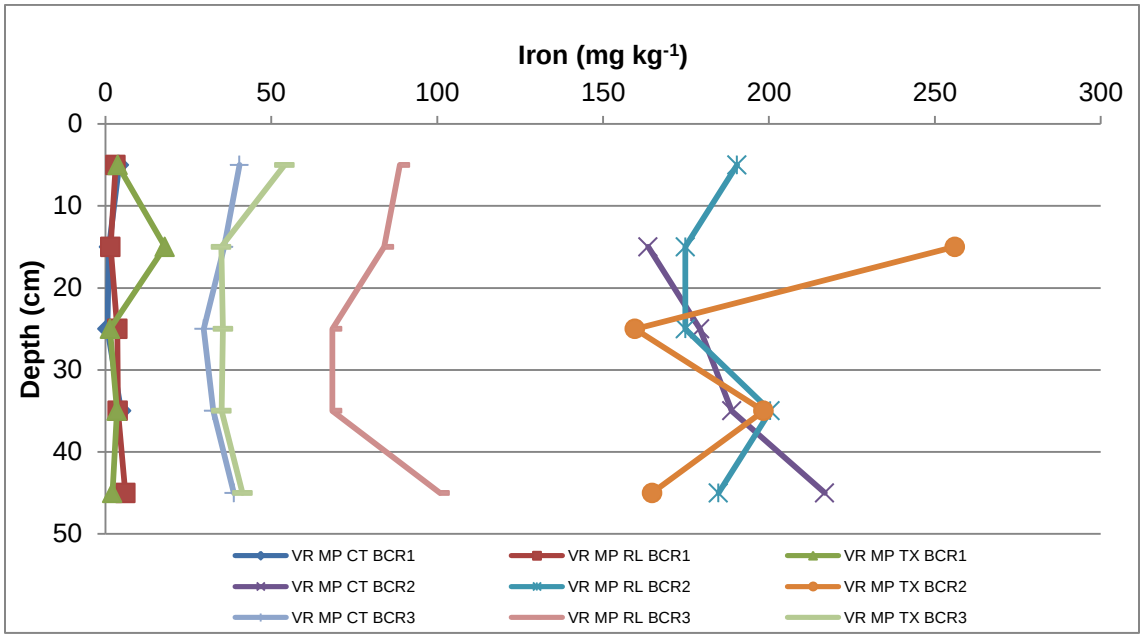

Figure 8.20 BCR sequential extraction curve with depth for iron at the Vaal River Mispah

Lead

Lead BCR extraction curves at the VRWC and VRMP are shown in Figures 8.21 and 8.22. In the control samples at both sites, lead was most mobile in the second fraction (oxide bound) and to a lesser extent in the third fraction (organic bound). At the VRWC *Rhus lancea* decreased the concentration of oxide bound lead in deeper samples (10-30 cm), while *Tamarix usneoides* decreased the concentration of the same fraction in the top layers of soil (0-10 cm). The third fraction remained the same as the control for both trees.

At the VRMP *Rhus lancea* decreased the concentration of oxide bound lead in deeper soil samples (20-50 cm), and *Tamarix usneoides* decreased the concentration of the same fraction in the middle layers (30-40 cm) of soil. Both trees decreased the concentration of the organic bound lead in the top layers of soil.

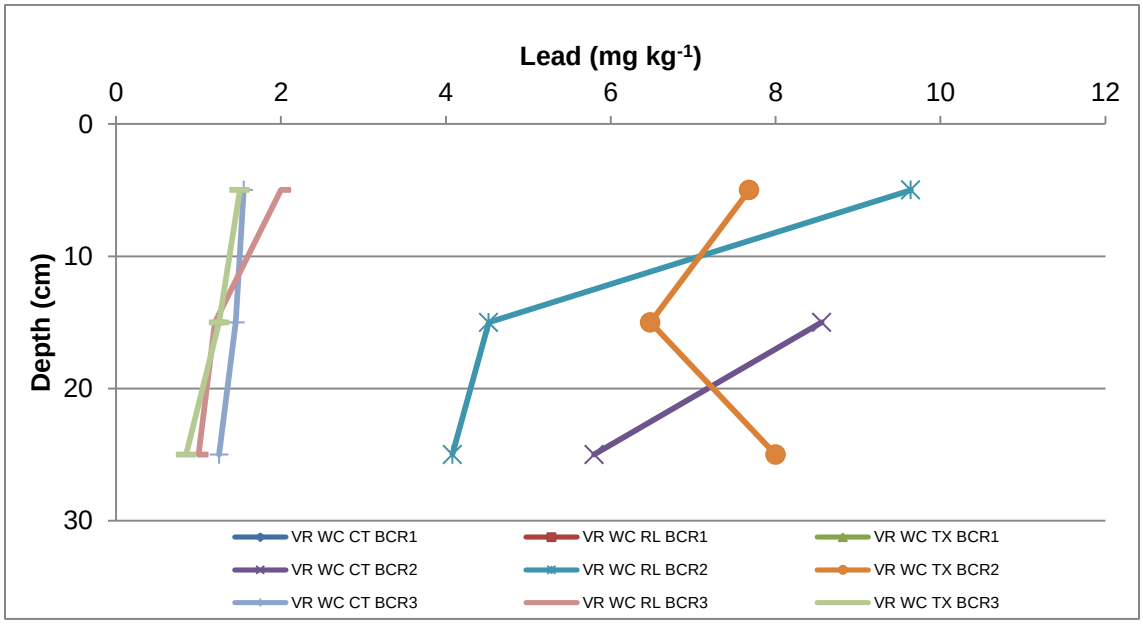

Figure 8.21 BCR sequential extraction curve with depth for lead at the Vaal River West Complex

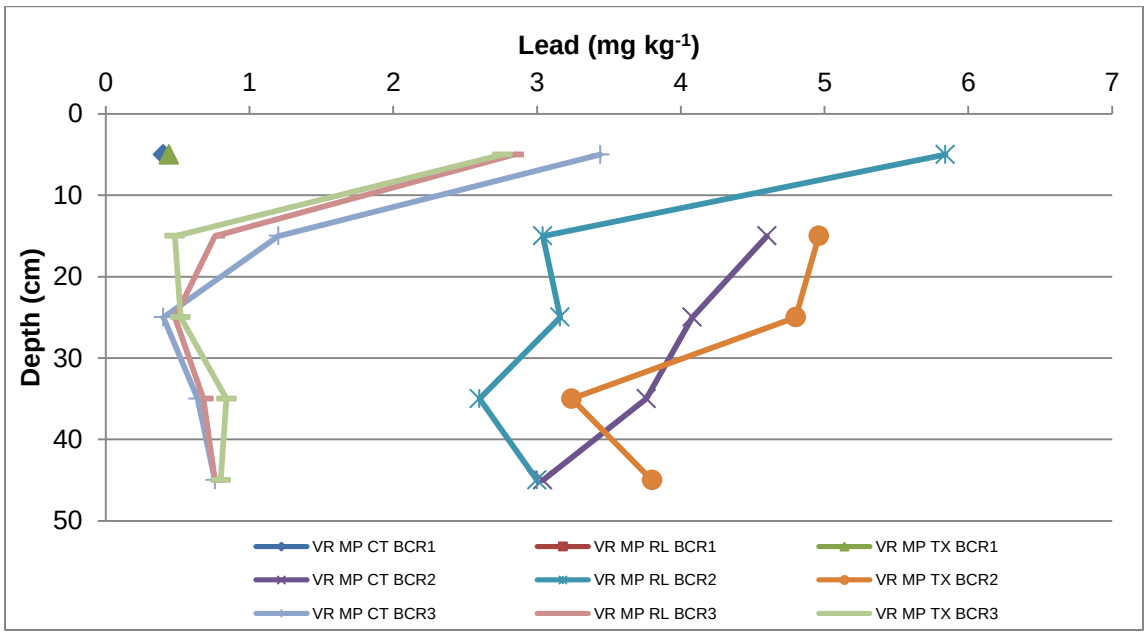

Figure 8.22 BCR sequential extraction curve with depth for lead at the Vaal River Mispah

Manganese

Manganese BCR extraction curves at the VRWC and VRMP are shown in Figures 8.23 and 8.24. Manganese is considered as a micronutrient, which is necessary for plant growth in low concentrations. Manganese showed a similar trend to that of iron, in that the control samples at the VRWC, manganese was most mobile in the oxide bound fraction. *Rhus lancea* decreased the concentration of oxide bound manganese in the top layers (0-10 cm) of soil, while *Tamarix usneoides* decreased the concentration in the same fraction in the top layers (0-10 cm), and in the deeper (20-30 cm) soil samples.

At the VRMP the control samples indicated that manganese was bound in the second fraction, and to a lesser extent in the first fraction. *Rhus lancea* and *Tamarix usneoides* decreased the carbonate bound manganese in all depths at this site. *Rhus lancea* also decreased the concentration of the oxide bound manganese in the top layers (0-10 cm) of soil, while *Tamarix usneoides* decreased the concentration of this fraction in the deeper soil samples (20-50 cm) at the VRMP.

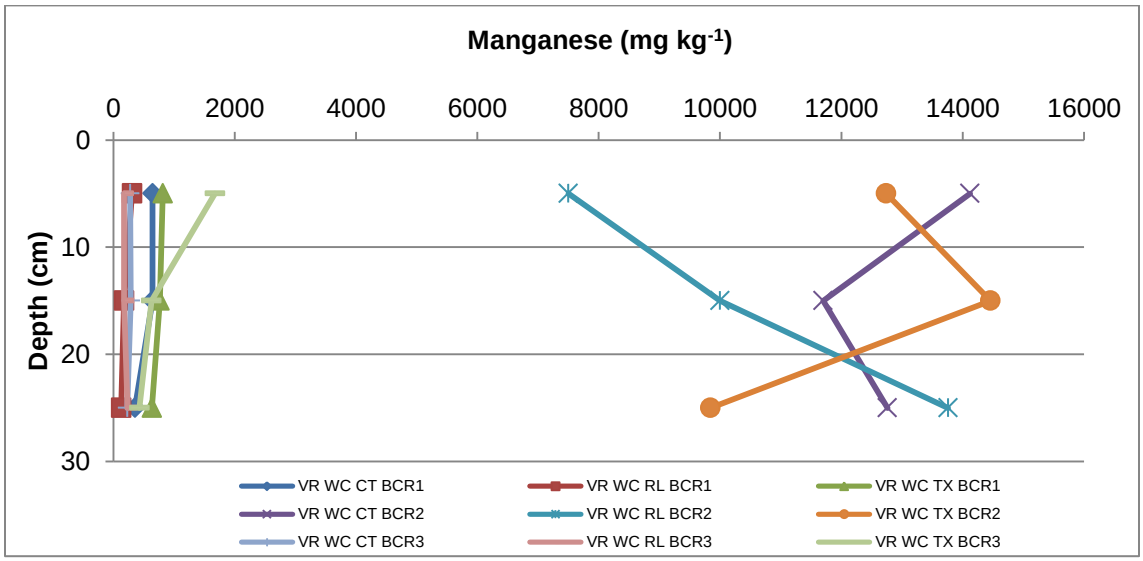

Figure 8.23 BCR sequential extraction curve with depth for manganese at the Vaal River West Complex

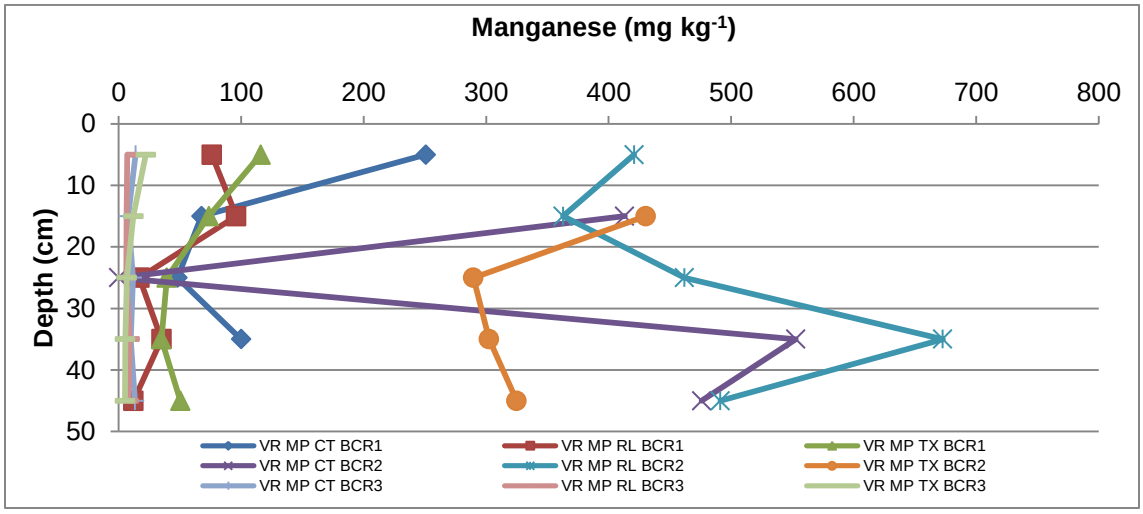

Figure 8.24 BCR sequential extraction curve with depth for manganese at the Vaal River Mispah

Mercury

Mercury BCR extraction curves at the VRWC and VRMP are shown in Figures 8.25 and 8.26.

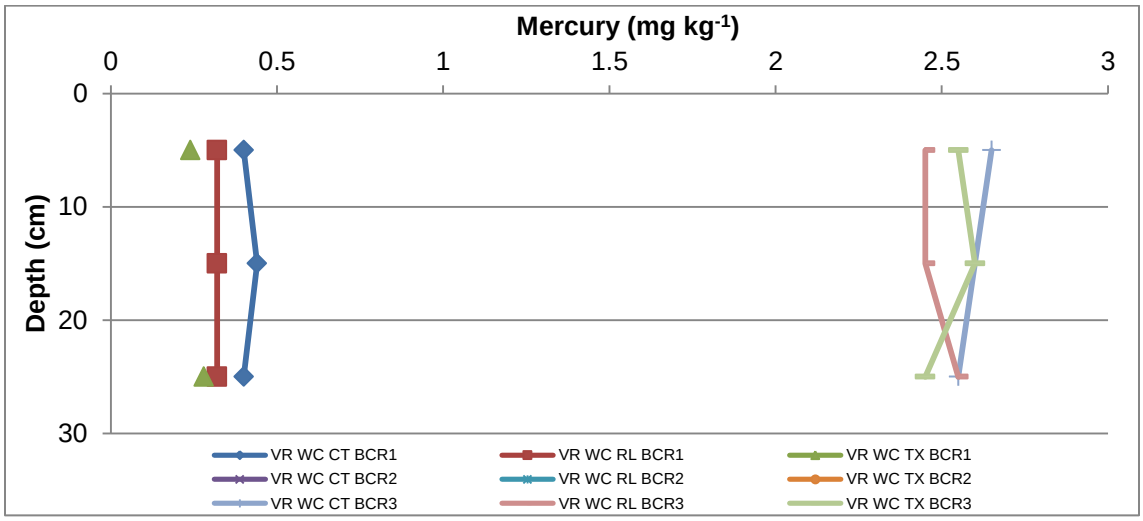

Figure 8.25 BCR sequential extraction curve with depth for mercury at the Vaal River West Complex

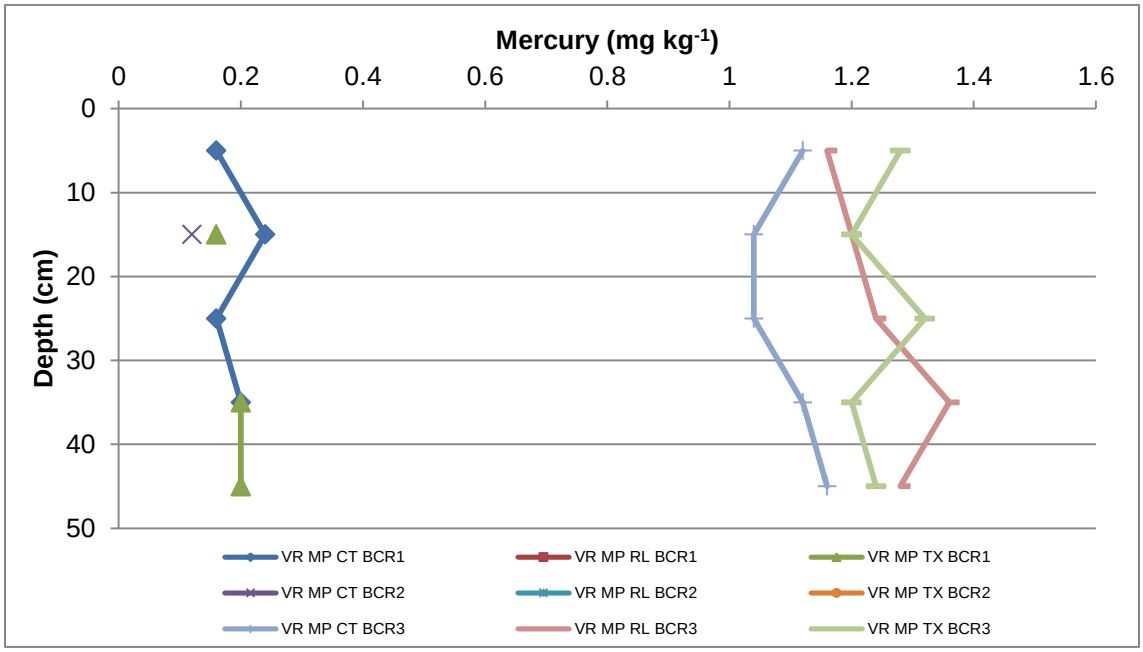

Figure 8.26 BCR sequential extraction curve with depth for mercury at the Vaal River Mispah

In the control samples at both sites, mercury was most mobile in the third fraction (organic bound). At the VRWC both trees decreased the concentration of organic bound mercury in all depths (0-30 cm), while at the VRMP both trees increased the concentration of mercury in the same fraction in all depths (0-50 cm).

Nickel

Nickel BCR extraction curves at the VRWC and VRMP are shown in Figures 8.27 and 8.28. At the VRWC nickel in the control samples was mobile in all three fractions with the most mobile fraction being the second fraction, followed by the third fraction and then the first fraction.

At the VRWC, *Rhus lancea* decreased: carbonate bound nickel in all sample depths (0-30 cm); oxide bound nickel in the top layers (0-10 cm) of soil, and organic bound nickel

in the top layer (0-10 cm) and deeper soil sample (20-30 cm) at this site. *Tamarix usneoides* decreased: carbonate bound nickel in the middle layer of soil (10-20 cm), oxide bound nickel in all sampled depths (0-30 cm), and organic bound nickel in the top layers (0-10 cm) of soil at the VRWC.

In the control samples at the VRMP, nickel was also mobilised in all three fractions, however the order differed in that the most mobile fraction was the third fraction, followed by the first fraction and then the second fraction. At this site *Rhus lancea* did not change the carbonate bound nickel, but increased the oxide bound nickel in the deeper soil samples (30-50 cm) and decreased the concentration of organic bound nickel in the top layers (0-10 cm) of soil. *Tamarix usneoides* on the other hand increased the carbonate and oxide bound nickel concentrations in the top layers (0-10 cm) of soil, and decreased the organic bound nickel concentration at depths 20-30 cm and 40-50 cm.

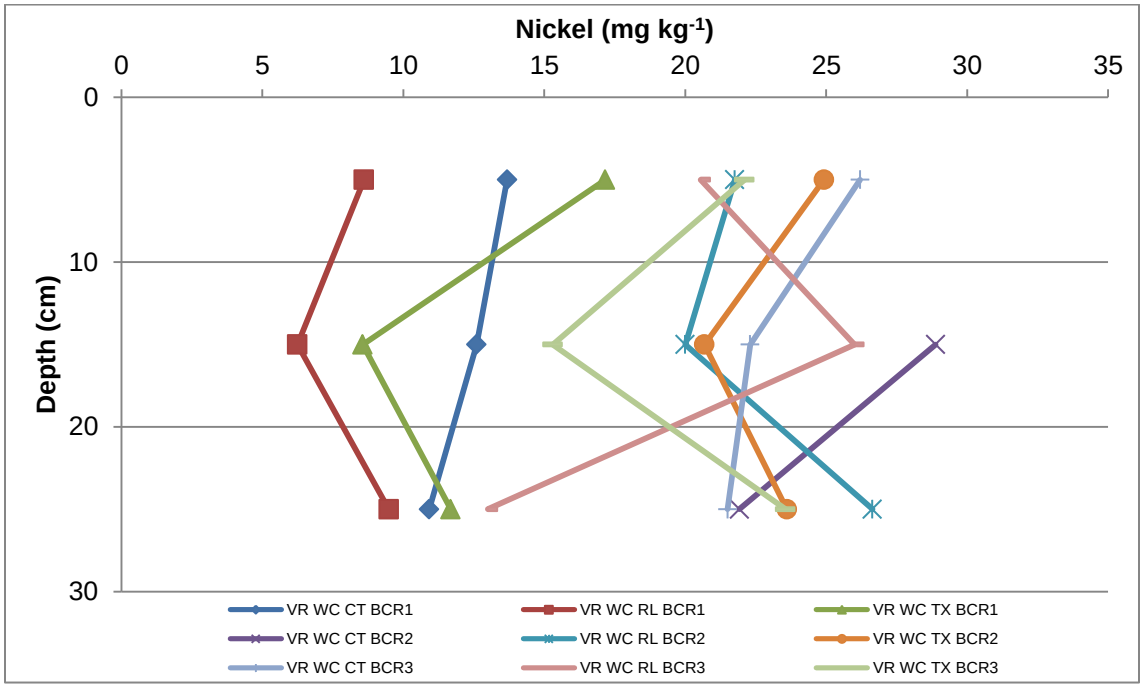

Figure 8.27 BCR sequential extraction curve with depth for nickel at the Vaal River West Complex

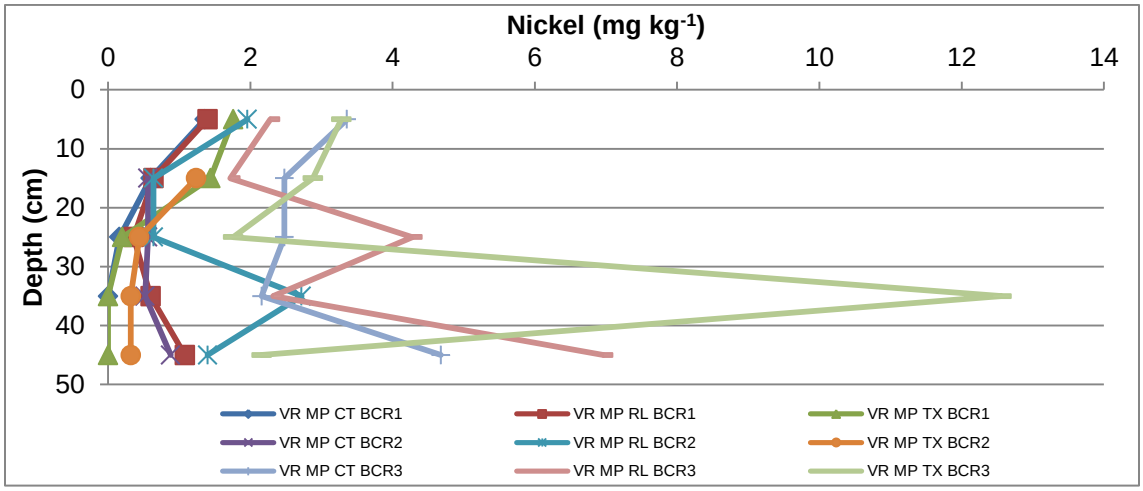

Figure 8.28 BCR sequential extraction curve with depth for nickel at the Vaal River Mispah

Titanium

Titanium BCR extraction curves at the VRWC and VRMP are shown in Figures 8.29 and 8.30.

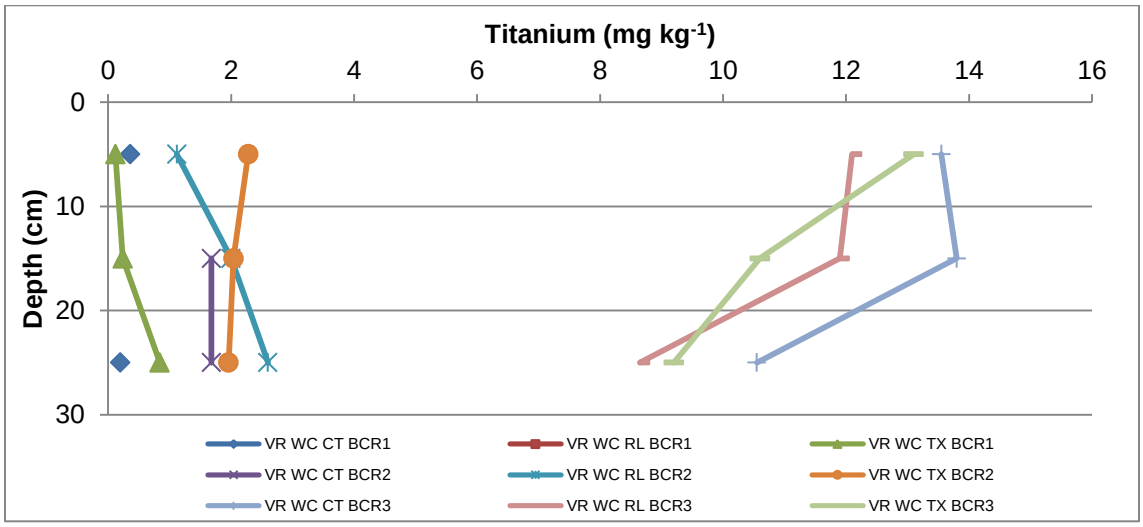

Figure 8.29 BCR sequential extraction curve with depth for titanium at the Vaal River West Complex

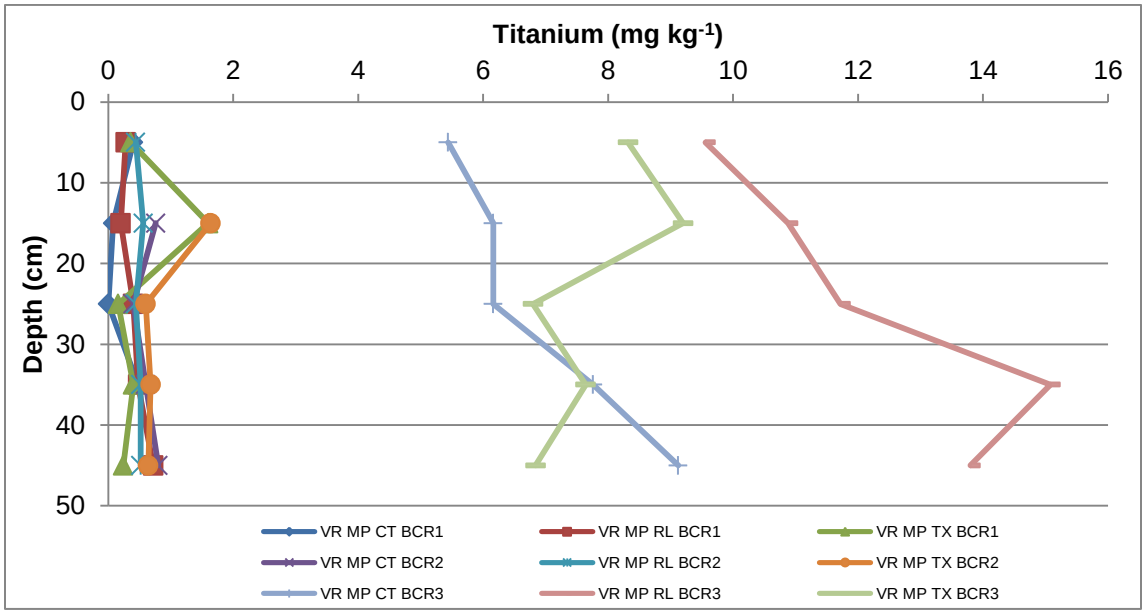

Figure 8.30 BCR sequential extraction curve with depth for titanium at the Vaal River Mispah

At both of the sites titanium in the control samples is most mobile in the third, organic bound fraction. At the VRWC *Rhus lancea* and *Tamarix usneoides* decreased the concentration of organic bound titanium in all depths (0-30 cm). At the VRMP *Rhus lancea* increased the concentration of organic bound titanium in all depths (0-50 cm), while *Tamarix usneoides* increased the same fraction in the top layers (0-10 cm) of soil and decreased the fraction in the deeper soil samples (40-50 cm).

Uranium

Uranium BCR extraction curves at the VRWC and VRMP are shown in Figures 8.31 and 8.32. Uranium in the control samples at both sites was mainly organic bound. At the VRWC *Rhus lancea* and *Tamarix usneoides* decreased the concentration of organic bound uranium, as the uranium concentrations were below the detection limit in the presence of the trees. Hence *Rhus lancea* and *Tamarix usneoides* decreased the concentration of uranium in the soil, which would limit uranium leaching into groundwater sources.

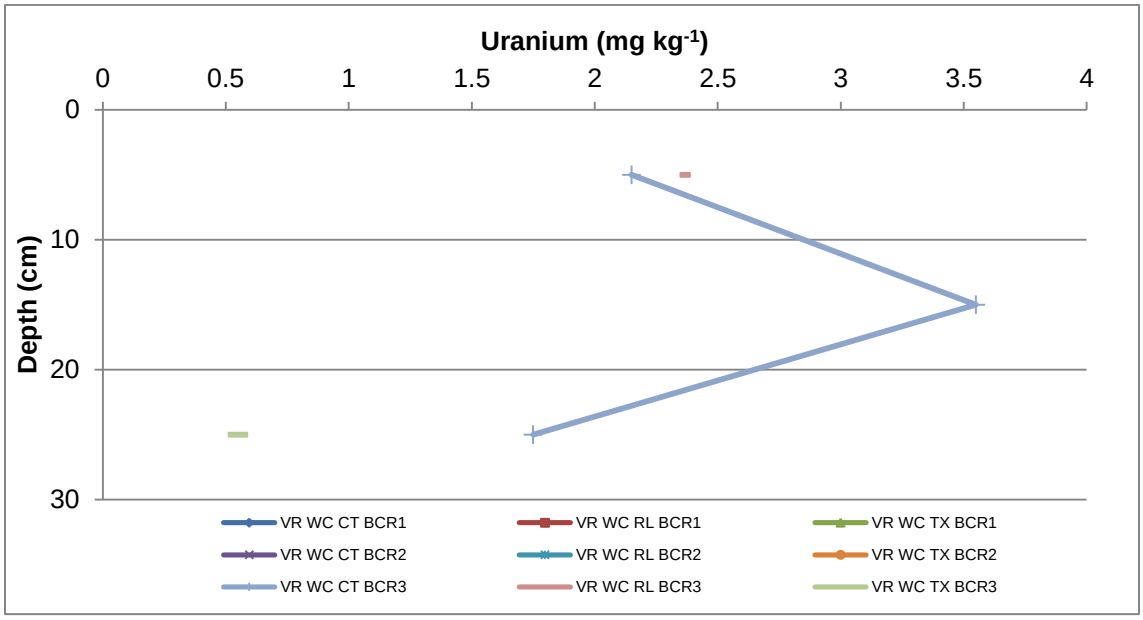

Figure 8.31 BCR sequential extraction curve with depth for uranium at the Vaal River West Complex

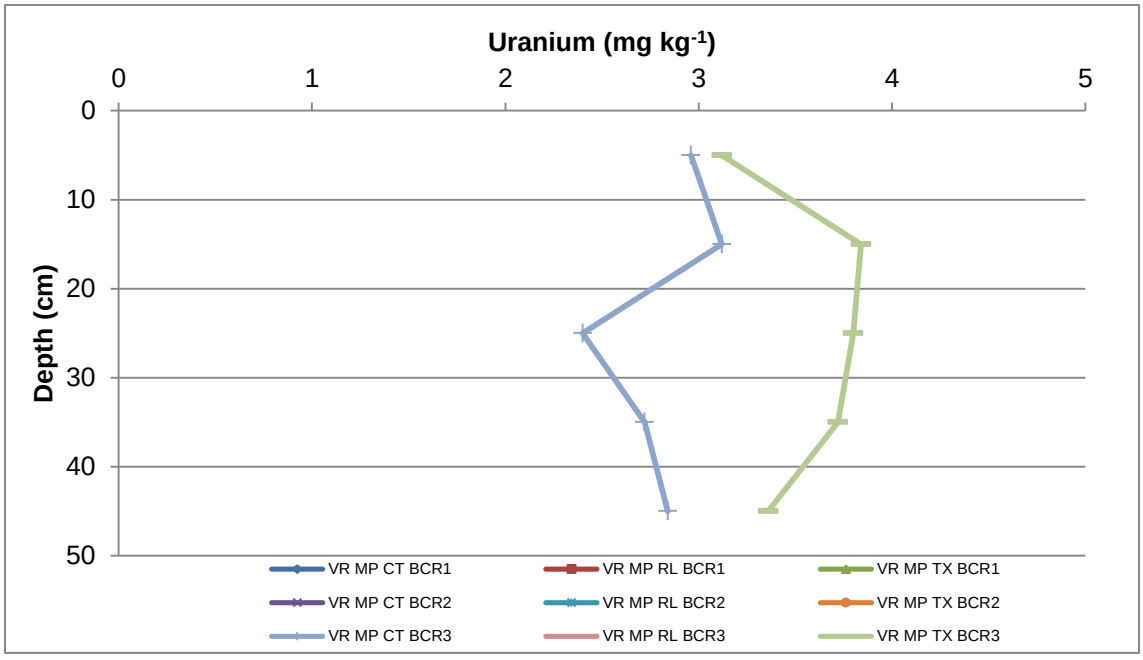

Figure 8.32 BCR sequential extraction curve with depth for uranium at the Vaal River Mispah

At the VRMP *Rhus lancea* decreased the concentration of organic bound uranium in all sample depths (0-50 cm), while *Tamarix usneoides* increased the concentration of the same fraction in all depths (0-50 cm).

Vanadium

Vanadium BCR extraction curves at the VRWC and VRMP are shown in Figures 8.33 and 8.34. At the VRWC, the control samples indicated that vanadium was mainly found bound to oxides and to a lesser extent to organics. At this site *Rhus lancea* and *Tamarix usneoides* decreased the concentration of vanadium in the third fraction in the top layers (0-10 cm) of soil. *Rhus lancea* increased the concentration of vanadium in the second fraction in the deeper soil samples (20-30 cm), and *Tamarix usneoides* increased the concentration of vanadium in the second fraction in all depths sampled (0-30 cm) at the VRWC.

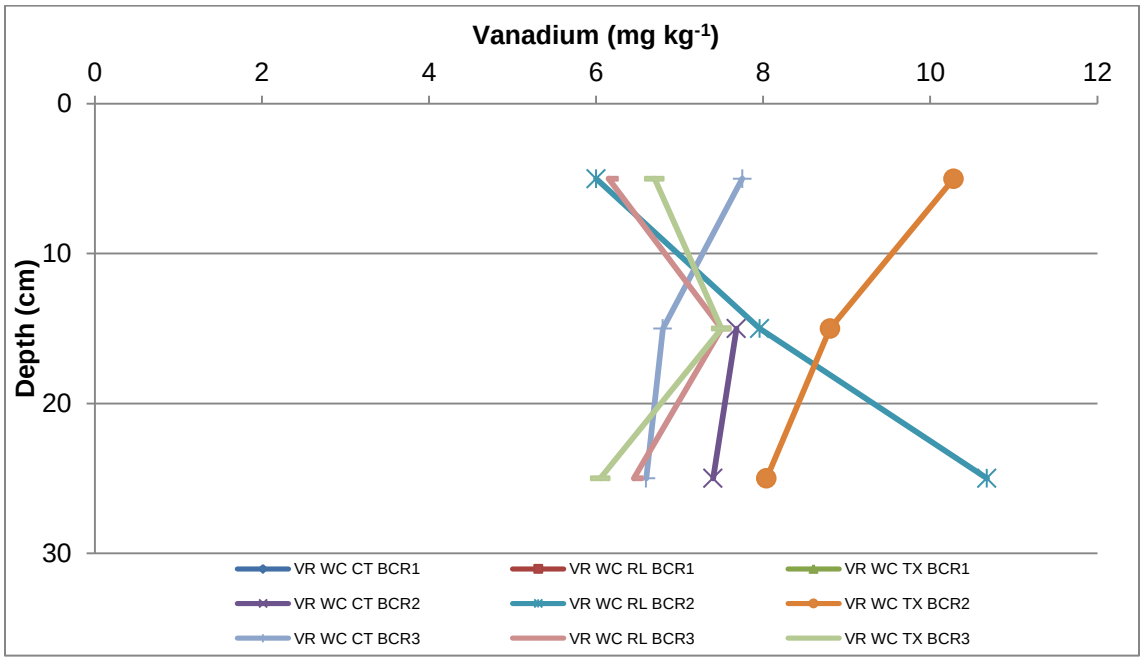

Figure 8.33 BCR sequential extraction curve with depth for vanadium at the Vaal River West Complex

In the control samples at VRMP, vanadium was mobilised in all three fractions with the most mobile being the organic, then the oxide and lastly carbonate bound fraction. At the VRMP, *Rhus lancea* decreased the concentration of carbonate and oxide bound vanadium, and increased the organic bound vanadium concentrations in all depths (0-50 cm). *Tamarix usneoides* did not change the concentration of vanadium in the first fraction; however it decreased the second and third fraction concentrations in the deeper soil samples (40 – 50 cm).

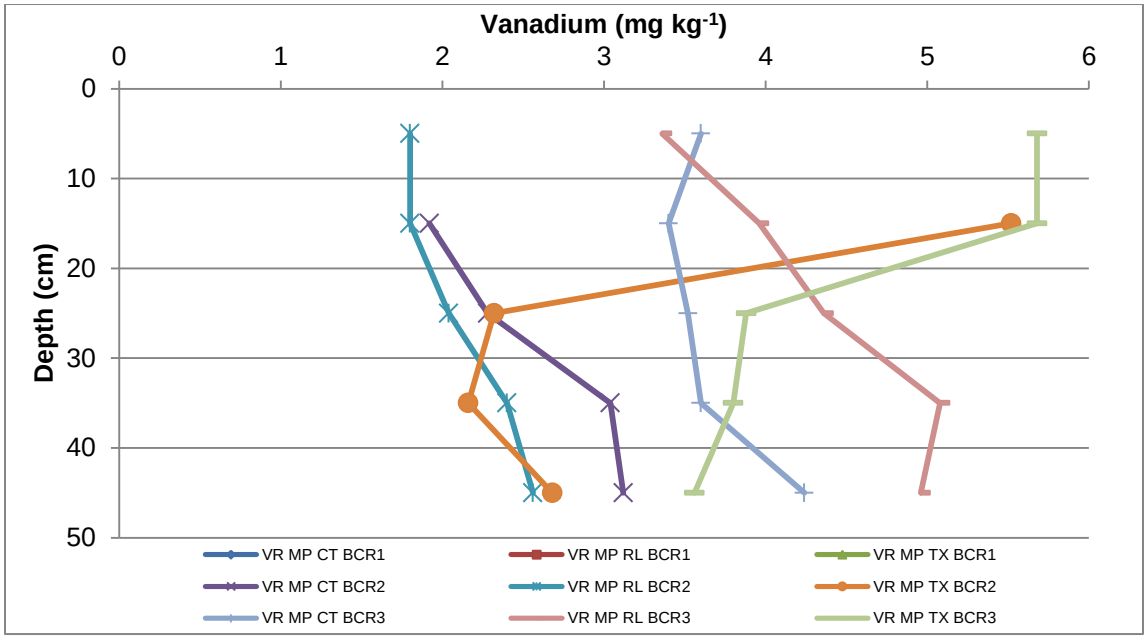

Figure 8.34 BCR sequential extraction curve with depth for vanadium at Vaal River Mispah

Zinc

Zinc BCR extraction curves at the VRWC and VRMP are shown in Figures 8.35 and 8.36. The mobility of zinc at the two sites differed in that at the VRWC zinc was mostly oxide bound, then, to a lesser extent, carbonate bound fraction. At the VRMP, zinc was most mobile in the organic fraction.

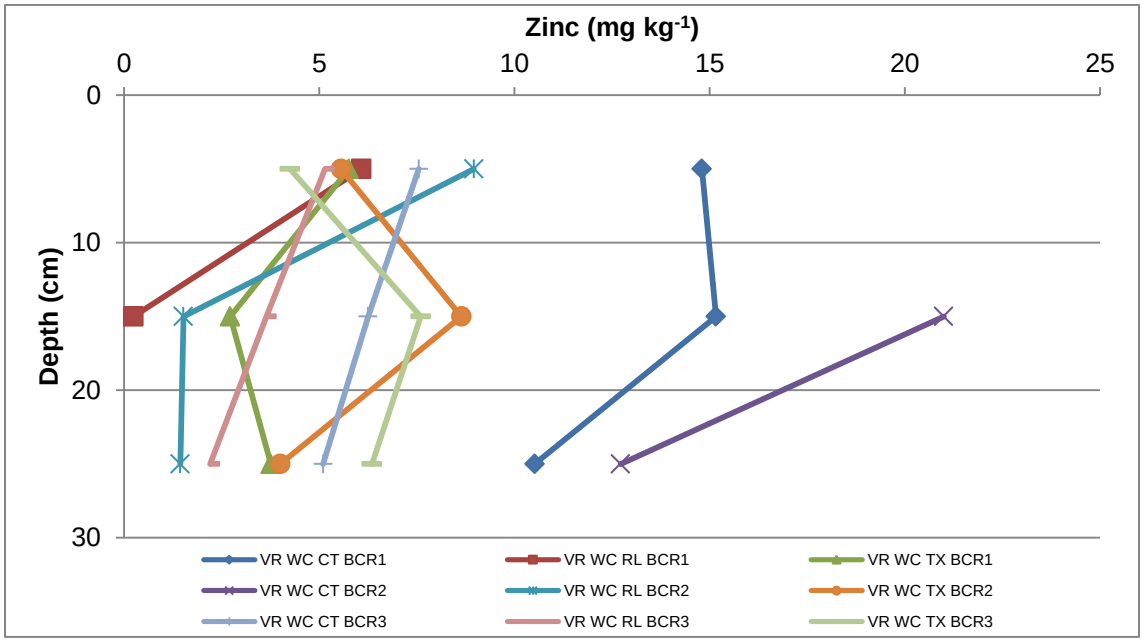

Figure 8.35 BCR sequential extraction curve with depth for zinc at the Vaal River West Complex

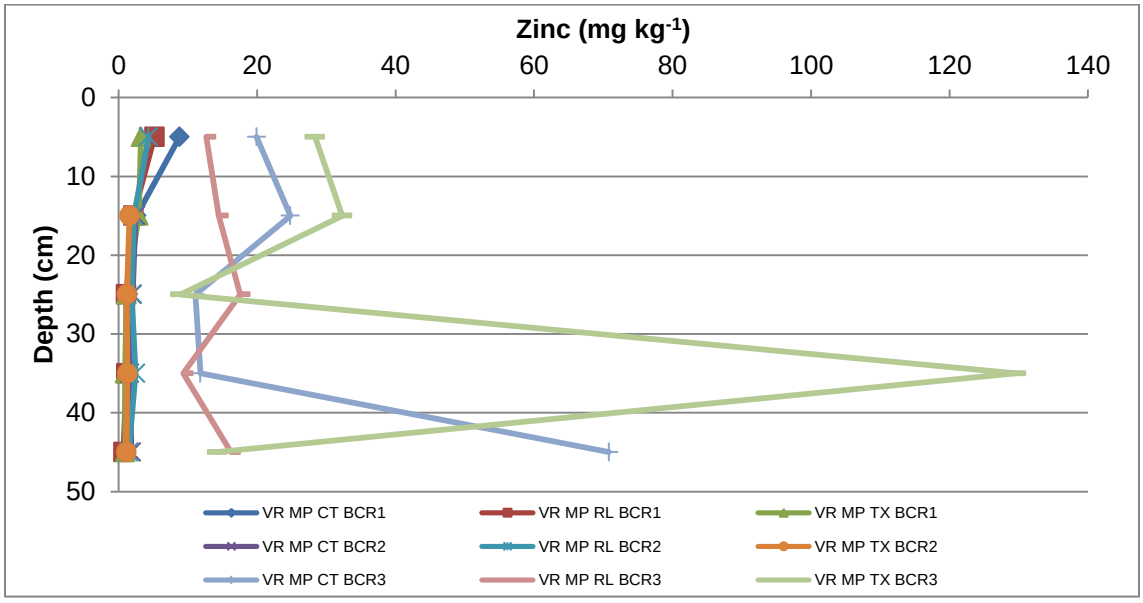

Figure 8.36 BCR sequential extraction curve with depth for zinc at the Vaal River Mispah

At the VRWC both trees decreased the concentration of zinc in the first and second fractions in all depths (0-30 cm). At the VRMP *Rhus lancea* decreased the concentration of organic bound zinc in the top layers (0-10 cm) of soil, and in the deepest soil sample (40-50 cm). *Tamarix usneoides* decreased the concentration in the same fraction in the middle depth, (20-30 cm) and also in the deepest soil sample (40-50 cm).

8.2.2 Statistical analysis

The descriptive statistics for the trace elements across site, treatment, type of tree, sequential extraction step and by depth for the two Vaal River sites are shown in Tables 8.9, 8.10, 8.11, 8.12 and 8.13. Tables 8.9, 8.10, 8.11 and 8.12 represent the composite sample at all depths. The tables include the mean, median and standard deviation for the initial soil solution determinants.

Table 8.9 indicated that manganese had the highest concentration of all the trace elements, followed by iron and then aluminium at both sites. Aluminium (p = 1.41E-7), arsenic (p = 3.29E-7), copper (p = 1.46E-8), iron (p = 4.06E-3), lead (p = 1.00E-5), manganese (p = 1.85E-14), mercury (p = 1.42E-3), nickel (p = 0.00) and vanadium (p = 0.00) concentrations were significantly different at the two sites; the concentrations were higher at the VRWC than at VRMB, with the percentage difference in brackets: aluminium (68%), arsenic (61%), copper (67%), iron (173%), lead (58%), manganese (186%), mercury (50%), nickel (97%), and vanadium (62%).

Table 8.10 showed that nickel was the only trace element that showed significantly different concentrations (p = 0.05) between the woodland and grassland treatment; the nickel concentration was 39% lower for the woodland treatment. Thus, the presence of the trees decreased the concentration of nickel in the soil.

Table 8.9 Descriptive statistics of trace elements by site

Determinant	Units	Site	Mean	Median	Standard Deviation	*p-value*
Aluminium	$mg\ kg^{-1}$	VRWC	753.56	898.00	657.89	1.41E-7
		VRMP	375.82	239.80	332.84	
Arsenic	$mg\ kg^{-1}$	VRWC	2.97	2.45	2.03	3.29E-7
		VRMP	1.60	0.64	1.32	
Chromium	$mg\ kg^{-1}$	VRWC	6.57	1.40	8.17	0.17
		VRMP	5.09	5.73	4.50	
Copper	$mg\ kg^{-1}$	VRWC	2.59	3.00	2.02	1.46E-8
		VRMP	1.28	1.16	1.17	
Iron	$mg\ kg^{-1}$	VRWC	1150.00	246.00	1536.08	4.06E-3
		VRMP	83.56	49.65	79.40	
Lead	$mg\ kg^{-1}$	VRWC	4.05	2.05	4.20	1.00E-5
		VRMP	2.24	2.04	1.64	
Manganese	$mg\ kg^{-1}$	VRWC	4272.11	636.00	5568.91	1.85E-14
		VRMP	161.06	48.40	195.37	
Mercury	$mg\ kg^{-1}$	VRWC	1.46	2.20	1.12	1.42E-3
		VRMP	0.95	1.30	0.67	
Nickel	$mg\ kg^{-1}$	VRWC	18.77	20.80	6.69	0.00
		VRMP	2.23	1.40	2.82	
Titanium	$mg\ kg^{-1}$	VRWC	5.16	2.00	5.17	0.35
		VRMP	4.41	0.64	5.56	
Uranium	$mg\ kg^{-1}$	VRWC	2.00	2.10	1.05	0.70
		VRMP	1.98	2.10	0.96	
Vanadium	$mg\ kg^{-1}$	VRWC	7.62	7.50	1.30	0.00
		VRMP	4.00	4.33	1.63	
Zinc	$mg\ kg^{-1}$	VRWC	7.29	5.95	5.52	0.16
		VRMP	11.46	2.20	2.56	

The *p-values* in Table 8.11 indicated that zinc was the only trace metal that had significantly different concentrations between the two trees; the zinc concentrations was 84% higher in the presence of *Tamarix usneoides* than *Rhus lancea*. These results showed that two tree species had a different affinity in terms of zinc.

Table 8.12 indicated that copper, iron, lead, and manganese were most mobile in the oxide fraction, while aluminium, arsenic, chromium, mercury, nickel, titanium, uranium, vanadium and zinc were most mobile in the organic fraction. The *p-values* indicated that all three fractions of each of the trace metals were significantly different ($p < 0.05$).

Table 8.10 Descriptive statistics of trace elements by treatment

Determinant	Units	Treatment	Mean	Median	Standard Deviation	*p-value*
Aluminium	mg kg^{-1}	Grassland	524.68	505.90	413.49	0.98
		Woodland	523.14	240.80	5.63	
Arsenic	mg kg^{-1}	Grassland	2.38	2.55	1.79	0.49
		Woodland	2.17	2.30	1.83	
Chromium	mg kg^{-1}	Grassland	6.63	5.58	6.57	0.39
		Woodland	5.58	1.40	6.74	
Copper	mg kg^{-1}	Grassland	1.92	1.20	2.02	0.48
		Woodland	1.74	1.30	1.50	
Iron	mg kg^{-1}	Grassland	572.00	47.30	1244.86	0.54
		Woodland	470.43	105.00	1018.79	
Lead	mg kg^{-1}	Grassland	3.13	1.90	2.58	0.45
		Woodland	2.80	2.10	2.41	
Manganese	mg kg^{-1}	Grassland	1993.65	279.00	4410.24	0.60
		Woodland	1677.92	176.80	3842.61	
Mercury	mg kg^{-1}	Grassland	0.99	1.48	0.92	0.08
		Woodland	1.27	0.40	0.91	
Nickel	mg kg^{-1}	Grassland	11.28	8.75	9.31	0.05
		Woodland	8.61	3.60	8.92	
Titanium	mg kg^{-1}	Grassland	4.43	1.50	4.93	0.60
		Woodland	4.80	1.56	5.64	
Uranium	mg kg^{-1}	Grassland	2.24	2.03	0.77	0.09
		Woodland	1.76	1.65	1.04	
Vanadium	mg kg^{-1}	Grassland	5.21	4.55	2.10	0.48
		Woodland	5.51	6.00	2.43	
Zinc	mg kg^{-1}	Grassland	10.73	8.33	11.11	0.17
		Woodland	9.45	3.70	23.66	

The trace elements by depth in Tables 8.13 (a), (b) and (c) at each site indicated that at VRWC aluminium, chromium, iron, lead, manganese, nickel, and zinc were more concentrated in the top layer of soil; while titanium and uranium were more concentrated in the middle layers of soil, i.e. at 10-20 cm. Arsenic, copper, mercury, and vanadium had similar concentrations through the whole depth of soil sampled. At VRMP chromium, lead and vanadium had their highest concentrations in the top layers of soil, while aluminium, arsenic, iron, and titanium were more concentrated in the deeper soil samples, i.e. 40-50 cm. Copper, manganese, nickel, uranium and zinc were

more concentrated in the middle layer of soil, i.e. 30-40 cm. Mercury had similar concentrations through the whole depth profile.

Similar to conductivity and some of the major nutrients, there were some cases of extremely high standard deviations, especially for aluminium, iron and manganese; which were also the trace elements with the highest concentrations at both sites. The high standard deviations indicate the variability in concentrations when comparing between the two sites, the woodland and grassland treatment, two tree types, three sequential extraction steps and the various depths, due to a composite sample being considered in the statistical analysis; for example for when comparing the sites, within one site both treatments, trees types and all depths were combined.

The trace elements for the soil core samples at the Vaal River sites were expressed into three components by PCA (Table C6, Appendix C), as shown in Table 8.14. The components included the following trace elements: mercury, vanadium, chromium, copper, arsenic, titanium, nickel, and zinc in Component 1; aluminium, manganese, and iron in Component 2; and uranium, and lead in Component 3. The components had a variance 82.56%. Histograms (Figures C10, C11, and C12, Appendix C) indicated that all the first and third components were normally distributed, and the second component was not normally distributed.

Table 8.15 shows the ANOVA results for the three trace element components (Tables C13, C14, C15, C16, C17, C18, C19, C20, C21, Appendix C). Groups within the following factors were not statistically different: Component 1 – treatment (p = 0.40) and tree (p = 0.70), Component 2 – site (p = 0.42), Component 3 – site (p = 0.67) and treatment (p = 0.20). Hence the trace elements within Component 1 showed no difference between the woodland versus grassland substrates, and in terms of the two tree types.

Table 8.11 Descriptive statistics of trace elements by type of tree

Determinant	Units	Tree	Mean	Median	Standard Deviation	*p-value*
Aluminium	mg kg^{-1}	*Tamarix usneoides*	574.29	268.00	681.75	0.29
		Rhus lancea	474.12	230.00	418.53	
Arsenic	mg kg^{-1}	*Tamarix usneoides*	2.20	2.35	1.90	0.84
		Rhus lancea	2.13	2.30	1.77	
Chromium	mg kg^{-1}	*Tamarix usneoides*	5.36	1.50	6.49	0.73
		Rhus lancea	5.80	1.40	7.03	
Copper	mg kg^{-1}	*Tamarix usneoides*	1.86	1.16	1.72	0.34
		Rhus lancea	1.62	1.51	1.26	
Iron	mg kg^{-1}	*Tamarix usneoides*	384.13	51.33	723.10	0.33
		Rhus lancea	551.90	114.00	1234.80	
Lead	mg kg^{-1}	*Tamarix usneoides*	2.73	1.40	2.53	0.75
		Rhus lancea	2.88	2.64	2.31	
Manganese	mg kg^{-1}	*Tamarix usneoides*	1900.64	301.60	4151.66	0.50
		Rhus lancea	1464.48	174.00	3537.36	
Mercury	mg kg^{-1}	*Tamarix usneoides*	1.33	1.40	0.94	0.09
		Rhus lancea	1.48	1.60	0.84	
Nickel	mg kg^{-1}	*Tamarix usneoides*	9.60	2.88	1.16	0.23
		Rhus lancea	7.74	4.10	1.02	
Titanium	mg kg^{-1}	*Tamarix usneoides*	4.14	1.68	4.57	0.16
		Rhus lancea	5.50	1.10	6.56	
Uranium	mg kg^{-1}	*Tamarix usneoides*	1.66	1.10	1.25	0.69
		Rhus lancea	1.80	1.90	0.95	
Vanadium	mg kg^{-1}	*Tamarix usneoides*	5.89	6.10	2.34	0.15
		Rhus lancea	5.16	5.78	2.49	
Zinc	mg kg^{-1}	*Tamarix usneoides*	13.46	4.00	32.63	0.04
		Rhus lancea	5.45	2.40	5.51	

Table 8.12 Descriptive statistics of trace elements by sequential extraction step

Determinant	Units	Tree	Mean	Median	Standard Deviation	*p-value*
Aluminium	mg kg^{-1}	Carbonates	54.24	51.60	22.69	0.00
		Oxides	550.20	268.20	390.87	
		Organics	949.09	855.00	493.06	
Arsenic	mg kg^{-1}	Carbonates	0.51	0.50	0.21	0.00
		Oxides	2.06	2.40	1.03	
		Organics	3.91	3.15	1.32	
Chromium	mg kg^{-1}	Carbonates	0.25	0.20	0.09	0.00
		Oxides	0.85	0.87	0.64	
		Organics	11.89	10.45	5.29	
Copper	mg kg^{-1}	Carbonates	0.32	0.32	0.14	0.00
		Oxides	2.62	1.60	1.73	
		Organics	2.45	2.10	1.51	
Iron	mg kg^{-1}	Carbonates	4.22	3.56	3.86	0.00
		Oxides	1411.05	209.00	1584.37	
		Organics	143.55	103.50	148.30	
Lead	mg kg^{-1}	Carbonates	0.36	0.36	0.10	0.00
		Oxides	5.02	4.24	2.09	
		Organics	1.41	1.10	0.98	
Manganese	mg kg^{-1}	Carbonates	233.63	100.00	257.2	0.00
		Oxides	5187.49	522.40	5861.43	
		Organics	178.70	15.60	353.16	
Mercury	mg kg^{-1}	Carbonates	0.26	0.24	0.10	0.00
		Oxides	0.15	0.16	0.03	
		Organics	1.90	1.70	0.55	
Nickel	mg kg^{-1}	Carbonates	5.42	1.60	5.50	1.37E-3
		Oxides	10.43	1.66	11.69	
		Organics	10.82	5.55	8.91	
Titanium	mg kg^{-1}	Carbonates	0.40	0.30	0.36	0.00
		Oxides	1.15	0.78	0.70	
		Organics	11.32	10.88	2.95	
Uranium	mg kg^{-1}	Carbonates	0.90	0.96	0.51	5.10E-4
		Oxides	*.	*.	*.	
		Organics	2.09	2.10	0.93	
Vanadium	mg kg^{-1}	Carbonates	0.87	0.88	0.05	0.00
		Oxides	4.96	3.06	0.01	
		Organics	5.84	6.10	1.17	
Zinc	mg kg^{-1}	Carbonates	3.94	2.16	4.35	5.69E-7
		Oxides	4.81	1.92	5.63	
		Organics	19.93	9.73	31.44	

* - No value computed.

Table 8.13(a) Descriptive statistics of aluminium, arsenic, chromium, copper, and iron by site and depth

Determinant	Units	Site	Depth	Mean	Median	Standard Deviation
Aluminium	mg kg^{-1}	VRWC	0-10	964.17	1012.00	940.62
			10-20	660.68	853.50	445.39
			20-30	635.84	812.00	423.33
		VRMP	0-10	362.74	209.20	320.31
			10-20	374.82	250.80	341.19
			20-30	341.62	196.00	315.06
			30-40	368.60	240.80	322.87
			40-50	424.99	259.20	383.08
Arsenic	mg kg^{-1}	VRWC	0-10	2.99	2.40	2.09
			10-20	2.90	2.40	2.06
			20-30	3.00	2.60	2.02
		VRMP	0-10	1.62	0.68	1.37
			10-20	1.33	0.46	1.29
			20-30	1.75	2.45	1.32
			30-40	1.57	0.48	1.37
			40-50	1.83	2.68	1.34
Chromium	mg kg^{-1}	VRWC	0-10	6.74	1.70	8.41
			10-20	6.65	1.40	8.44
			20-30	6.31	1.40	7.94
		VRMP	0-10	6.66	7.23	4.42
			10-20	4.81	6.75	4.63
			20-30	4.35	5.50	3.82
			30-40	4.08	5.70	3.38
			40-50	5.92	5.55	5.91
Copper	mg kg^{-1}	VRWC	0-10	2.60	3.30	1.99
			10-20	2.85	3.30	2.26
			20-30	2.32	2.40	1.82
		VRMP	0-10	1.18	1.30	0.85
			10-20	1.20	1.16	0.70
			20-30	0.94	0.90	0.51
			30-40	1.73	1.16	2.10
			40-50	1.34	1.22	0.81
Iron	mg kg^{-1}	VRWC	0-10	1272.28	301.50	1671.80
			10-20	1006.61	258.00	1317.12
			20-30	1171.76	139.50	1641.04
		VRMP	0-10	60.28	50.03	67.84
			10-20	89.75	44.85	86.92
			20-30	76.30	44.35	73.29
			30-40	85.55	43.80	83.43
			40-50	101.93	87.68	82.21

Table 8.13(b) Descriptive statistics of lead, manganese, mercury, nickel, and titanium by site and depth

Determinant	Units	Site	Depth	Mean	Median	Standard Deviation
Lead	mg kg^{-1}	VRWC	0-10	4.87	2.10	3.63
			10-20	3.73	1.60	2.96
			20-30	3.53	2.70	2.78
		VRMP	0-10	2.99	3.48	2.03
			10-20	2.62	2.30	1.77
			20-30	1.89	0.75	1.57
			30-40	1.87	1.10	1.30
			40-50	1.93	1.15	1.30
Manganese	mg kg^{-1}	VRWC	0-10	4250.50	811.20	5472.93
			10-20	4302.47	630.00	5695.41
			20-30	4263.82	426.00	5747.33
		VRMP	0-10	131.07	76.40	145.00
			10-20	164.04	73.60	174.97
			20-30	138.79	39.30	185.00
			30-40	191.90	35.00	247.48
			40-50	173.39	33.50	209.25
Mercury	mg kg^{-1}	VRWC	0-10	1.43	1.30	1.18
			10-20	1.53	2.30	1.15
			20-30	1.44	1.35	1.15
		VRMP	0-10	1.02	1.35	0.66
			10-20	0.80	0.77	0.65
			20-30	0.92	1.23	0.70
			30-40	0.99	1.45	0.69
			40-50	1.05	1.40	0.70
Nickel	mg kg^{-1}	VRWC	0-10	20.42	21.80	6.13
			10-20	17.85	20.10	7.42
			20-30	18.04	21.60	6.38
		VRMP	0-10	2.52	1.96	1.16
			10-20	1.54	1.24	1.10
			20-30	1.45	0.56	1.71
			30-40	3.63	2.65	5.16
			40-50	2.99	1.40	2.96
Titanium	mg kg^{-1}	VRWC	0-10	5.09	1.50	5.85
			10-20	6.05	2.00	5.50
			20-30	4.47	2.30	4.08
		VRMP	0-10	4.37	0.44	4.95
			10-20	4.19	1.52	5.10
			20-30	3.94	0.44	5.21
			30-40	4.58	0.60	6.38
			40-50	5.02	0.76	6.27

Table 8.13(c) Descriptive statistics of uranium, vanadium and zinc by site and depth

Uranium	mg kg^{-1}	VRWC	0-10	2.00	2.20	0.67
			10-20	3.57	3.60	0.15
			20-30	1.15	1.20	0.65
		VRMP	0-10	3.79	3.80	0.49
			10-20	1.59	1.43	0.90
			20-30	1.82	1.64	1.03
			30-40	2.26	2.13	1.14
			40-50	1.83	1.65	0.83
Vanadium	mg kg^{-1}	VRWC	0-10	7.58	7.25	1.54
			10-20	7.72	7.60	0.61
			20-30	7.56	7.05	1.58
		VRMP	0-10	4.41	4.35	1.95
			10-20	4.25	4.60	1.96
			20-30	3.56	3.38	1.42
			30-40	3.87	3.74	1.52
			40-50	4.05	3.82	1.41
Zinc	mg kg^{-1}	VRWC	0-10	8.50	6.10	4.65
			10-20	7.43	6.30	6.53
			20-30	5.77	4.55	3.80
		VRMP	0-10	11.30	6.96	9.24
			10-20	9.10	2.16	11.28
			20-30	4.93	1.60	5.90
			30-40	20.78	1.24	50.29
			40-50	11.13	1.48	16.86

For Component 2, in Table 8.15, the concentration of the trace elements showed no difference between the two sites. Trace elements in Component 3, showed no difference between the two sites, and between the woodland versus grassland treatment substrates.

Groups within the following factors were statistically different: Component 1 – site (p = 0.00), Component 2 – treatment (p = 0.00) and tree (p = 0.02), and Component 3 – tree (p = 0.000). The concentration of the trace elements within Component 1 differed between the two sites. The trace elements in Component 2 showed a significant difference between the woodland versus grassland treatment substrates, and also between the two tree species. Trace elements in Component 3, showed a significant difference between *Rhus lancea* versus *Tamarix usneoides*.

Table 8.14 The PCA of the trace elements

Data set	Component	Parameters included	Normally distributed
Trace elements	1	Mercury, vanadium, chromium, copper, arsenic, titanium, nickel, zinc	Yes
Trace elements	2	Aluminium, manganese, iron	No
Trace elements	3	Uranium, lead	Yes

The LRA for the trace elements (Figures C15, C16, C17, Tables C28, C29, C30, C31, C32, C33, C34, C35, C36, Appendix C) are shown in Table 8.16. Components 1 and 2 of the trace elements both had a negative, linear correlation with depth. The *p-values* were both greater than 0.05 (p = 0.08 and p = 0.17), thus the regression model equations were not statistically significant in being able to predict the elemental concentration based on the depth. The correlation coefficients had values of 0.373 and 0.294 respectively for Component 1 and 2, thus the relationship between elemental mobility of the trace elements in both components versus depth was not very strong. This was further highlighted by the variability, i.e. only 13.9% of the elemental mobility of the major nutrients in Component 1 could be explained by depth, and only 8.7% of the elemental concentration of the major nutrients in Component 2.

Component 3 of the trace elements was fitted with a negative, linear correlation and a quadratic correlation with depth. The correlation coefficient was 0.513 for the linear correlation curve, a fairly high degree of correlation, with a variability of 26.4%. The correlation coefficient for the quadratic correlation curve was 0.632, also a fairly high degree of correlation, with a variability of 39.9%. The quadratic curve had a better fit for the data, because the correlation coefficient and the variability were higher. The *p-value* for the quadratic equation was less than 0.05 (p = 0.01), thus the regression model equation was statistically significant in being able to predict the elemental concentration based on the depth.

Table 8.15 A summary of the one-way ANOVA results for the components of the trace elements

Component	Factor	Test used	*p-value*
1	Site	One-way ANOVA	0.00
	Treatment	One-way ANOVA	0.40
	Tree	One-way ANOVA	0.70
2	Site	Mann-Whitney	0.42
	Treatment	Mann-Whitney	0.00
	Tree	Kruskal-Wallis	0.02
3	Site	One-way ANOVA	0.67
	Treatment	One-way ANOVA	0.20
	Tree	One-way ANOVA	0.00

Table 8.16 A summary of the LRA for the components of the trace elements

Component	Correlation	R	R^2	*p-value*	Model
1	Linear - negative	0.373	0.139	0.08	$y = 0.773 - 0.33(Depth)$
2	Linear - negative	0.294	0.087	0.17	$y = 0.579 - 0.26(Depth)$
3	Linear - negative	0.513	0.264	Not computed as the quadratic was the best fit.	
3	Quadratic	0.632	0.399	0.01	$y = 2.276 - 0.172(Depth) + 0.003(Depth)^2$

8.3 Distribution curves

Percentage distribution curves at the Vaal River West Complex for the control, *Rhus lancea* and *Tamarix usneoides* are shown in Figures 8.37, 8.38 and 8.39. The

percentage distribution curves at the Vaal River Mispah are shown in Figures 8.40, 8.41, and 8.42. The curves show the distribution of each element, i.e. aluminium, calcium, chromium, iron, magnesium, manganese, nickel, phosphorous, potassium, titanium and vanadium, through the three BCR fractions and the extraction residual at depths 0-10 cm and 20-30 cm at the VRWC and 0-10 cm and 40-50 cm at the VRMP.

The percentage distribution curves showed that aluminium, chromium, iron, phosphorous, potassium, titanium and vanadium were mainly present in the residual fraction, indicating that these elements were mainly in mineral form in the soil. Hence these elements are less likely to leach into groundwater. Nickel at the VRMP was also included in this list. In the presence of *Rhus lancea* and *Tamarix usneoides* the percentage distribution of these elements did not change drastically.

Calcium, magnesium, manganese and nickel at the VRWC showed percentage distribution curves where the BCR fractions (as a combination of all three fractions or one dominant fraction) were more than 30% of the total elemental concentration.

Calcium occurred in the carbonate bound fraction in the control samples at both sites. At the VRWC the trees changed the percentage distribution, by increasing the calcium concentration in this fraction, in the top layer of soil. At the VRMP the trees decreased the same fraction in the top layer of soil.

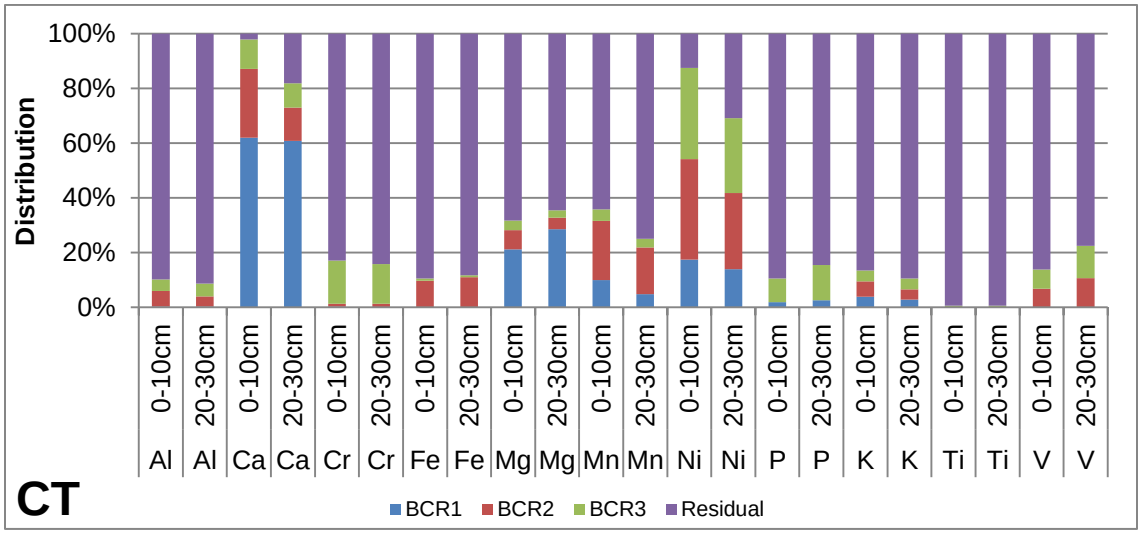

Figure 8.37 Elemental percentage distribution curves at the Vaal River West Complex for the control samples at 0-10 cm and 20-30 cm

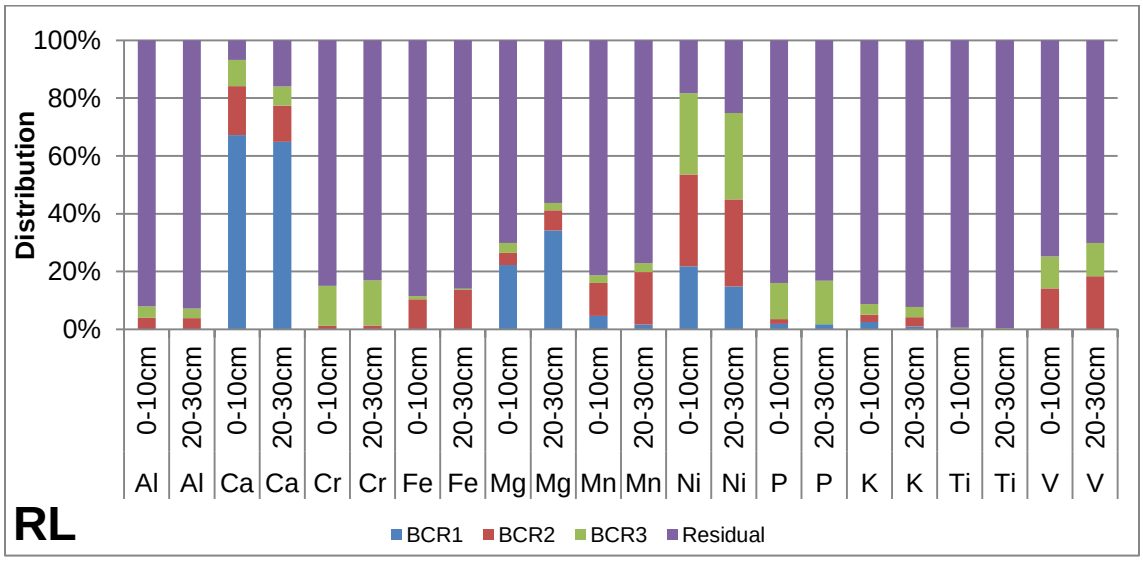

Figure 8.38 Elemental percentage distribution curves at the Vaal River West Complex for *Rhus lancea* at 0-10 cm and 20-30 cm

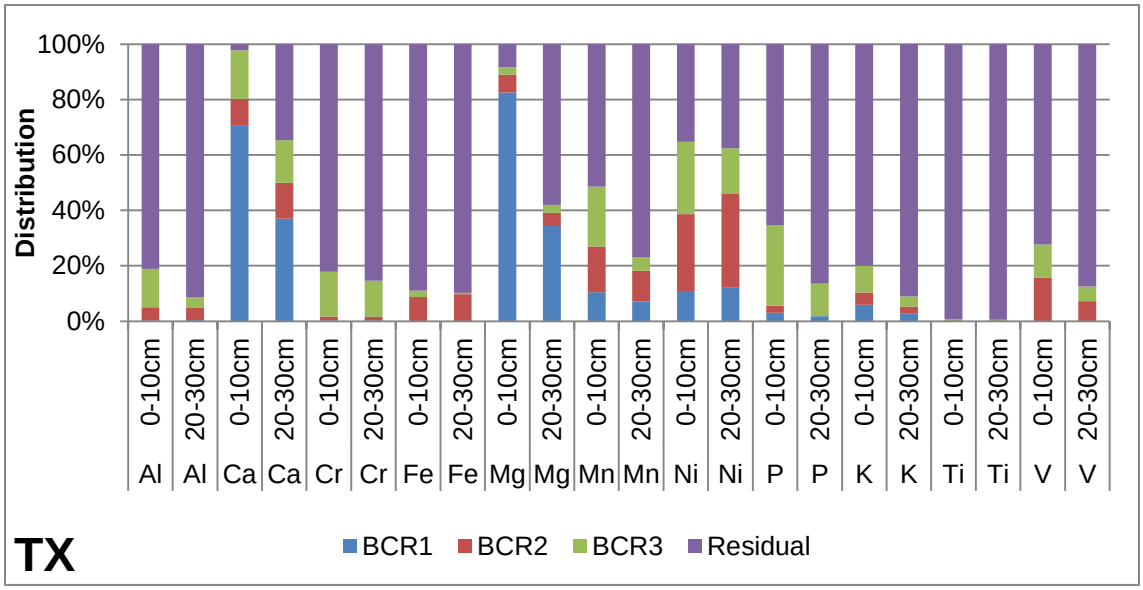

Figure 8.39 Elemental percentage distribution curves at the Vaal River West Complex for *Tamarix usneoides* at 0-10 cm and 20-30 cm

Magnesium was similar to calcium in that it also occurred mainly in the first BCR fraction of the control samples. *Rhus lancea* and *Tamarix usneoides* increased the carbonate bound magnesium in the top layer of soil at both sites.

Manganese was dominant mainly in the oxide bound fraction, at both sites of the control samples. At the VRWC *Rhus lancea* and *Tamarix usneoides* decreased the oxide bound manganese concentration at depth 0-10 cm, while *Tamarix usneoides* also increased the organic bound manganese at the same depth. At the VRMP the trees again decreased the manganese concentration in the oxide bound fraction in the top layer of soil.

At the VRWC nickel occurred in all three BCR fractions, i.e. bound to carbonates, oxides and organics, in the control sample. The trees changed the distribution by decreasing the carbonate bound nickel in the top layer of soil at the VRWC.

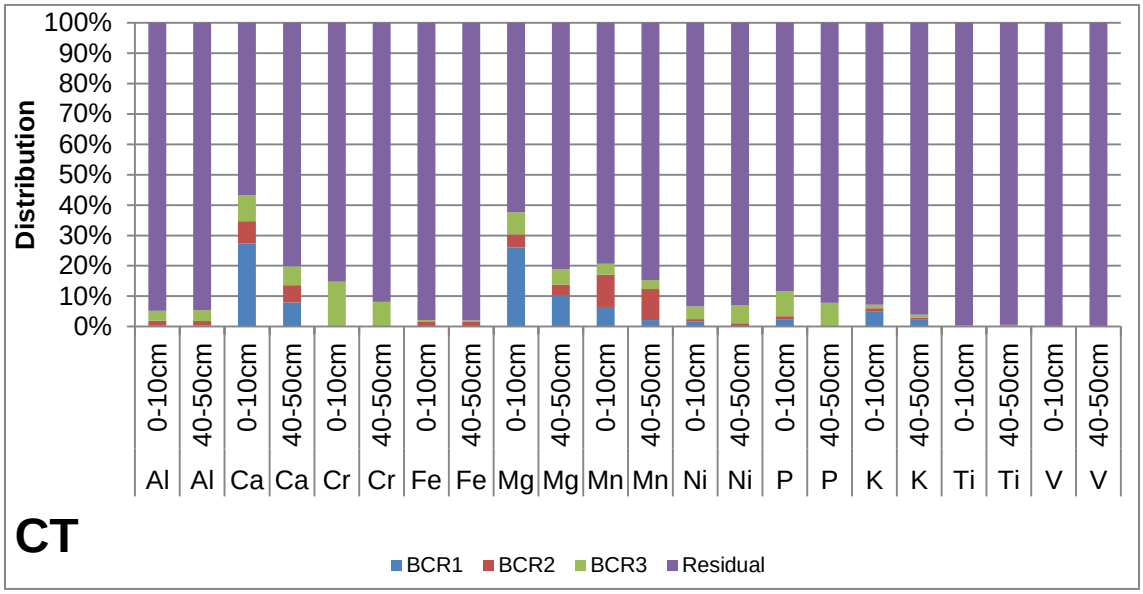

Figure 8.40 Elemental percentage distribution curves at the Vaal River Mispah for the control samples at 0-10 cm and 40-50 cm

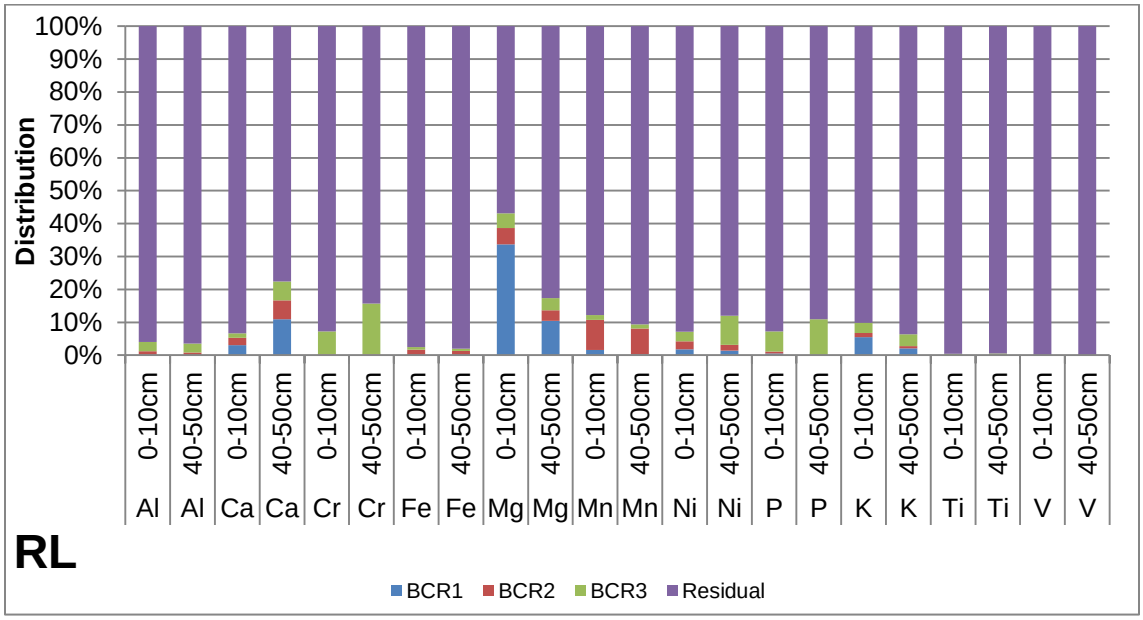

Figure 8.41 Elemental percentage distribution curves at the Vaal River Mispah for *Rhus lancea* at 0-10 cm and 40-50 cm

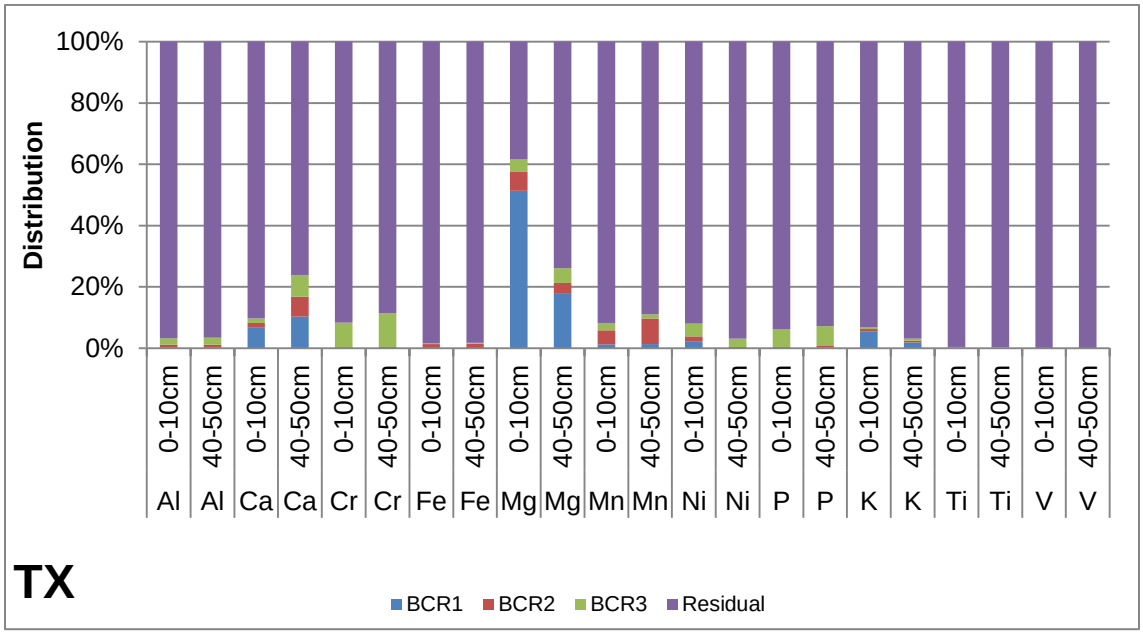

Figure 8.42 Elemental percentage distribution curves at the Vaal River Mispah for *Tamarix usneoides* at 0-10 cm and 40-50 cm

8.4 Summary and conclusions

8.4.1 Major nutrients

Phosphorous had the highest concentration of the major nutrients at both sites. Calcium, magnesium and sulphur were carbonate bound, phosphorous was organic bound and potassium was bound equally in all three fractions (p = 0.05).

At a landfill site where a similar study was done, calcium was found to have the highest concentration at the site, and calcium, magnesium, and potassium were found to be carbonate bound, while phosphorous and sulphur were found to be organic bound (Arendze, unpublished).

The calcium concentration was 14% higher in the woodland substrate than in the grassland substrate, and the difference was significant (p = 0.01), hence the presence of the trees increased the calcium concentration in the soil.

Calcium, magnesium, phosphorous, potassium and sulphur were 133%, 120%, 126%, 96% and 183% respectively higher at VRWC than at VRMB, and the difference was statistically significant (p <0.05) hence the soil was richer in terms of the major nutrients at VRWC.

The magnesium concentration was 71% higher in the soil surrounding *Tamarix usneoides* than *Rhus lancea*, and the difference was statistically significant (p = 0.03), thus *Tamarix usneoides* was more effective in improving the magnesium concentration in the soil.

Calcium, magnesium, and potassium had higher concentrations in the top layer of soil, while sulphur was found to be more concentrated in the deeper soil sample at the two sites i.e. 20-30 cm for VRWC and 40-50 cm for VRMP. Phosphorous had the highest concentrations in the top layer of soil at VRWC, and the in deeper soil sample at VRMP.

Calcium, magnesium and phosphorous had high standard deviations, due to a composite sample being used for the statistical analysis; these high standard deviations are indicative of high variability of the concentration of major nutrients in the study, and not outliers. Calcium, magnesium and phosphorous concentrations showed big variability at VRWC compared to VRMP, in the woodland substrate compared to the grassland substrate, and in the presence of *Tamarix usneoides* instead of *Rhus lancea*.

Calcium also showed high standard deviation for a landfill site where the same trees have been planted (Arendze, unpublished), so the high variability in data is not isolated to the VRWC and VRMP sites; this high variability could likely be due to the high hyperaccumulation capabilities of the trees.

The PCA expressed the major nutrients into two components: Calcium, magnesium and sulphur in Component 1, and phosphorous and potassium in Component 2. The ANOVA results indicated that the major nutrient concentrations in both components showed a significant difference between the two sites (p = 0.00 for Component 1, p = 0.00 for Component 2). However both components showed no significant difference between the woodland and grassland substrates (p = 0.40 for Component 1, p = 0.41 for Component 2) and between the tree types (p = 0.67 for Component 1, p = 0.12 for Component 2).

In comparison, phosphorous, potassium, and sulphur formed one component and calcium and magnesium formed another component of the PCA of the major nutrients at a landfill site; here Component 1 showed no significant difference between treatment (p = 0.27) and tree (p = 0.39), while Component 2 showed a significant difference between treatment (p = 0.00) and tree (p = 0.00) (Arendze, unpublished).

The LRA indicated that the concentration of both components of the major nutrients had a linear, negative relationship with depth, and that the correlation model was significant (p = 0.00 for Component 1, p = 0.00 for Component 2), hence the respective equations could be used to predict the concentration based on depth.

In comparison to a landfill site where a similar study was done, the major nutrient components formed linear, positive LRA relationships with depth (Arendze, unpublished).

8.4.2 Trace elements

The trace elements were mainly bound in the oxide and organic bound fractions. Copper, iron, lead and manganese were oxide bound, while aluminium, arsenic, chromium, mercury, nickel, titanium, uranium, vanadium and zinc were organic bound. Manganese, followed by iron and then aluminium had the highest concentrations of all the trace elements at both sites

At a landfill site, where the same trees have been planted, it was found that aluminium had the highest concentration in the soil, followed by iron and then manganese (Arendze, unpublished). It was also found that aluminium, copper, iron, lead, manganese and zinc were oxide bound, while arsenic, chromium, mercury, nickel, titanium, uranium, and vanadium were organic bound at the landfill site (Arendze, unpublished). The trend with regards to the organic bound fractions is very similar.

Nickel was 39% lower in the woodland substrate compared to the grassland substrate, and this difference was significant (p = 0.05), which indicated that the presence of the trees have decreased the concentration of nickel in the soil. Nickel was the only trace elements that showed a significant difference between treatments.

Aluminium, arsenic, copper, iron, lead, manganese, mercury, nickel, and vanadium were respectively 68%, 61%, 67%, 173%, 58%, 186%, 50%, 97%, and 62% higher at VRWC than at VRMB, and the differences was significant (p <0.05).

The trees showed different affinity for zinc, as the concentration was 84% higher in the presence of *Tamarix usneoides* compared *Rhus lancea*; and the difference was significant (p = 0.04).

At VRWC aluminium, chromium, iron, lead, manganese, and zinc were more concentrated in the top layer of soil, while copper, titanium and uranium, were more concentrated in the middle layer of soil, i.e. at 10-20cm. Arsenic, mercury, nickel and vanadium had similar concentrations through the whole depth of soil sampled.

At VRMP chromium and lead had highest concentrations in the top layer of soil, while aluminium, arsenic, iron, titanium and vanadium were more concentrated in the deeper soil sample, i.e. 40-50 cm. Copper, manganese, nickel, uranium and zinc had higher concentrations in the middle layer of soil, i.e. 30-40 cm. Mercury had similar concentrations through the whole depth profile.

Aluminium, iron and manganese had extremely high standard deviations, similar to conductivity and major nutrients: calcium, magnesium and phosphorous. The high standard deviations indicate the variability in concentrations when comparing between the two sites, the woodland and grassland treatment, the two tree types, the three sequential extraction steps and the various depths, due to a composite sample being used for the statistical analysis. The variability of aluminium, iron and manganese was higher at VRWC than at VRMP, and for the woodland treatment than the grassland treatment. Aluminium and manganese had higher variability in the presence of *Tamarix usneoides*, while iron had higher variability in the presence of *Rhus lancea*.

When comparing to the landfill study, aluminium, iron and manganese also showed extremely high standard deviations (Arendze, unpublished), hence the variability in

these three trace elements is not and isolated occurrence; this high variability could likely be due to the high hyperaccumulation capabilities of the trees

PCA represented the trace elements in 3 components, Component 1: mercury, vanadium, chromium, arsenic, titanium, nickel, and zinc, Component 2: aluminium manganese, and iron, and Component 3: uranium, and lead.

The ANOVA data indicated that the trace metals in Component 1 showed a significant difference between the two sites (p = 0.00), but no significant difference between the treatment substrate (p = 0.40) and the tree species (p = 0.70). Trace metals in Component 2 showed a significant difference between the woodland and grassland treatment substrates (p = 0.00), and also a significant difference between the trees (p = 0.02), but no significant difference between the sites (p = 0.42). Trace metals in Component 3 showed a significant difference between *Tamarix usneoides* and *Rhus lancea* (p = 0.00), and showed no significant difference between the sites (p = 0.67) and between treatment substrates (p = 0.20).

For the landfill study, where there was a similar experimental design, all the trace elements were combined into only one component (Arendze, unpublished); which showed a significant difference in terms of treatment (p = 0.01) and tree (p = 0.01).

The LRA data indicated that the trace elements in Components 1 and 2 did not have a significant correlation with depth, while Component 3 had a significant, quadratic correlation with depth, hence the equation could be used to predict the concentration based on depth.

In comparison to a landfill site where a similar study was done, the LRA showed that the trace metal component had a linear, positive relationship with depth (Arendze, unpublished).

8.4.3 Distribution curves

Aluminium, chromium, iron, phosphorous, potassium, titanium, vanadium and nickel (at the VRMP), were predominantly present in the residual fraction of the percentage distribution curves, hence they were for the most part in mineral form in the soil, making them less probable to leach into groundwater. The percentage distribution of these elements did not change hugely in the presence of the trees.

Calcium, magnesium, manganese and nickel (at the VRWC) showed minor residual percentages in their percentage distribution curves, with the BCR fraction accounting for more 30% of the total elemental concentration.

Calcium was mainly carbonate bound and the trees increased this fraction at the VRWC at 0-10 cm. At the VRMP calcium in the first fraction decreased at 0-10 cm due to the trees. Magnesium was also mainly carbonate bound, and the trees increased the carbonate bound magnesium at 0-10 cm at both sites.

Manganese mainly occurred bound to oxides, and the trees decreased manganese in this fraction at 0-10 cm at both sites. At the VRWC *Tamarix usneoides* had increased the manganese in the third fraction at 0-10 cm. Nickel (at the VRWC) was present in all three BCR fractions, and the trees decreased the carbonate bound nickel at 0-10 cm.

CHAPTER NINE - SUMMARY AND CONCLUSIONS

The effect of trees on the physical and chemical properties of soil contaminated by gold mine waste disposal was successfully investigated. Conclusions were drawn based on the effectiveness of the trees to change the characteristics of the soil, i.e. physical and chemical characteristics. Conclusions were also drawn based on the differences between the sites and the differences between the trees.

9.1 The potential of the trees for acid rock drainage remediation

The trees have shown great potential for the remediation of acid rock drainage as the physical and chemical characteristics of the soil substrate have been improved. The improvements in the physical and chemical characteristics are summarised as follows.

Generally, the pH of the soil was increased by 7% due to the alkalinising effects of the trees. The conductivity was increased by 88% due to the hyperaccumulation capabilities of the trees, thus increasing the amount of cations and anions in the soil. The redox potential of the soil was decreased by 15%, thus decreasing the oxidation potential of the soil environment. No conclusions could be drawn with regards to the effect of the trees on the soil moisture, as there was no significant difference in the presence of the trees.

The trees were found to increase finer clay particles in the soil, by 18%, and decreasing the bulk density by 1%, thus improving the soil texture and the water retention within the soil. No conclusions could be made in terms of the effect of the

trees on the soil fertility, and CHNS concentration, as there was no significant difference in the presence of the trees.

The trees also improved the chemical condition of the soil by increasing the concentration of calcium in the soil by 14%, due to topsoil enrichment. PCA showed that calcium, magnesium and sulphur grouped together while phosphorous and potassium formed their own grouping, each grouping indicating similarities in elemental behaviour and influence. The ANOVA results indicated that the concentration of the major nutrients showed no significant difference between the woodland and grassland treatment substrates. The LRA indicated that the major nutrients had a significant, linear, negative relationship with depth.

The trees also decreased the nickel concentration in the soil by 39%. The trees absorbed the nickel ions from the soil, causing a decrease from the soil solution.

PCA showed that mercury, vanadium, chromium, arsenic, titanium, nickel, and zinc, were grouped together, aluminium manganese, and iron formed another grouping while uranium and lead formed the last grouping; again indicating similarities in behaviour in each grouping. The ANOVA results indicated that aluminium, manganese and iron showed a significant difference between the woodland and the grassland treatment substrates; while mercury, vanadium, chromium, copper, arsenic, titanium, nickel, zinc, uranium and lead showed no significant difference between the treatment substrates. The LRA data showed that mercury, vanadium, chromium, arsenic, titanium, nickel, zinc, aluminium manganese, and iron did not have a significant correlation with depth while uranium and lead had a significant quadratic correlation with depth.

Distribution curves showed that the following elements were primarily present in the residual fraction: aluminium, chromium, iron, phosphorous, potassium, titanium,

vanadium and nickel (at the VRMP), hence they were less probable to leach into groundwater. The trees had no effect on the percentage distribution of these elements.

The BCR fractions of calcium, magnesium, manganese and nickel (at the VRWC) accounted for more than 30% of the total elemental concentration in the percentage distribution curves. The trees changed the percentage distribution of these elements as follows: carbonate bound calcium at the VRWC increased at 0-10 cm, and decreased at the VRMP at 0-10 cm; carbonate bound magnesium increased at 0-10 cm at both sites; oxide bound manganese decreased manganese at 0-10 cm at both sites, with *Tamarix usneoides* increasing the organic bound manganese at 0-10 cm; carbonate bound nickel (at the VRWC) decreased at 0-10 cm.

9.2 Differences between the Vaal River Sites

Even though the two sites were within the same geographical area and characterised by the same climate, soil genesis and amount of rainfall, there were distinct differences between the two sites in terms of the physical and chemical properties of the soil. The overall soil quality was better at the VRWC in terms of soil fertility, physical and chemical characteristics.

The differences between the Vaal River West Complex and the Vaal River Mispah sites were as follows:

- Soil colour - Soil at the VRMP had a distinct red colour, and the soil was more uniform and brighter in colour than that of the VRWC, which indicated that it was better drained.
- Conductivity - The conductivity values were 168% significantly higher at the VRWC than at VRMP.

- Soil texture – The VRMP had 26%, 15%, and 6% significantly higher percentages of clay, silt and sand in the soil than the VRWC.
- Soil fertility - The CEC, organic carbon and total cation values were 129%, 112% and 89% significantly higher at the VRWC compared to those for the VRMP, thus the soil condition for growth was better at the VRWC.
- CHNS – The percentages of carbon (121%), and hydrogen (48%), were significantly higher at VRWC compared to that of VRMP.
- Major nutrients - The major nutrients had significantly higher concentrations at the VRWC compared to the VRMP. The calcium, magnesium phosphorous, potassium and sulphur were 133%, 120%, 126%, 96% and 183% higher at VRWC compared to VRMB. Thus at VRWC the soil was more beneficial for plant growth.
- Trace elements - The concentrations of the following trace elements were significantly higher at the VRWC than at the VRMB by the percentage shown in brackets: aluminium (68%), arsenic (61%), copper (67%), iron (173%), lead (58%), manganese (186), mercury (50%), nickel (97%), and vanadium (62%).
- Variability – The variability of the aluminium, iron, manganese, calcium, magnesium and phosphorous concentrations were higher at the VRWC site, than at the VRMP site.

9.3 Differences between the tree species

Due to the varying characteristics of the two tree species, differences in the physical and chemical properties of the soil were expected. Generally, it seemed that due to its hyperaccumulation capabilities *Tamarix usneoides* was more effective in improving the overall quality of the soil.

Differences between the trees were as follows:

- Buffer pH - *Tamarix usneoides* was 10% more effective than *Rhus lancea* in raising the buffer pH of the soil.
- Conductivity - *Tamarix usneoides* had 107% higher conductivity values than *Rhus lancea*, indicating that it had greater hyperaccumulation capabilities.
- Redox potential - *Tamarix usneoides* was 18% more effective than *Rhus lancea* in reducing the redox potential of the soil, by introducing a reducing environment in the soil.
- Soil texture – There was no significant difference in the soil texture between the two trees.
- Soil fertility – There was no significant difference in soil fertility between the two trees.
- CHNS – The soil around *Tamarix usneoides* was found to have 46% higher percentage nitrogen compared to *Rhus lancea*.
- Major nutrients - *Tamarix usneoides* was more effective than *Rhus lancea* in increasing the magnesium in the soil; the magnesium was 71% greater in the soil surrounding *Tamarix usneoides*.
- Trace elements - The trees showed a significant different affinity for zinc; zinc was 84% higher in the presence of *Tamarix usneoides* compared to *Rhus lancea.*
- Variability – The variability of the aluminium, iron, manganese, calcium, magnesium and phosphorous concentrations were higher in the presence of *Tamarix usneoides*, than *Rhus lancea*.

10 REFERENCES

Akcil, A., & Koldas, S. (2006). Acid Mine Drainage (AMD): Causes, Treatment and Case Studies, *Journal of Cleaner Production*, No. 14, pp. 1139-1145.

Amberger, A. (2006). Soil fertility and plant nutrition in the tropics and subtropics, First version, published by IFA and IPI, Paris, France, Horgen, Switzerland.

AngloGold Ashanti (AGA). (2007). Vaal River Groundwater Plume Delineation Update, Internal reference number ANGGA.07.175/70563 VRW, Vaal River, South Africa.

Arendze, S. (unpublished). The effect of *Tamarix usneoides* and *Rhus lancea* on the physical and chemical properties of soil at a landfill site in Ekurhuleni, University of the Witwatersrand, South Africa.

Baumann, A. (1885). Das Verhalten von Zinksatzen gegen Pflazen und im Boden Landwirtsch. *Vers.-Statn*, No. 31 pp. 1-53.

Brodie, M.J., Robertson, A. MacG. & Gadsby, J.W. (1992). Cost Effective Closure Plan Management for Metal Mines, Steffen Robertson and Kirsten Inc., Vancouver, B.C.

Camberato, J.J. (2001). Cation exchange capacity – Everything you want to know and more, *South Carolina Turfgrass Foundation news*, October-December.

Chaney, R.L. (1983). Plant uptake of Inorganic Waste. In Parr, J.E., Marsh, J.B., and Kla, J.M. (eds), *Land Treatment of Hazardous Waste*, Noyes Data Corp, Park Ridge, IL, pp. 50-76.

Coulter, B.S., & Lalor, S. (2008). Major and minor nutrient advice for productive agricultural crops, Teagasc, Carlow, Ireland.

Cukrowska, E.M., Tutu, H. & Weiersbye, I.M. (2006). Assessment of chemical composition, potential mobility and toxicity of elements in water, sediments and

evaporated salts of mine evaporative pans, Advances in Mineral Resources Management and Environmental Geotechnology, Hania, Greece, 25-27 September, *AMIREG 2006,* pp. 567-572.

Dye, P.J., Jarmain, C., Oageng, B., Xaba, J. & Weiersbye, I.M. (2008). The Potential of Woodlands and Reed-beds for Control of Acid Mine Drainage in the Witwatersrand Gold Fields, South Africa, *In: A.B. Fourie, M. Tibbett, I.M. Weiersbye and P.J. Dye (eds), Mine Closure 2008, Proceedings of the 3rd International Seminar on Mine Closure, Johannesburg, pp. 487-497.*

Espinoza, L., Slaton, N., & Mozaffari, M. (2006). Understanding the numbers of your soil test report, FSA2118-PD-1-12RV, University of Arkansas, Division of Agriculture, Research and Extension, Texas, USA,.

Fadeeva, V.P., Tokhova, V.D. & Nikulicheva, O.N. (2008). Elemental analysis of Organic Compounds with the Use of Automated CHNS Analyzers, *Journal of Analytical Chemistry*, Vol. 63, No. 11 pp. 1094-1106.

FAO/IIASA/ISRIC/ISS-CAS/JRC, 2009. *Harmonized World Soil Database (version 1.1)*. FAO, Rome, Italy and IIASA, Laxenburg, Austria.

Fisher, P., Aumann, C., O'Halloran, N., Kirkby, C., Lacy, J. & Skjemstad, J. (2007). More organic matter leads to more soil carbon & better soils, *IREC Farmers Newsletter*, No. 176.

Growitz, D. (2002). Factors Controlling Acid Mine Drainage Formation, *US Department of the Interior, Office of Surface Mining*, Washington.

Harris, D.C. (2002). Quantitative Chemical Analysis, W.H. Freeman and Company, New York.

Hill Laboratories (2015). Soil tests and interpretation, Technical notes, Hamilton, New Zealand.

Hlavay, J., Prohaska, T., Weisz, M., Wenzel, W.W. & Stigeder, G.J. (2004). Determination of Trace Elements bound to Soils and Sediment Fractions, *Pure Appl. Chem.*, Vol. 76, No. 2 pp. 415-442.

Hodges, S. C. (2010). Soil Fertility Basics, Soil Science Extension, North Carolina State University. *In* Imtiaz, M., A. Rashid, P. Khan, M. Y. Memon and M. Aslam, 2010. *The Role of Micronutrients in Crop Production and Human Health. Pakistan Journal of Botany,* Vol. 42 No. 4 pp. 2565-2578.

ITRC (Interstate Technology & Regulatory Council). (2009). Phytotechnology Technical and Regulatory Guidance and Decision Trees, Revised. PHYTO-3. Washington, D.C.: Interstate Technology & Regulatory Council, Phytotechnologies Team, Tech Reg Update. www.itrcweb.org

Jenkins, R. (2000). X-Ray Techniques: Overview, Encyclopaedia of Analytical Chemistry: 13269-13288.

Johnson, D.B. & Hallberg, K.B. (2005). Acid Mine Drainage Remediation Options: A Review, *Science of the Total Environment*, No. 338 pp. 3-14.

Khalid, A., Khan, A.T. & Anwar, M.S. (2011). X-Ray Fluorescence (XRF) spectrometry for materials analysis and “discovering” the atomic number, LUMS, School of Science and Engineering.

Kumah, A. (2006). Sustainability and Gold Mining in the Developing World, *Journal of Cleaner Production*, No. 14, pp. 315-323.

Manson, A.D. & Roberts, V.G. (2000). Analytical methods used by the soil fertility and analytical services section. *KZN Agri-report*, No. N/A/2001/04. Pietermaritzburg, South Africa.

Martinez-Sanchez, M.J., Navarro, M.C., Perez-Sirvent, C., Marimon, J., Vidal, J., Garcia-Lorenzo, M.L., & Bech, J. (2008). Assessment of the mobility of metals in a mining-impacted coastal area (Spain, Western Mediterranean), *Journal of Geochemical Exploration*, No. 96 pp. 171-182.

McCarthy, T.S & Venter, J.S. (2006). Increasing Pollution Levels on the Witwatersrand recorded on the Peat Deposits of the Klip River Wetland, *South African Journal of Science*, No. 102, January/February pp. 27-34.

McGrath, S.P. & Zhao, F.-J. (2003). Phytoextraction of Metals and Metalloids from Contaminated Soils, *Current Opinion in Biotechnology*, No. 14 pp. 277-282.

Mitchell, C.C., & Everest, J.W. (1995). Soil testing and plant analysis – Interpreting soil organic matter tests, Southern regional fact sheet, *SERA-IEG-6*1*, Dept. Agronomy & Soils, Auburn University, Alabama.

Naiker, K., Cukrowska, E. & McCarthy, T.S. (2003). Acid Mine Drainage arising from Gold Mining Activity in Johannesburg, South Africa and Environs, *Environmental Pollution*, No. 122 pp. 29-40.

Prasad, M.N.V. & De Oliveira Freitas, H.M. (2003). Metal Hyperaccumulation in Plants – Biodiversity Prospecting for Phytoremediation Technology, *Electronic Journal of Biotechnology*, Vol. 6, No. 3 pp. 285-321.

Rauret, J.F., Lopez-Sanchez, J.F., Sahuquillo, A., Barahona, E., Lachica, M., Ure, A.M., Davidson, C.M., Gomez, A., Luck, D., Bacon, J., Yli-Halla, M., Muntau, H. & Quevauviller, Ph. (2000). Application of a modified BCR Sequential Extraction (Three-Step) Procedure for the Determination of Extractable Trace Metal Contents in a Sewage Sludge amended Soil Reference Material (CRM 483), complemented by a Three-Year Stability Study of Acetic Acid and EDTA Extractable Metal Content, *J. Environ. Monit*., No. 2 pp. 228-233.

Reeves, R.D. & Baker, A.J.M. (2000). Metal accumulating plants, In: *Phytoremediation of Toxic Metals: Using Plants to clean up the Environment*, Raskin, I. and Ensley, B.D. (Eds.), John Wiley & Sons Inc, New York, USA, pp. 193 – 229.

Rodriguez, L., Lopez-Bellido, F.J., Carnicer, A. & Alcalde-Morano, V. (2003). Phytoremediation of Mercury-Polluted Soils using Crop Plants, *Fresenius Environmental Bulletin*, Vol. 12, No. 9 pp. 967-971.

Sahuquillo, A., Lopez-Sanchez, J.F., Rubio, R., Rauret, G., Thomas, R.P., Davidson, C.M. & Ure, A.M. (1999). Use of a Certified Reference Material for Extractable Trace Metals to Asses Sources of Uncertainty in the BCR Three-Stage Sequential Extraction Procedure, *Analytica Chimica Acta*, No. 382 pp. 317-327.

Salido, A. L., Hasty, K.L., Lim, J.-M. & Butcher, D.J. (2003). Phytoremediation of arsenic and Lead in Contaminated Soil using Chinese Brake Ferns (*Pteris vittata*) and Indian Mustard (*Brassica juncea*), *International Journal of Phytoremediation*, Vol. 5, No. 2 pp. 89-103.

Soriano, M.A. & Fereres, E. (2003). Use of Crops for In Situ Phytoremediation of Polluted Soils Following a Toxic Flood from a Mine Spill, *Plant and Soil*, No. 256 pp. 253-264.

State of Victoria (2011). Practical Note: Soil Colour, Victorian Resources Online, Department of Primary Industries, The State of Victoria, Australia.

Steffen, R. (1986). Studies Relating to Evaluation of Alternative Abandonment Measures for Faro Mine Tailings, Report 60601 to Curragh Resources.

Sulkowski, M. & Hirner, A.V. (2006). Element Fractionation by Sequential Extraction in Soil with High Carbonate Content, *Applied Geochemistry*, No. 21 pp. 16-28.

Sutton, M.W., Weiersbye, I.M., Galpin, J.S. & Heller, D. (2006) A GIS-based history of gold mine residue deposits and risk assessment of post-mining land-uses on the Witwatersrand Basin, South Africa. In A.B. Fourie and M. Tibbett (eds), *Mine Closure 2006: Proceedings of the 1st International Seminar on Mine Closure,* Australian Centre for Geomechanics, Perth, ISBN 0-9756756-6-4, pp. 667–678.

Symons, J.M., Bradley L.C.Jr. & Cleveland T.C. (2000). The Drinking Water Dictionary, American Water Works Association, Colorado.

Tan, K.H. (2005). Soil sampling, preparation, and analysis, Marcel Dekker Inc., New York. Cited at http://books.google.co.za on 16 December 2009.

Terry, N., Sambukumar, S.V. & LeDuc, D.L. (2003). Biotechnological Approaches for Enhancing Phytoremediation of Heavy Metals and Metalloids, *Acta Biotechnol.*, Vol. 23 Nos. 2-3 pp. 281-288.

Thompson, M. (2008). CHNS Elemental analysers, *Royal Society of Chemistry*, AMCTB 29 ISSN 1757-5958.

Tokalioglu, S., Kartal, S., & Birol, G. (2003). Application of a Three-Stage Sequential Extraction Procedure for the Determination of Extractable Metal Contents in Highway Soils, *Turk J Chem.*, No. 27 pp. 333-346.

Tutu, H. (2005). Determination and geochemical modelling of the dispersal of uranium in gold-mine polluted land on the Witwatersrand, Ph. D. Thesis, University of the Witwatersrand, Johannesburg.

Tutu H., McCarthy T.S. & Cukrowska E. (2008a). The chemical characteristics of acid mine drainage with particular references to sources, distribution and remediation: The Witwatersrand Basin, South Africa as a case study. *Applied Geochemistry*, No. 23 pp. 3666-3684.

Tutu, H., Cukrowska, E. & McCarthy, T.S. (2008b). Geochemical modelling of the speciation of uranium in an acid mine drainage environment in the Witwatersrand Basin, In: A.B. Fourie, M. Tibbett, I.M. Weiersbye and P.J. Dye (eds). *Mine Closure 2008: Proceedings of the 3rd International Seminar on Mine Closure*, Johannesburg, South Africa, pp. 631 – 638.

Wanenge, M.T. (2009). Growth, biomass production, and carbon, sulphur and nitrogen contents of two *Rhus* species (Anacardiaceae) planted to control acid mine drainage: A case study on Highveld gold mines, Honours Project, University of Witwatersrand, Johannesburg, South Africa.

Watzlaf, G.R., Schroeder, K.T., Kleinmann, R.L.P., Kairies, C.L. & Nairn, R.W. (2004). The Passive Treatment of Coal Mine Drainage, National Energy Technology Laboratory, US Department of Energy, Pittsburgh.

Weber, P.A., Stewart, W.A., Skinner, W.M., Weisener, C.G., Thomas, J.E. & Smart, R.St.C. (2004). Geochemical Effects of Oxidation Products and Framboidal Pyrite Oxidation in Acid Mine Drainage Prediction Techniques, *Applied Geochemistry,* No. 19 pp. 1953-1974.

Weiersbye, I.M., Witkowski, E.T.F. & Reichardt, M. (2006). Floristic composition of gold and uranium tailings dams, and adjacent polluted areas, on South Africa's deep level mines. *Bothalia,* Vol. 36, No. 1 pp. 101-127.

Weiersbye I.M. & Witkowski, E.T.F. (2007). Impacts of acid mine drainage on the regeneration potential of Highveld phreatophyte trees. In J.J. Bester, Seydack, A.H.W., Voster T., Van der Merwe, I.J., and Dzivhani S., *Multiple use management of natural forests and woodlands: Policy Refinement and scientific progress IV*. Department of Water Affairs and Forestry of South Africa, pp. 224-237. www.dwaf.gov.za/forestry

Weiersbye, I.M. (2007). Global review and cost comparison of conventional and phyto-technologies for mine closure, Plenary paper in A.B. Fourie, M. Tibbett and J. Wiertz (eds), *Mine Closure 2007, Proceedings of the 2nd International Seminar on Mine Closure,* Santiago, Australian Centre for Geomechanics, ISBN 978-0-9804185-0-7, pp. 13-19.

Weiersbye, I.M. (2008). An Overview of Phyto-technologies Applicable to Mine Remediation in southern Africa, University of Witwatersrand, South Africa.

Weiersbye, I.M., (unpublished). Phyto-technologies at Anglo Gold Ashanti: The mine woodlands project, PowerPoint presentation slides.

Willard, H.H., Merrit Jr., L.L., Dean, J.A. & Settle Jr., F.A. (1981). Instrumental methods of analysis, sixth edition, Wadsworth Publishing company, Blemont, California.

Winde, F., Wade, P. & Van der Walt, I.J. (2004). Gold Tailings as a Source of Waterborne Uranium Contamination of Streams – The Koekemoerspruit (Klerksdorp goldfield, South Africa) as a case study Part I of III: Uranium Migration along the Aqueous Pathway, *Water SA*, Vol. 30, No. 2 pp. 219-225.

Winde, F. & Van der Walt, I.J. (2004). Gold Tailings as a Source of Waterborne Uranium Contamination of Streams – The Koekemoerspruit (Klerksdorp goldfield, South Africa) as a case study Part II of III: Dynamics of Groundwater-Stream Interactions, *Water SA*, Vol. 30, No. 2 pp. 227-232.

Winde, F., Wade, P. & Van der Walt, I.J. (2004). Gold Tailings as a source of Waterborne Uranium Contamination of Streams – The Koekemoerspruit (Klerksdorp goldfield, South Africa) as a case study Part III of III: Fluctuations of Stream Chemistry and their Impacts on Uranium Mobility, *Water SA*, Vol. 30, No. 2 pp. 233-239.

Winde, F. (2005). Long Term Impacts of Gold and Uranium Mining on Water Quality in Dolomitic Regions – Examples from the Wonderfonteinspruit Catchment in South Africa, North West University, Potchefstroom, South Africa.

Yara Analytical Services (2011). Cation exchange capacity, Yara Phosyn Ltd., Technical bulletin, York.

Zimmerman, A.J. & Weindorf, D.C. (2010). Heavy Metal and Trace Metal Analysis in Soil by Sequential Extraction: A Review of Procedures, *International Journal of Analytical Chemistry*, Vol. 2010, Article ID 387803, 7 pages, doi: 10.1155/2010/387803.